Report No. FAA-RD-75-141

COPY 1

FAA WJH Technical Center
00090610

# A REVIEW AND ANALYSIS OF THE SIERRA DME COLLISION AVOIDANCE SYSTEM

**(IDA Study S-456)**

Arthur Krinitz

Science and Technology Division
Institute for Defense Analyses
Arlington, Virginia 22202

NAFEC
LIBRARY
AUG 16 '76

October 1975

FINAL REPORT

Document is available to the public through the
National Technical Information Service,
Springfield, Virginia 22161.

**Prepared for**

**U.S. DEPARTMENT OF TRANSPORTATION**
**FEDERAL AVIATION ADMINISTRATION**
**Systems Research & Development Service**
**Washington, D.C. 20590**

The United States Government does not endorse products or manufacturers. Trade or manufacturer's names appear herein solely because they are considered essential to the object of the report.

This document is disseminated under the sponsorship of the Department of Transportation in the interest of information exchange. The United States Government assumes no liability for its contents or use thereof.

The work reported in this document was conducted under Contract No. DOT FA 74WA-3498 for the Department of Transportation. The publication of this IDA Study does not indicate endorsement by the Department of Transportation, nor should the contents be construed as reflecting the official position of that agency.

**Technical Report Documentation Page**

| 1. Report No. | 2. Government Accession No. | 3. Recipient's Catalog No. |
|---|---|---|
| FAA-RD-75-141 | | |

| 4. Title and Subtitle | 5. Report Date |
|---|---|
| A REVIEW AND ANALYSIS OF THE SIERRA DME COLLISION AVOIDANCE SYSTEM | October 1975 |
| | 6. Performing Organization Code |
| 7. Author(s) Arthur Krinitz | 8. Performing Organization Report No. Study S-456 |
| 9. Performing Organization Name and Address INSTITUTE FOR DEFENSE ANALYSES 400 Army-Navy Drive Arlington, Virginia 22202 | 10. Work Unit No. (TRAIS) |
| | 11. Contract or Grant No. ARPA DAHC 15 73 C 0200 |
| 12. Sponsoring Agency Name and Address Department of Transportation Federal Aviation Adminstration Systems Research & Development Service Washington, D.C. 20590 | 13. Type of Report and Period Covered Final July 1974 - September 1975 |
| | 14. Sponsoring Agency Code |

15. Supplementary Notes

N/A

16. Abstract


The purpose of this study is to evaluate SIERRA's concept for a collision avoidance system, referred to as DME/CAS. The evaluation is one of a series of studies of various collision avoidance concepts carried out by IDA under contract to the FAA.

The DME/CAS is an air-derived synchronous concept intended to exploit the proliferated network of DME ground facilities to obtain synchronization and to adapt airborne DME designs for time-sharing between the DME and CAS functions. DME ground facilities would be augmented to transmit a CAS time reference signal, in addition to normal DME replies; airborne clocks would be synchronized to the received reference, after correction for the propagation delay obtained by DME techniques. Synchronized CAS participants transmit and receive one-way range and encoded altitude signals for threat evaluation in accordance with the ANTC-117 threat logic.

The areas addressed in this study include the impact of time sharing between DME and CAS functions; the impact of various interference mechanisms (fruit, co-slot and adjacent slot occupancy, multipath), and threat parameter measurement accuracies. The main findings of the study are as follows:

(1) With two-frequency channels and appropriate pulse pair decoders, the DME/CAS should have adequate capacity to accommodate the 800 aircraft of the 1982 Los Angeles Basin traffic model.

(2) Two CAS frequency channels will preempt four out of 252 DME reply channels. This will affect the DME frequency allocations of 16 (expected number) VORTAC facilities, their neighbors, and neighbors' neighbors, etc., in a population of 1000 VORTAC stations. The overall effect could not be dismissed as an insignificant dislocation.

(3) Reliable synchronization performance in the presence of DME-generated "fruit" can be attained, provided that ground transmission of the CAS time reference signal is given priority over conventional DME replies.

(4) In DME/CAS, DME ground facility standards (as promulgated by FAA/ICAO) will have to be upgraded to meet the CAS range accuracy specifications of ANTC-117.

(5) The use of range difference measurements (at 6-sec intervals) for range-rate estimation introduces bias errors in the tau alarm boundary. Although, at short ranges, the error exceeds the allowed (by ANTC-117) value by wide margins, there is only an 8 percent to 10 percent increase in the overall alarm rate.


| 17. Key Words | 18. Distribution Statement |
|---|---|
| Air-Derived Collision Avoidance System, Synchronous, Distance Measuring Equipment, Range and Range-Rate Measurement Accuracy, Synchronization, Fruit, Multipath, Interference | Document is available to the public through the National Technical Information Service, Springfield, Virginia 22151 |

| 19. Security Classif. (of this report) | 20. Security Classif. (of this page) | 21. No. of Pages | 22. Price |
|---|---|---|---|
| UNCLASSIFIED | UNCLASSIFIED | 127 | |

Form DOT F 1700.7 (8-72) Reproduction of completed page authorized

# METRIC CONVERSION FACTORS

## Approximate Conversions to Metric Measures

| Symbol | When You Know | Multiply by | To Find | Symbol |
|---|---|---|---|---|
| | | **LENGTH** | | |
| in | inches | *2.5 | centimeters | cm |
| ft | feet | 30 | centimeters | cm |
| yd | yards | 0.9 | meters | m |
| mi | miles | 1.6 | kilometers | km |
| | | **AREA** | | |
| $in^2$ | square inches | 6.5 | square centimeters | $cm^2$ |
| $ft^2$ | square feet | 0.09 | square meters | $m^2$ |
| $yd^2$ | square yards | 0.8 | square meters | $m^2$ |
| $mi^2$ | square miles | 2.6 | square kilometers | $km^2$ |
| | acres | 0.4 | hectares | ha |
| | | **MASS (weight)** | | |
| oz | ounces | 28 | grams | g |
| lb | pounds | 0.45 | kilograms | kg |
| | short tons (2000 lb) | 0.9 | tonnes | t |
| | | **VOLUME** | | |
| tsp | teaspoons | 5 | milliliters | ml |
| Tbsp | tablespoons | 15 | milliliters | ml |
| fl oz | fluid ounces | 30 | milliliters | ml |
| c | cups | 0.24 | liters | l |
| pt | pints | 0.47 | liters | l |
| qt | quarts | 0.95 | liters | l |
| gal | gallons | 3.8 | liters | l |
| $ft^3$ | cubic feet | 0.03 | cubic meters | $m^3$ |
| $yd^3$ | cubic yards | 0.76 | cubic meters | $m^3$ |
| | | **TEMPERATURE (exact)** | | |
| °F | Fahrenheit temperature | 5/9 (after subtracting 32) | Celsius temperature | °C |

*1 in = 2.54 (exactly). For other exact conversions and more detailed tables, see NBS Misc. Publ. 286, Units of Weights and Measures, Price $2.25, SD Catalog No. C13.10:286.

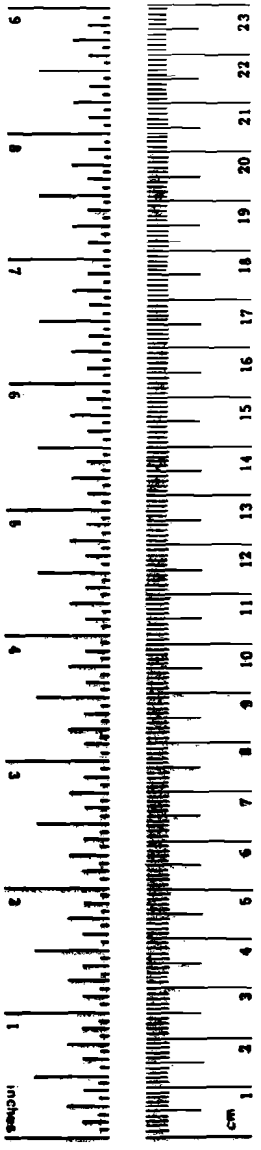


## Approximate Conversions from Metric Measures

| Symbol | When You Know | Multiply by | To Find | Symbol |
|---|---|---|---|---|
| | | **LENGTH** | | |
| mm | millimeters | 0.04 | inches | in |
| cm | centimeters | 0.4 | inches | in |
| m | meters | 3.3 | feet | ft |
| m | meters | 1.1 | yards | yd |
| km | kilometers | 0.6 | miles | mi |
| | | **AREA** | | |
| $cm^2$ | square centimeters | 0.16 | square inches | $in^2$ |
| $m^2$ | square meters | 1.2 | square yards | $yd^2$ |
| $km^2$ | square kilometers | 0.4 | square miles | $mi^2$ |
| ha | hectares (10,000 $m^2$) | 2.5 | acres | |
| | | **MASS (weight)** | | |
| g | grams | 0.035 | ounces | oz |
| kg | kilograms | 2.2 | pounds | lb |
| t | tonnes (1000 kg) | 1.1 | short tons | |
| | | **VOLUME** | | |
| ml | milliliters | 0.03 | fluid ounces | fl oz |
| l | liters | 2.1 | pints | pt |
| l | liters | 1.06 | quarts | qt |
| l | liters | 0.26 | gallons | gal |
| $m^3$ | cubic meters | 35 | cubic feet | $ft^3$ |
| $m^3$ | cubic meters | 1.3 | cubic yards | $yd^3$ |
| | | **TEMPERATURE (exact)** | | |
| °C | Celsius temperature | 9/5 (then add 32) | Fahrenheit temperature | °F |

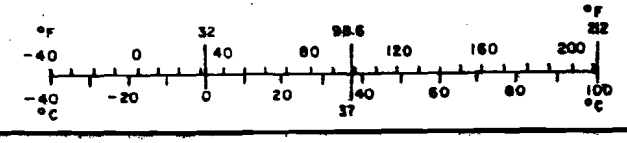

## FOREWORD

In this report, the evaluation of the Collision Avoidance System (CAS) has been based on the criteria and specifications, insofar as they are applicable, of ANTC-117. No direct conclusion about the efficacy of the CAS, as such, should be drawn from the fact that the system evaluated herein conforms to the requirements set down by that document. In another concurrent study by IDA, described in the IDA Report S-450 (FAA Report No. FAA-RD-75-72), an evaluation of ANTC-117 itself was made. The results of that study indicate that ANTC-117 requirements do not guarantee the safe avoidance of collision between encountering aircraft in all circumstances. Moreover, they predict excessive alarm rates in high density traffic such as forecast by the FAA for the Los Angeles Basin in 1982.

## CONTENTS


| | | |
|---|---|---|
| I. | Introduction | 1 |
| II. | Summary and Conclusions | 5 |
| | A. Statement of the Problem and Study Approach | 5 |
| | B. System Description | 8 |
| | C. Study Scope | 11 |
| | D. Study Findings | 13 |
| III. | Brief Functional Description of the DME/CAS Concept | 21 |
| IV. | CAS Frequency Allocations | 25 |
| V. | Acquisition of the CAS Time Reference Signal (CASTRS) | 39 |
| VI. | Updating of the Airborne CAS Clock | 47 |
| VII. | Range Rate Measurement Errors | 57 |
| | References | 76 |
| | Appendix A--Accuracy of Leading Edge Time-of-Arrival Measurements | A-1 |
| | Appendix B--Synchronization Loop Analysis | B-1 |
| | Appendix C--Effect of Multipath on Range Rate Error | C-1 |
| | Appendix D--Undetected Co-Slot Occupants | D-1 |
| | Appendix E--Copy of DOT/FAA Task Order | E-1 |
| | Appendix F--Summary of ANTC-117 Evaluation and Maneuver Logic | F-1 |
| | Appendix G--Effect of Correlated Errors | G-1 |
| | Appendix H--The Impact of Range Difference Measurements on the Tau Alarm Criteria | H-1 |

## LIST OF FIGURES


1. The Basic DME Pulse (Ref. 4) 24
2. DME Frequency Allocations 25
3. Slot-to-Slot Spillover in a Single-Frequency CAS 27
4. Transmitted CAS Signal Format 31
5. Synchronization Sequence 48
6. Synchronization Error as a Function of Loop Settling Time, for a 48-msec Update Interval 52
7. Mean Accuracy Requirements 58
8. Noise Jitter Contribution: Airliner-to-Airliner Link, Tau Zone 2 61
9. Noise Jitter Contribution: Airliner-to-GA Link, Tau Zone 2 62
10. Noise Jitter Contribution: GA-to-Airliner Link, Tau Zone 2 63
11. Noise Jitter Contribution: GA-to-GA Link, Tau Zone 2 64
12. Noise Jitter Contribution: Airliner-to-Airliner Link, Tau Zone 1 65
13. Noise Jitter Contribution: Airliner-to-GA Link, Tau Zone 1 66
14. Noise Jitter Contribution: GA-to-Airliner Link, Tau Zone 1 67
15. Noise Jitter Contribution: GA-to-GA Link, Tau Zone 1 68
16. Maximum Range-Rate Error for 6-sec Data (Ranges and Altitudes Producing Maximum Error are Shown in Fig. 17) 71
17. Altitude and Range Producing the Maximum Range-Rate Error Shown in Fig. 16 72
18. Downrange-versus-Crossrange Plot for a Relative Speed of 600 Knots 74

C-1. Multipath Parameters C-4

D-1. Geometrical Factors D-3

H-1. Aircraft Encounter Kinematics in Reference Aircraft Coordinates H-4

H-2. Threat Evaluation; Range and Range Rate H-6

## LIST OF TABLES

1. Study Scope 12

2. Interpulse Interval Coding 23

3. Nominal Power Budgets 28

4. Probability of Obtaining a 6 dB Margin At The Tau 2 Threat Range 30

5. Power and Range Excess Above Nominal Value 30

6. CAS Transmission Time Budget 31

7. Probability That The CAS Threshold is Exceeded By The Interslot Spillover Signal (Single-Frequency CAS) 33

8. Altitude Decode Accuracies 36

9. Uplink and Downlink Measurement Accuracies Per Pulse 50

10. One-Sigma Contribution of the Synchronization Error to the Range Rate Estimation Error 69

11. Score of Range Rate Error Performance (No Multipath) 69

12. Range-Rate Bias Errors (From Appendix H, Eq. H-9) For A 600-Knot Relative Speed, A 6-Sec Time Base, and Tau Zone 1 Parameters 73

A-1. Calculations Relating To Eq. A-16 A-7

D-1. Summation of Expected New Aircraft Within Communication Range D-5

## GLOSSARY

| | |
|---|---|
| ACAS | Airborne Collision Avoidance System |
| ANTC-117 | Air Navigation and Traffic Control Report No. 117 |
| ATA | Air Transport Association |
| BUM | back-up mode |
| CAS | Collision Avoidance System |
| CASTRS | CAS Time Reference Signal |
| DME | distance measuring equipment |
| DOT | Department of Transportation |
| ERP | effective radiated power |
| FAA | Federal Aviation Administration |
| GA | general aviation |
| ICAO | International Civil Aviation Organization |
| SMR | signal-to-multipath ratio |
| SNR | signal-to-noise ratio |
| TACAN | tactical air navigation |
| T/F | time/frequency |
| TOA | time of arrival |
| VCO | Voltage-Controlled Oscillator |
| VOR | VHF omnidirectional range |
| VORTAC | VHF omnidirectional range tactical air navigation |

# I. INTRODUCTION

The purpose of this study is to evaluate Sierra's (Ref. 1) concept for a collision avoidance system, referred to as DME/CAS.* The evaluation is conducted in response to the DOT/FAA task order reproduced in Appendix E. This is one of a series of evaluations of various collision avoidance systems performed by IDA under contract to the FAA.

DME/CAS is an air-derived synchronous concept intended to exploit the proliferated network of DME ground facilities to obtain synchronization and to adapt airborne DME designs to fulfill the CAS function. DME ground facilities would be augmented to transmit a CAS time reference signal, in addition to normal DME replies; airborne clocks would be synchronized to the received reference after correction for the propagation delay obtained by DME techniques.

The basic information exchanged between the CAS participants, *i.e.*, transmitting and receiving aircraft, consists of three threat parameters: one-way range, range rate as obtained from range difference measurements, and aircraft altitude. These are the only parameters employed for threat evaluation (as specified in Ref. 2) and their measurement accuracies have a direct impact on the rate of illegitimate alarms and on delays of legitimate alarms. For this reason, a portion of the study effort was devoted to an analysis of errors in the measurement of the threat parameters. The results are compared with the ANTC-117 (Ref. 2) specifications which reflect the user's perception of the required performance.

---

*Distance Measuring Equipment/Collision Avoidance System.

The so-called "ANTC-117" is an airline industry (as represented by the Air Transport Association of America) document designed to provide a statement of airline policy and requirements and a technical description of an Airborne Collision Avoidance System (ACAS). The document was prepared under the auspices of the Airline Air Traffic Control Committee, CAS Technical Working Group, and issued by the Air Navigation/Traffic Control Division of the Air Transport Association (ATA) of America. The CAS working group, formed in 1967, included representatives from the ATA, the airlines, the avionics and aircraft manufacturers, ARINC, and observers from the FAA and DoD. The working group recommended the Tau criteria (described in Appendix F of this study) for the threat evaluation logic; time/frequency (T/F) techniques for the transmission and reception of signals; one-way ranging, doppler techniques, and encoded altitude, for threat evaluation.

The ANTC-117 specifications include both functional criteria (*e.g.*, threat logic, threat parameter accuracy requirements, capacity, interference protection, etc.) as well as detailed hardware specifications. In general, all of the ACASs evaluated by IDA purported to meet the essential functional specifications of ANTC-117 without, necessarily, complying with the specified hardware implementation (the one exception being the McDonnell Douglas CAS). Because of this, and because ANTC-117 provides the only articulated set of requirements, ANTC-117 functional specifications were adopted as the common standard of comparison for all of the ACASs studied by IDA. The adequacy of ANTC-117 was examined separately (Ref. 3) and is not addressed in the present study.

A significant portion of the IDA effort on other ACAS studies was devoted to the relationship between traffic density and missed and false alarms. This problem has been of primary concern in the asynchronous CAS concepts, and is the result of

"fruit" effects within their target tracker algorithms. For the DME/CAS, the relationship between interference and "fruit" on the one hand, and false alarms and false dismissals on the other hand, depends on the type of pulse coding/decoding and number of frequency channels envisioned for the CAS function. Sierra (Ref. 1) identified a variety of options without sufficient detail to permit an evaluation of false alarms and false dismissal probabilities. For this reason, the study was confined to a description of the generic type of decoder(s) and frequency assignments needed to protect against interference. In accordance with the admonition in the task order, no detailed functional design of the decoder was attempted. The special forms of "fruit" and interference characteristic of the DME/CAS are addressed in the appropriate section of the study.

Chapter II of the study provides a summary and conclusions which cover: (a) the implications of time sharing between the DME and CAS functions in DME/CAS; (b) accuracies of threat parameter measurements; (c) airborne clock synchronization; and (d) interference mechanisms and their implications on traffic handling capacity.

Chapter III provides a brief functional description of the DME/CAS; more detailed descriptions are given in the course of the analysis in subsequent sections.

Chapter IV addresses the impact of DME/CAS on existing DME service. This includes considerations of frequency channel needs of CAS as determined by the CAS signal format, power budget factors, and interslot interference considerations.

Chapter V examines the procedure for acquiring the CAS time reference signal. Acquisition delays and probabilities of lock-up on fruit are evaluated, together with the CAS-imposed load on the DME ground facility.

Chapter VI analyzes the airborne clock update requirements, clock errors, and their implication on CAS capacity and accuracy of threat parameter measurements.

Chapter VII evaluates the accuracy of CAS range rate measurements, including the impact of clock errors and multipath.

Appendix A derives a lower bound, used in this analysis, on time-of-arrival errors in leading edge measurements.

Appendix B analyzes the synchronization loop behavior and performance characteristics.

Appendix C evaluates the multipath contribution to range rate measurement errors.

Appendix D examines interference resulting from undetected co-slot occupants.

Appendix E provides a copy of the DOT/FAA task order.

Appendix F describes the Tau criteria of ANTC-117 for collision avoidance.

Appendix G examines the effect of correlation between range and range-rate errors.

Appendix H evaluates the range-rate bias errors resulting from range difference measurements.

# II. SUMMARY AND CONCLUSIONS

## A. STATEMENT OF THE PROBLEM AND STUDY APPROACH

The DME/CAS is one of several CAS concepts that have been analyzed and reviewed in a series of IDA studies. The common elements in all cases are as follows:

1. Each of the proposed systems represents a unique technical approach to an air-derived CAS concept. The basic aim of the proponents of the systems (with the exception of the McDonnell Douglas CAS) is to provide a competitive alternative to the so-called ATA CAS as defined in Ref. 2.
2. All of the CASs purported to meet the essential functional specifications (e.g., capacity, alarm criteria, threat parameter measurement accuracies, protection against interference, etc.) of ANTC-117 (Ref. 2) without necessarily meeting the detailed technical design approach specified in ANTC-117.

Thus, the basic study problems are (1) the derivation of the functional performance characteristics from the detailed technical descriptions of the CAS, and (2) comparison with the ANTC-117 functional specifications to the extent that these apply in the specific case.

The so-called "ANTC-117" is an airline industry (as represented by the Air Transport Association of America) document designed to provide a statement of airline policy and requirements and a technical description of an Airborne Collision Avoidance System (ACAS). The document was prepared under the

auspices of the Airline Air Traffic Control Committee, CAS Technical Working Group, and issued by the Air Navigation/ Traffic Control Division of the Air Transport Association (ATA) of America. The CAS working group, formed in 1967, included representatives from the ATA, the airlines, the avionics and aircraft manufacturers, ARINC, and observers from the FAA and DoD. The working group recommended the Tau criteria (described in Appendix F of this study) for the threat evaluation logic; time frequency (T/F) techniques for the transmission and reception of signals; one-way ranging, doppler techniques, and encoded altitude for threat evaluation.

The ANTC-117 specifications include both functional criteria (*e.g.*, threat logic, threat parameter accuracy requirements, capacity, interference protection,) as well as detailed hardware specifications. In general, all of the ACASs evaluated by IDA purported to meet the essential functional specifications of ANTC-117 without necessarily complying with the specified hardware implementation (the one exception being the McDonnell Douglas CAS). Because of this, and because ANTC-117 provides the only articulated set of requirements, ANTC-117 functional specifications were adopted as the common standard of comparison for all of the ACASs studied by IDA.

The adequacy of the ANTC-117 specifications was examined in a companion study (Ref. 3) and is not addressed in this paper (see Foreword).

Each of the CAS studies at IDA was focused on the unique technical features of the specific system under examination. In the case of the DME/CAS, these are (1) time sharing between DME and CAS functions and (2) reliance on the basic DME pulse for both functions. The first will impact both the CAS functions as well as the conventional DME functions, while the second imposes some basic constraints on the threat parameter measurement accuracies. Accordingly, a significant portion of the study was devoted to these problem areas.

The basic assumptions and ground rules adopted in the study are listed below:

1. The technical characteristics of the DME ground facilities conform to the FAA specifications and ICAO standards (Refs. 4 and 5).
2. The essential elements of the DME/CAS are represented in Sierra's Report TR-1115 (Ref. 1) with two amendments:
   a. Synchronization logic changes communicated to IDA in a letter dated 9 December 1974.
   b. Introduction of a pulse peak detector which was not described in TR-1115 and which was communicated to the author through telephone conversations.
3. All of the analyses must be presented in explicit form to insure that the results can be reproduced by the interested reader. Standard analytical tools of modern electronic engineering are used throughout the study--new and startling models are avoided to prevent any spurious controversies about the credibility of the analytical methods.
4. Interference effects which depend on traffic density are evaluated on the basis of the FAA traffic model. This provides a static snapshot of aircraft positions (in three coordinates) and aircraft types projected for the Los Angeles Basin for 1982.
5. A detailed analysis of DME coverage throughout continental United States is beyond the scope of the study. Although Sierra had considered (Ref. 1) some aspects of the problem, a much more detailed assessment will be needed in any future planning for DME/CAS.

IDA studies of the asynchronous CAS systems had devoted a significant portion of the effort to the relationship between traffic density and missed and false alarms. This problem is a primary concern in asynchronous CAS concepts, and is the result of "fruit" effects within their target tracking algorithms.

On the other hand, the synchronous DME/CAS will be subjected to other forms of interference. The impact on false alarms and false dismissals depends on the type of pulse coding/decoding and the number of frequency channels that are envisioned for the CAS function. Sierra (Ref. 1) identified a variety of options without sufficient detail to permit an evaluation of false-alarm and missed-alarm probabilities. For this reason, the study was confined to a description of the generic type of decoder(s) and frequency assignments needed to protect against interference. In accordance with the admonition in the task order, no detailed functional design of the decoder was attempted.

## B. SYSTEM DESCRIPTION

DME/CAS is an air-derived synchronous concept intended to exploit the proliferated network of DME ground facilities to obtain synchronization, and to adapt airborne DME designs to fulfill the CAS function. DME ground facilities would be augmented to transmit a CAS time reference signal, in addition to normal DME replies. Airborne clocks, included in the airborne DME/CAS units, would be synchronized to the received reference after correction for the propagation delay obtained by DME techniques.

The conventional DME is a standardized, L-band, pulse-ranging system designed for airborne navigation applications. It consists of airborne interrogation-and-reception equipment and ground-based transponders or beacons. DME-equipped aircraft interrogate the ground transponder and determine range from the time elapsed between the transmission of an interrogation and the reception of the corresponding reply. DME functions are incorporated into four types of ground facilities:

1. TACAN is an L-band Tactical Air Navigation system which, in addition to DME service, provides bearing information to appropriately equipped aircraft. TACAN ranging is compatible with the conventional airborne DME units.

2. VOR/DME consists of two co-located facilities: one is a VHF omnidirectional range system operating in the VHF band providing only azimuth information, while the DME component, operating at L-band, provides range.
3. VORTAC consists of co-located VOR and TACAN facilities where the DME ranging function is provided by the TACAN component.
4. DME-only facilities operating at L-Band, which provide only ranging.

Approximately* 1000 VORTAC stations cover the continental United States. The most powerful among these, the so-called class H stations, provide DME service out to a range of 130 nmi.

VORTAC stations have been identified by Sierra (Ref. 1) as the prime candidates for the dissemination of the CAS time reference signal for synchronization of the airborne CAS units. The required modifications/additions to these stations include: an atomic clock, timing generation circuitry, and some means for disseminating master time among the ground stations. Sierra (Ref. 1) has not identified any method for providing a common time base for ground stations. This problem is of particular significance to the DME/CAS, which, in contrast to the ATA CAS, has no air-to-air synchronization relay capability and will, therefore, have to rely on a much larger number of ground stations. Although a number of different methods for master time dissemination are available, it is not clear at present which of these can meet the accuracy specifications at a cost acceptable to the FAA.

As far as the airborne equipment is concerned, the transmitter and antenna installation of the conventional DME appears to be appropriate for the DME/CAS. However, the DME/CAS transceiver must be time-shared between five functions:

1. Transmission of conventional DME interrogations to the ground-based DME transponder,

*950 stations in 1967 and 1050 projected for 1981.

2. Reception of conventional DME replies from the ground transponder,
3. Reception of the CAS time reference signal from the augmented DME transponder (ground-based),
4. Transmission of the CAS signal, *i.e.*, one-way range and encoded altitude,
5. Reception of the CAS signal from other aircraft.

Of these five functions, only (1) and (2) are incorporated in the conventional airborne DME transceiver. Thus, the DME/CAS transceiver will require frequency switching hardware (crystal oscillators, frequency multipliers, voltage-controlled oscillator) in addition to the CAS time-crystal-controlled oscillator and a new receiver with appropriate gain control and peak detector circuitry.

Overall system operation is as follows. The airborne CAS unit synchronizes its clock on the basis of DME measurements and time-of-arrival measurements of the CAS time reference signal from the ground (Chapters V and VI provide additional descriptions). The synchronization signal provides the common timing format for 2000 1.5-ms time slots within a 3-second epoch. After synchronization, the airborne CAS selects an unoccupied time slot for transmission of the CAS signal. This consists of two pulse pairs: (1) a marker pulse pair, and (2) an altitude pulse pair. The first pair is transmitted at a fixed time relative to slot start time while the second pair is delayed relative to the first. The delay consists of a relatively large component minus a component which is proportional to aircraft altitude. Thus, a synchronized CAS receiver obtains range to the transmitter by measuring the delay between reception of the marker pulse pair and its known transmission time, while the transmitter's altitude is decoded from the separation between the received marker pulse pair and the altitude pulse pair. Range rate is obtained from the change of range in successive epochs. The three measurements, range,

range rate, and altitude are used (in accordance with Ref. 2) to determine whether or not the transmitting aircraft poses a potential collision threat. An alarm/warning is generated when an intruder appears within prescribed altitude band(s) of the receiving aircraft and when the intruder range is less than a minimum range or the sum of: (1) the prescribed (by ANTC-117) Tau value, in units of time, multiplied by the range rate, plus (2) an offset range to allow for unexpected aircraft maneuvers. The resultant warning time for aircraft on a collision course is greater than the Tau value.

The DME/CAS frequencies are selected from the 960 to 1213 MHz band allocated to DME service. DME interrogation and reply frequencies are separated by the usual 63 MHz; the CAS time reference signal is transmitted (and received) on the uplink DME reply frequency, while the CAS signals are transmitted and received on one or more exclusive frequencies. The DME interrogation and reply frequencies, as well as the CAS time reference signal frequency, are determined by the frequency allocation to the local DME facility. These frequencies change as the aircraft crosses the adjacent service volumes covered by the ground transponders. However, the CAS frequencies are common throughout the continental United States. A CAS time slot is preempted by each DME measurement and by each airborne clock update requiring a time-of-arrival measurement of the CAS time reference signal. The latter is carried out in the presence of "fruit" generated by the conventional DME replies.

## C. STUDY SCOPE

The broad areas covered in this study include the impact of time sharing between DME and CAS functions, interference mechanisms, and threat parameter measurement accuracies. A more detailed breakdown of the specific technical areas and the factors addressed in each area are provided in Table 1.



FAA WJH Technical Center
00090610

TABLE 1. STUDY SCOPE

| Areas Covered in the Study | | Factors Addressed in the Indicated Area |
|---|---|---|
| A. Interslot interference, its impact on frequency channel requirements and dislocation to conventional DME service. | 1. | Power budget factors (transmitted power, antenna gain, receiver sensitivities) and their fluctuation over the equipment population. |
| | 2. | CAS signal format, altitude encoding/decoding scale, pulse pair decoder characteristics. |
| B. CAS load imposed on DME ground transponders. | 1. | Relative priorities assigned to DME and CAS transmissions. |
| | 2. | Synchronization acquisition delays and "fruit" lock-up probabilities. |
| C. Reduction in CAS capacity due to preemption by DME functions. | 1. | DME interrogation rate needed for navigation and for airborne clock updates. |
| | 2. | Airborne clock update requirements as determined by the specified synchronization accuracy, range rate measurement accuracy, clock drift, and synchronization loop design. |
| D. Threat parameter measurement accuracies. | 1. | Power budget factors, random errors, and bias errors. |
| | 2. | DME accuracy, synchronization loop design, and clock drift. |
| | 3. | Multipath. |
| E. Impact of interference on CAS capacity. | 1. | CAS signal format, number of frequency channels, power budget factors, undetected co-slot occupants. |
| | 2. | Pulse-pair decoder characteristics. |

The following are beyond the scope of the present study:

1. Analysis of DME coverage throughout the continental United States. In spite of the 1000 VORTAC stations, some coverage gaps can be anticipated where the asynchronous Back-Up Mode (BUM) will have to be invoked.*
2. Dissemination of master time among ground stations: Ref. 1 has not identified any method for establishing a common time base.

Finally, it should be noted that the analysis of the BUM was omitted from this study because of the incomplete description in Ref. 1 (Appendix D entitled "Back-Up Mode Considerations"). Specifically, the quantitative alarm criteria in terms or range and range rate (or, in fact, whether range rate would be used at all) were not identified by Sierra (Ref. 1).

## D. STUDY FINDINGS

### 1. Frequency Channels

The original ATA CAS (Ref. 2) had been allocated four exclusive frequencies: 1600, 1605, 1610, and 1615 MHz. However, the DME/CAS will have to be accommodated within the DME band around 1 GHz. Here, a single airborne interrogation frequency channel allocated to the CAS function will eliminate 3 out of 252 DME reply channels (Chapter IV). For example, if the airborne frequency channel at 1041 MHz is selected, three ground reply frequency channels will be preempted:

1. 987 MHz = 1041 - 63, corresponding to the so-called channel number 17X,
2. 1104 MHz = 1041 + 63, corresponding to the so-called channel number 17Y, and
3. 1041 MHz, corresponding to channel 80Y, which replies to interrogations on 1104 (= 1041 + 63).

If two airborne frequencies separated by 63 MHz are used for CAS, only three ground reply channels are displaced. On the

*The DME/CAS has no air-to-air synchronization relay capability.

other hand, if the spacing between airborne frequencies is less than or greater than 63, six channels are displaced. The dislocation to DME service will depend on the number of frequencies needed for CAS which, in turn, depends on the CAS signal format, power budgets, and interslot interference protection requirements. Interference may be produced by a CAS transmission after a propagation delay which is long enough to place the trailing end of the CAS signal in a subsequent time slot belonging to a different CAS participant. In this regard, the factors examined in the study (Chapter IV) were: (1) Nominal power budget factors (*i.e.*, transmitter power, antenna gain, losses, receiver sensitivity) and their fluctuations over the equipment population. (2) The CAS signal format and, in particular, the altitude encoding/decoding scale. It was found that the proposed 1-μsec delay per 250 ft of altitude would not meet the specified (Ref. 2) accuracy; accordingly, the scale was changed to 1-μsec delay per 100 ft of altitude (Chapter IV, Eqs. 4 and 6, and Table 6). (3) Pulse pair decoder characteristics.

> Conclusion (Chapter IV): Two frequency channels allocated to the CAS function should provide adequate protection against interslot interference. With appropriate channel spacing, such an allocation will preempt four out of 252 DME reply channels (otherwise, six would be preempted); its impact will be reflected in the frequency reallocation of 16 (expected number) VORTAC facilities, their neighbors, and neighbors' neighbors, etc., in a population of 1000 VORTAC stations. The overall effect could not be dismissed as an insignificant dislocation.

The full impact will depend on the interference protection margins employed in present allocation.

## 2. CAS Load on DME Ground Facilities

A CAS load is imposed on the DME facility by the CAS time reference signal transmissions. Their priority, relative to

conventional DME replies, affect the synchronization acquisition performance of the airborne unit: both acquisition delays and probabilities of lockup on "fruit" were examined in Chapter V.

> Conclusion (Chapter V): The transmission of the CAS time reference signal ($\approx$ 83 pulse pairs per sec) should receive priority over DME replies. The result is a 3-percent reduction in transponder capacity ($\approx$ 2800 pulse pairs per sec) for DME service.

### 3. Impact of DME Functions on CAS Capacity

The CAS traffic handling capacity of the DME/CAS depends (Chapter III) on the number of CAS slots, out of 2000, that will be preempted by DME interrogation/reply sequences and by the airborne clock update requirements (Chapter VI). DME interrogations (typically, 150 Hz during search and 30 Hz during track) can be scheduled for time slots occupied by remote aircraft which pose no threat to the interrogator. However, clock updates can only be made at the scheduled transmission times of the CAS time reference signal. Clock update requirements are determined by the specified synchronization accuracy, the specified range rate measurement accuracy, receiving system noise level, clock drift, and the synchronization loop design, all of which were examined in Chapter VI.

> Conclusion (Chapter VI): In the absence of bias errors, a properly designed synchronization loop can meet the accuracy requirements with lead/lag measurements every 48 msec. Under such conditions, the synchronization maintenance function will preempt 3 percent of the 2000 CAS slots.

### 4. Threat Parameter Measurement Accuracies

Synchronization bias errors, introduced on the DME interrogation channel (Chapter VI) are not affected by update rates nor synchronization loop design. In an encounter between two

aircraft with different effective radiated powers (e.g., an airliner and a general aviation aircraft), the bias error difference can reach 1.25 μsec (Chapter VI) when the encounter takes place near the edge of the service volume of the DME facility (120 nmi from a class H station*). The error is 2.5 times larger than the specified (by ANTC-117) value. When the range to the DME station is 0.4 its maximum range, then the bias error difference is reduced by a factor of 2.5 to that specified by ANTC-117.

An additional source of potential range bias errors is the reply delay accuracy of the DME transponder. The nominal value of the delay between interrogation reception and reply is 50 μsec, which is compensated by the airborne receiver (see discussion in connection with Fig. 5). The present standard (Ref. 4, p. 35, paragraph 3.5.3.5) allows a maximum delay error of ±1 μsec (two-way), which is also reflected in the requirements (Ref. 5, p. 32, paragraph 5.4.1b) for continuous monitoring of the ground facility. Thus, the combination of the two error sources, one from interrogator amplitude disparity and one from transponder delay errors, may exceed the range error allowance (±0.5 μsec) of ANTC-117.

> Conclusion: In DME/CAS, DME ground facility standards on accuracy will have to be upgraded to meet the CAS specifications of ANTC-117.

It is conceivable that many stations provide better accuracies than is called for in the ICAO/FAA specifications. The available measurements (Ref. 6) show a bias error of 0.8 nmi (or 0.5 μsec of one-way delay). However, this result includes aggregated data from short- and long-range measurements, and the transponder delay monitoring and calibration procedures were not identified. Still, the experimental results suggest that

---

*This is the most powerful ground facility whose nominal range extends out to 130 nmi.

sufficient accuracy for CAS operation may be achievable.

Range rate measurement errors, which were examined in Chapter VII, depend on the basic pulse shape, receiver system noise levels, synchronization errors, multipath effects, receiver bandwidth restrictions imposed by electromagnetic compatibility requirements within the congested DME frequency band, and the time available between the two range measurements. Calculated one-sigma errors were compared to the root sum square of two specified (in Ref. 2) error components:

1. The specified one-sigma error, and
2. The specified bias divided by $\sqrt{3}$,

the latter being the one-sigma value of a random error uniformly distributed between the bias limits. The result is a somewhat relaxed one-sigma specification and the justification is that the original bias error specification was intended to accommodate FM discriminator errors in doppler (range rate) measurements.

> <u>Conclusion</u> (Chapter VII): When the CAS range data interval is increased from 3 sec to 6 sec, and when multipath is negligible, then all CAS equipment pair categories (combination/permutations of airliner and general aviation categories) can meet the relaxed range rate accuracy specification in both Tau zones.

However, the data interval envisioned in ANTC-117 (Ref. 2) is 3 sec, in which case the bulk of the aircraft population will not meet the relaxed accuracy specification. This applies to general aviation CAS pairs in both Tau zones (Chapter VII, Figs. 11 and 15) as well as to general aviation CAS units evaluating airliner threats in Tau zone 2 (Chapter VII, Fig. 9).

The multipath contribution to range rate error was examined in Chapter VII (Figs. 16 and 17) and Appendix C. At a signal-to-multipath ratio of 10 dB (as specified in Ref. 2, p. 107, paragraph 2.5.1) and a data interval of 6 sec, the one-sigma

error can be as high as 61 knots, depending on altitude and range (see Figs. 16 and 17). This error component alone exceeds the relaxed one-sigma specification, *i.e.*, 20 knots, for ranges less than 3 nmi (see Fig. 15). However, preliminary calculations for doppler system, addressed in the ANTC-117 specifications, indicate that this system would also fail to meet the specified accuracy for the specified multipath conditions. Because of this inconsistency, no inference can be drawn about noncompliance with ANTC-117 specifications.

Time-of-arrival measurement techniques, other than the peak detector method used in DME/CAS, might reduce the range rate error due to multipath. Some of the alternative approaches include a modification in the threshold control logic in combination with leading--as well as trailing-edge--measurements.

The overall picture emerging from the preceding discussions is that, from the standpoint of random range rate errors, the 6-sec data interval would be preferable to 3 sec. However, the consequence of such an increase is a very large range rate bias error (see Chapter VII, Table 12) due to an overestimate of the actual range rate.

The impact of the bias error on the alarm rate was estimated in Chapter VII (see discussion associated with Fig. 18). For this purpose, intruder aircraft trajectories were characterized by the distance at closest approach, or crossrange, relative to the threat-evaluating aircraft. If these cross ranges are assumed to be uniformly distributed, the increase in the alarm rate due to bias errors amounts to 8 percent to 10 percent, depending on relative speeds.

Conclusion: The use of range difference measurements for range-rate estimation introduces bias errors between the actual Tau alarm boundary and the specified boundary. In spite of the fact that the error, at short ranges, exceeds the specified value by wide margins (see Table 12

in Chapter VII), there is only an 8 percent to 10 percent increase (depending on relative speeds) in the overall alarm rate.

## 5. Interference and Its Impact on CAS Capacity

The interference mechanisms encountered by the DME/CAS in its CAS mode are as follows. (1) Interslot interference due to spillover of the CAS signal. It was estimated (Chapter IV) that, given two frequency channels, the interference probability will be greater than 0.5 percent and less than 0.8 percent per high-altitude encounter, at about 300 nmi from the Los Angeles Basin. (2) Interference to the altitude pulse pair from the range pulse pair arriving via multipath (last paragraphs in Chapter IV). (3) Undetected co-slot occupants which appear between the checks for co-slot occupancy (last paragraph of Chapter IV and Appendix D). The corresponding interference probability can reach 1.3 percent per 40-sec interval (Appendix D).

The impact on the CAS functions depends on the pulse pair decoder for range and altitude pulse pairs. Unfortunately, the simplest decoder, which is very attractive from the standpoint of convenience of implementation, is also the most vulnerable. Such a decoder is preempted by the first interference pulse which exceeds the CAS threshold (12.7 dB above receiver system noise), and is blocked for the duration of the interpulse code interval. The mechanization of the DME/CAS decoder had not been described in Ref. 1 and its design was beyond the scope of this study. However, decoder techniques do exist which incorporate amplitude discrimination and which can eliminate the interference vulnerabilities of the simple decoder. Under such conditions, virtually all of the 2000 CAS slots (minus the 3 percent needed for the clock update function) will be available for transmission/reception of CAS signals.

Conclusion (Chapter IV): Given two frequency channels, and appropriate pulse pair decoders, the DME/CAS should have more than adequate capacity to accommodate the 797 aircraft of the Los Angeles Basin model.

## III. BRIEF FUNCTIONAL DESCRIPTION OF THE DME/CAS CONCEPT

The DME/CAS is a concept for an air-derived synchronous collision avoidance system proposed by the Sierra Research Corporation (Ref. 1). The basic approach attempts to exploit the proliferated network of DME ground transponders* for synchronization and to adapt airborne DME designs to fulfill the CAS function. DME transponders would be augmented to transmit a CAS time reference signal (CASTRS) in addition to normal DME replies, and airborne clocks would be synchronized to the received reference signal after correction for the propagation delay obtained by DME techniques.

The CASTRS provides the common timing format for 2000 1.5-ms time slots within a 3-sec epoch. In essence, the CASTRS is composed of two components: (1) a fine cynchronization component and (2) an epoch synchronization component. The first consists of pulse pairs transmitted at the start of slot numbers 16, 24, 32,..., 1992; the separation between pulse pairs being 8 slots = 12 msec. The epoch-start component is transmitted once every 6 sec as two pulse pairs in slot number 0 and in slot number 8. In both slots, the first pulse of the first pair is transmitted 6 μsec after slot start time. However, the second pulse pair is delayed relative to the first pulse pair by 128.8 μsec in slot number 0 and by 140.8 μsec in slot number 8. Thus, the transmissions in slot numbers 0 and 8 delineate epoch start

*DME transponders are a part of all VORTAC stations. In addition, DME is available in VOR/DME stations and DME-only stations. The total number of DME-equipped stations in CONUS is approximately 1000.

time, while the remaining transmissions provide a refined reference for slot start times.

After synchronization, the airborne CAS selects an unoccupied time slot for transmission of the CAS signal. This consists of two pulse pairs: (1) a marker pulse pair, and (2) an altitude pulse pair. The first pair is transmitted at a fixed time relative to slot start time, while the second pair is delayed relative to the first. The delay consists of a relatively large component minus a component which is proportional to aircraft altitude. Thus, a synchronized CAS receiver obtains range to the transmitter by measuring the delay between reception of the marker pulse pair and its known transmission time, while the transmitter's altitude is decoded from the separation between the received marker pulse pair and the altitude pulse pair. Range rate is obtained from the change of range in successive epochs. The three measurements, range, range rate, and altitude are used (in accordance with Ref. 2) to determine whether or not the transmitting aircraft poses a potential collision threat. An alarm/warning is generated when an intruder appears within prescribed altitude bands of the receiving aircraft and when the intruder range is less than a minimum range or the sum of: (1) the prescribed Tau value, in units of time, multiplied by the range rate, plus (2) an offset range to allow for unexpected aircraft maneuvers. The resultant warning time, for aircraft on a collision course, is somewhat greater than the Tau value.

The airborne DME/CAS transceiver is time shared among five functions:

(1) Transmission of conventional DME interrogations to the ground-based DME transponder,

(2) Reception of conventional DME replies from the ground transponder,

(3) Reception of the CAS time reference signal from the augmented DME transponder (ground based),

(4) Transmission of the CAS signal, i.e., one-way range and encoded altitude.

(5) Reception of the CAS signal from other aircraft. Transmitter and receiver radio frequencies are selected from the 960 MHz to 1213 MHz band allocated to DME service; frequencies for functions (1) and (2) are separated by 63 MHz, (2) and (3) are received on the same frequency, while (4) and (5) will employ one or more frequencies which differ from those used for functions (1), (2), and (3). Clearly, all of the 2000 time slots will not be continuously available for CAS functions (4) and (5), while synchronization, i.e., function (3), will have to be carried out in the presence of fruit generated by the conventional DME replies to other aircraft interrogations.

All transmissions, air-to-ground, ground-to-air, and air-to-air, employ pulse pairs composed from the basic DME pulse shown in Fig. 1. The separation between the constituent pulses of the pulse pairs are summarized in Table 2.

TABLE 2. INTERPULSE INTERVAL CODING

| Pulse Pair | Interpulse Interval (μsec) |
|---|---|
| DME interrogation | 12 |
| DME reply | 12 |
| CAS time reference signal | 60 to 130 |
| Marker pair (CAS range pair) | 140 to 210 |
| Altitude | |

*The indicated range of possible intervals is provided by Ref. 1 pp. 4-107); the preferred design value has not been specified.

Conclusion: The salient features of DME/CAS concept are: (1) time sharing between DME and CAS functions, and (2) reliance on the basic DME pulse for both functions.

A more detailed description of system operation will be provided in the course of the analysis in subsequent sections.

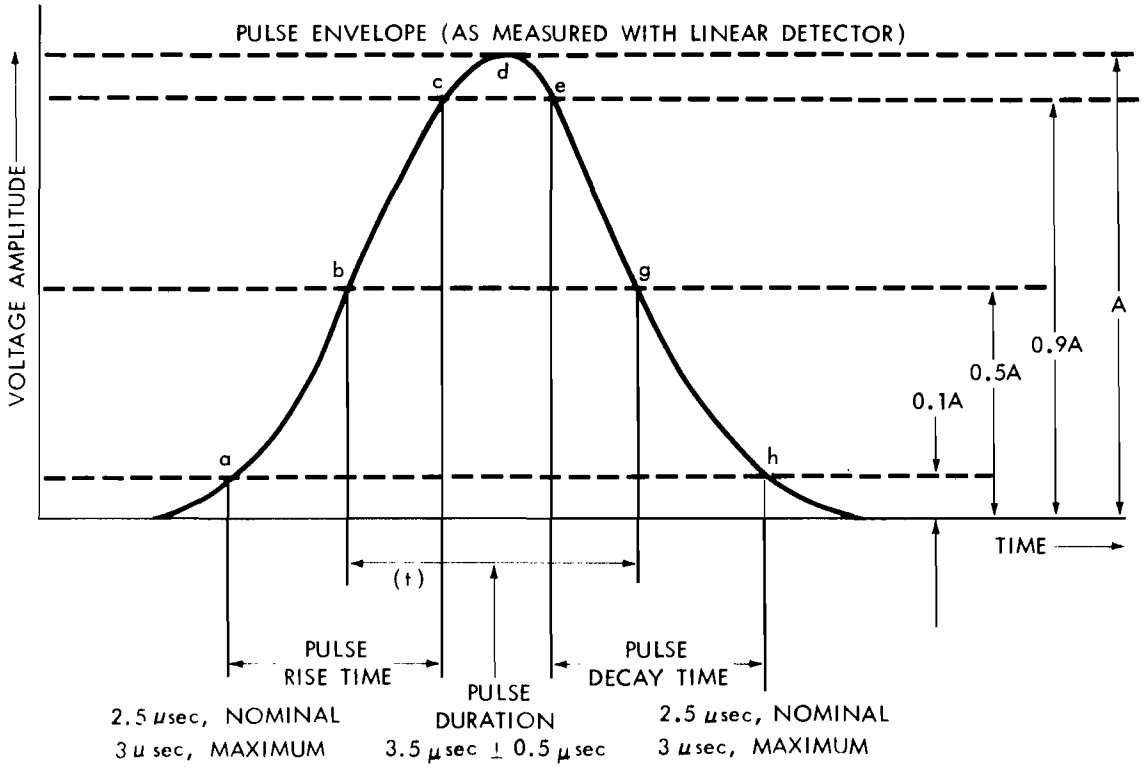


DEFINITION OF PULSE SHAPE (See diagram)

a) Denote 0.1A and 0.9A on leading edge of pulse by a and c respectively, and 0.9A and 0.1A on trailing edge of pulse, as e and h respectively.

b) Denote 0.5A by b and g respectively.

c) Denote A by point d at peak of pulse envelope.

DEFINITIONS

Pulse amplitude A. The peak amplitude of the pulse envelope.

Pulse duration t. The time interval between 0.5A points on leading and trailing edges of the pulse envelope.

Pulse rise time. The rise time as measured between 0.1A and 0.9A on the leading edge of the pulse envelope.

Pulse decay time. The decay time as measured between 0.9A and 0.1A on the trailing edge of the pulse envelope.

6-27-75-1

FIGURE 1. The Basic DME Pulse (Ref. 4)

## IV. CAS FREQUENCY ALLOCATIONS

The original ATA CAS (Ref. 2) had been allocated four exclusive frequencies: 1600, 1605, 1610, and 1615 MHz. Unfortunately, the DME/CAS will have to be accommodated within the DME band around 1 GHz.

The DME band consists of 126 frequency triplets selected from 252 frequencies. Each triplet is composed of a downlink interrogation frequency and two uplink reply frequencies, the so-called X and Y channels. For any given interrogation frequency, the reply frequency is either 63 MHz above or 63 MHz below the interrogation, depending on the interrogator pulse coding. The disposition of the frequency channels is shown in Fig. 2.

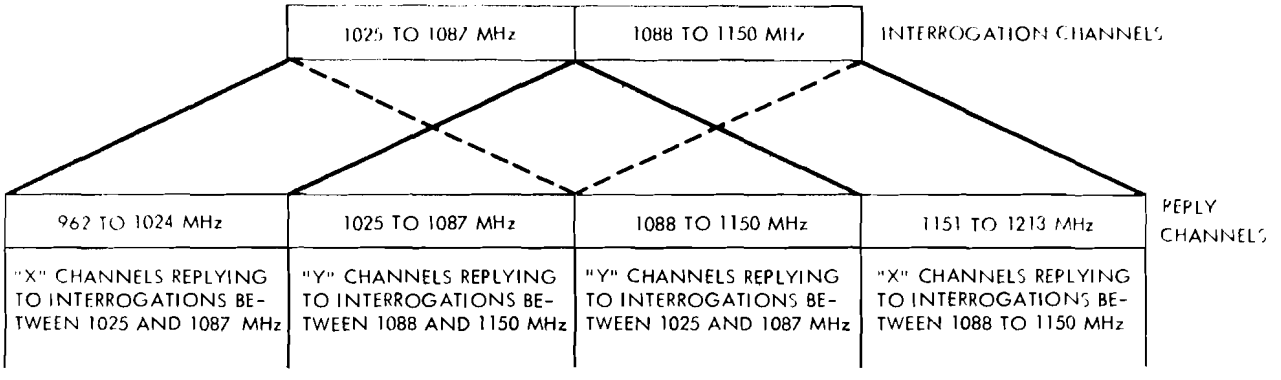


NOTES: (1) CHANNELS ARE SPACED AT 1 MHz INTERVALS
(2) REPLY CHANNELS ARE 63 MHz AWAY FROM THE INTERROGATION CHANNEL

FIGURE 2. DME Frequency Allocations

Inasmuch as airborne transmissions are confined to the 1025 to 1150 MHz band, the CAS signal will have to be accommodated in this band. Here, a single frequency allocated to CAS eliminates three DME reply channels: 63 MHz above, 63 MHz below, as well as a "Y" reply channel of the same frequency. For example, if the airborne frequency channel at 1041 MHz is selected, three ground reply frequency channels will be preempted (see Ref. 4, pp. 30, 31, 32):

1. 987 MHz = 1041 - 63, corresponding to the so-called channel number 17X.
2. 1104 MHz = 1041 + 63, corresponding to the so-called channel number 17Y, and
3. 1041 MHz corresponding to channel 80Y which replies to interrogations on 1104 (= 1041 + 63) MHz.

If two airborne frequencies separated by exactly 63 MHz are used for CAS, only three ground reply channels are displaced. On the other hand, if the spacing between airborne frequencies is less than or greater than 63 MHz, then six channels are displaced.*

The latter implies that for a population of 1000 stations, (4/252) x 1000 = 16 stations**, as well as their neighbors and neighbors' neighbors, etc., may have to have their frequencies reallocated. Thus, the dislocation to DME service will depend on the number of frequencies needed for CAS operation and this depends on the CAS signal format, CAS power budgets, and interslot interference protection requirements.

---

*Reallocation of present ground frequencies for airborne use and a modification of the standard DME transceiver design might alleviate some of the dislocation to DME service.

**This figure is probably higher because some of the nominally DME frequencies are not available to DME users and because the population of 1000 stations does not include DME facilities associated with stations other than VORTAC.

The interslot interference mechanism for a single frequency CAS is illustrated in Fig. 3. Here $t_1$, is the time, relative to slot start time, of the start of transmission of the CAS message, $t_2$ is the end of the transmission, $t_1$ + delay is the arrival time of the leading edge of the transmission at a remote receiver, and $t_2$ + delay is the arrival time of the trailing edge of the transmission. Thus, a CAS transmission in any one slot may reach a remote CAS receiver after a propagation delay which places the trailing end of the CAS signal in a subsequent time slot belonging to a different CAS participant. Whether or not the spillover (see Fig. 3) exceeds the CAS receiver

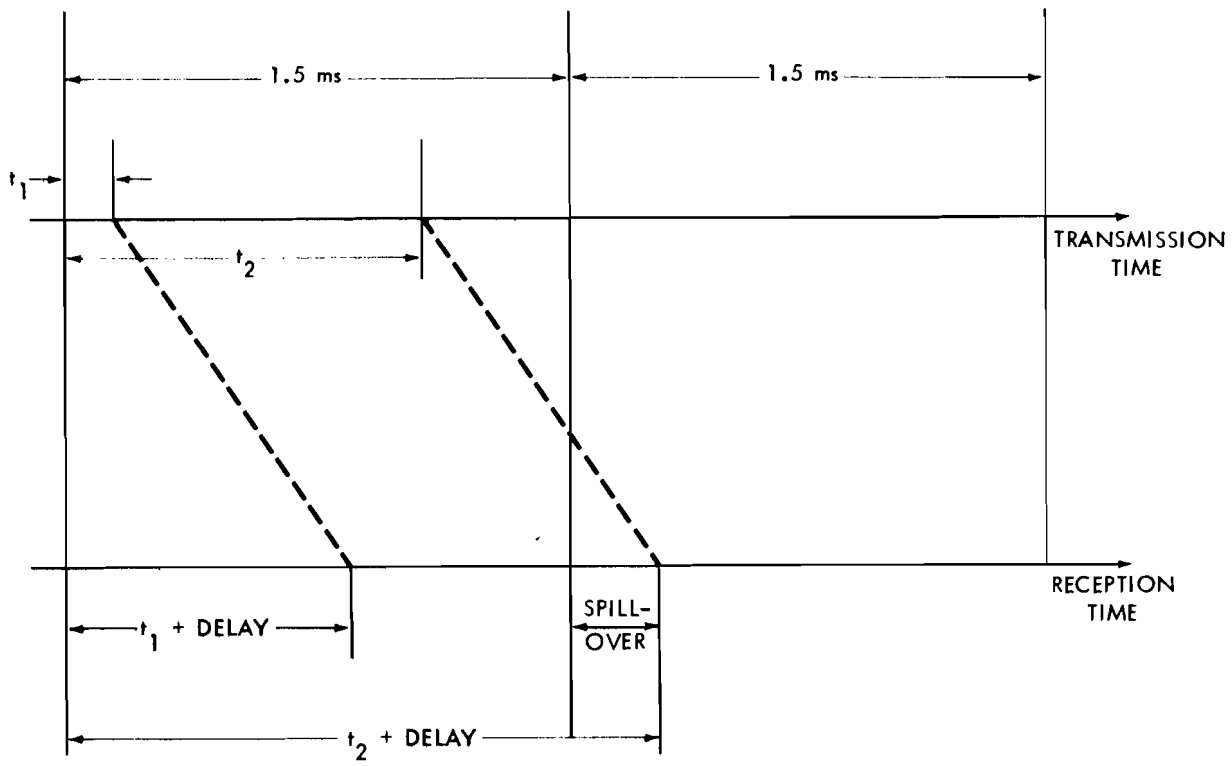


NOTE: $t_1$ = transmission time of the leading end of the CAS signal

$t_2$ transmission time of the trailing end of the CAS signal

6-22-75-3

FIGURE 3. Slot-to-Slot Spillover in a Single-Frequency CAS

threshold is determined from power budgets and from the signal format. The first is evaluated from

$$\frac{PG^2\lambda^2}{(4\pi)^2 R_t^2 L} = \text{CAS threshold}, \qquad (1)$$

where P is the transmitted power, G is the antenna gain, $\lambda$ is the wavelength, L is the total cable loss, and $R_t$ is the threshold range at which the signal level is equal to the CAS receiver threshold; results of this calculation are shown in Table 3

TABLE 3. NOMINAL POWER BUDGETS

| Power Budget Factors | Airline Transmitter to | | GA(1) Transmitter to | |
|---|---|---|---|---|
| | Airline Receiver | GA(1) Receiver | Airline Receiver | GA(1) Receiver |
| a. Transmitter power (W) | 500 | 500 | 100 | 100 |
| b. Average antenna gain(2) product (dB) | 4 | 4 | 4 | 4 |
| c. Receiver sensitivity(3) (dBm) | -90 | -80 | -90 | -80 |
| d. Cable losses for both ends (dB) | 9 | 7 | 7 | 5 |
| e. CAS threshold above sensitivity (dB) | 3.7 | 3.7 | 3.7 | 3.7 |
| f. Resultant threshold range(4) (nmi) | 101 | 40 | 57 | 22 |
| g. Probability that threshold range exceeds nominal value(5) | 93% | 80% | 58% | 61% |

(1) GA denotes general aviation equipments

(2) Assumed frequency is 1050 MHz (wavelength = 0.9374 ft)

(3) Sensitivity is 9 dB above the noise

(4) Free space calculation

(5) Based on data in Ref. 1, Figs. 4-13 through 4-16

for the four combinations of transmitter-receiver pairs. Equipment characteristics are the same as those of the airborne DME transceivers which will be shared with CAS. The indicated receiver sensitivity is 9 dB above the receiver noise level, and the CAS threshold is 3.7 dB above the sensitivity, or 12.7 dB above the noise. This threshold was selected by Sierra (Ref. 1) on the basis of tradeoffs between the probability of threshold crossings by noise and signal detection margins needed to protect against variations in equipment characteristics (power, antenna gain, and sensitivity) below the nominal specifications.

The last row of Table 3 shows the probability that the threshold range exceeds its nominal value because of variations over the population of airborne equipments. The probability is obtained from a convolution (extracted from Ref. 2) of the histograms for transmitted power, antenna gains, and receiver sensitivities, expressed in decibel units.

A similar computation, shown in Table 4, yields the probability that a 6 dB margin will be available at the Tau 2 threat range.

The deviations from nominal values are characterized in terms of a margin, defined as the ratio of the received signal-to-CAS-threshold ratio to its nominal value. The upper 5 percentile, and 1 percentile values of the margin, together with the corresponding threshold range, are shown in Table 5.

The threshold range is converted into one-way delay (approximately 6.2 μsec/nmi which, when added to the transmission time of the trailing end of the CAS signal, will determine the spillover (see Fig. 3), if any, into the subsequent time slot. CAS signal transmission times, as envisioned in Ref. 1, are shown in Fig. 4, and the resultant time budget is summarized in

TABLE 4. PROBABILITY OF OBTAINING A 6 dB MARGIN AT THE TAU 2 THREAT RANGE

| Encounter Parameters | Airline Transmitter to | | GA Transmitter to | |
|---|---|---|---|---|
| | Airline Receiver | GA Receiver | Airline Receiver | GA Receiver |
| a. Maximum closing rate (knots) | 1200 | 800 | 800 | 400 |
| b. Tau two threat range, (nmi) | 15.1 | 10.7 | 10.7 | 6.24 |
| c. Margin available over nominal threshold[1] range (dB) | 16.5 | 11.5 | 14.5 | 10.9 dB |
| d. Probability that a 6 dB margin will be available at the threat range | Over 99%[2] | Over 99%[2] | 99% | 93% |

[1] These are shown in row (f) of Table 3.

[2] The available data do not extend beyond the 99% point.

TABLE 5. POWER AND RANGE EXCESS ABOVE NOMINAL VALUE

| Statistics | | Airline Transmitter to | | GA[1] Transmitter to | |
|---|---|---|---|---|---|
| | | Airline Receiver | GA[1] Receiver | Airline Receiver | GA[1] Receiver |
| Upper five percentile | margin[2] (dB) | 6.5 | 9.0 | 8.0 | 8.0 |
| | threshold range (nmi) | 213 | 113 | 143 | 55 |
| Upper one percentile | margin[2] (dB) | 9 | 13 | 11.5 | 14 |
| | threshold range (nmi) | 285 | 179 | 214 | 110 |

[1] GA denotes general aviation equipments.

[2] Based on data in Ref. 1, Figs. 4-13 through 4-16.

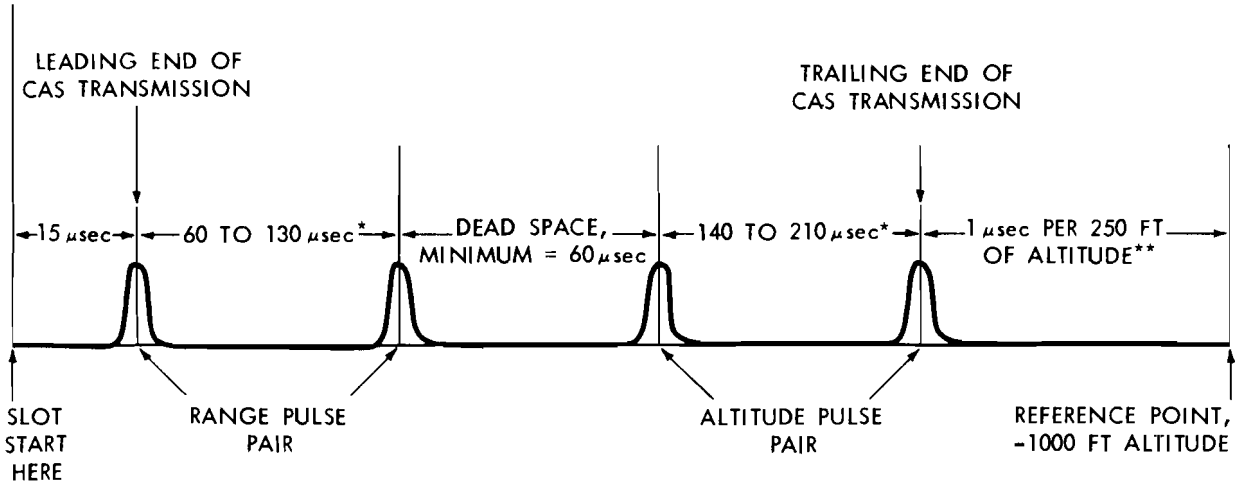


*Reference 1 does not provide a specific value; only the range of possible values is given.

**Reference 1 discusses two scales: 1 μsec per 250 ft, and 1 μsec per 500 ft. The choice of the scale factor is discussed in greater detail in the subsequent analysis.

FIGURE 4. Transmitted CAS Signal Format (Not to Scale)

TABLE 6. CAS TRANSMISSION TIME BUDGET

| | |
|---|---|
| a. Transmission time of the first pulse of the marker pulse pair (relative to slot start) | 15 μsec |
| b. Range pulse position coding delay(1) | 60 to 130 μsec |
| c. Dead space for 80,000-ft altitude(2) | 60 μsec |
| d. Dead space for -1000-ft altitude(3) | 384 μsec |
| e. Altitude pulse position coding delay(1) | 140 to 210 μsec |
| f. Transmission time (relative to slot start) of trailing end of CAS signal from a minimum altitude aircraft | 599 to 739 μsec |

(1) Reference 1 does not provide a specific value, only range is given.

(2) Maximum design altitude.

(3) This value is the sum of 60 μsec and (81,000 ft x 1 μsec/250 ft) = 324 μsec.

Table 6. Clearly, the trailing end of a low-altitude CAS transmission will arrive at the start of the subsequent time slot at a receiver at a range equal to

$$\frac{1500\ \mu\text{sec} - 599\ \mu\text{sec}}{6.18\ \mu\text{sec/nmi}} = 146\ \text{nmi}, \qquad (2)$$

where 1500 μsec is the slot duration; 599 μsec is the transmission time relative to slot start time of the trailing end of the CAS signal, for the minimum pulse position coding delay, and for an aircraft at minimum altitude (see item f in Table 6); and where 6.18 μsec is the one-way propagation delay per nautical mile of range. The probability that a transmission received from 146 nmi range exceeds the CAS threshold is simply the probability that the power budget margin, in dB, is equal to or greater than

$$10 \log_{10} \left(\frac{146}{R_{nom}}\right)^2,$$

where $R_{nom}$ is the nominal threshold range (see item f in Table 3). The required margin, and the probability of attaining that margin, is shown in Table 7.

The effect of spillover depends on the pulse pair decoder. For the Sierra implementation, the decoder will be preempted by the spillover signal when its time of arrival precedes the range and/or altitude pulse pair from the desired signal. Although the problem could be solved with a more sophisticated decoder, Sierra's implementation appears to be the preferred approach from the standpoint of simplicity and cost considerations for the general aviation CAS units.

TABLE 7. PROBABILITY THAT THE CAS THRESHOLD IS EXCEEDED BY THE INTERSLOT SPILLOVER[1] SIGNAL (SINGLE-FREQUENCY CAS)

| Transmitter-Receiver Pair | Margin Needed to Exceed the CAS Threshold at 146 nmi Range[2] | Probability of Obtaining Indicated Margin[3] (%) |
|---|---|---|
| Airliner-to-Airliner | 3.2 dB | 42 |
| Airliner-to-GA | 11.2 dB | 1 |
| GA-to-Airliner | 8.2 dB | 4 |
| GA-to-GA | 16.4 dB | 0 |

(1) This is defined in connection with Fig. 3

(2) Minimum range at which the trailing end of the CAS transmission, from a low-altitude aircraft, will arrive at the start of the subsequent time slot (see Eq. 2 and associated discussion).

(3) These probabilities were read off from Figs. IV-13 through IV-16 of Ref. 1.

The risks of spillover interference could be reduced through the use of two CAS frequencies--one for transmissions in even slots and another for transmission in odd slots. Reception will take place on both frequencies, in synchronism with the transmissions. Under such conditions, Eq. 2 is replaced by

$$\frac{3000\ \mu\text{sec} - 599\ \mu\text{sec}}{6.19\ \mu\text{sec}} = 388\ \text{nmi}, \qquad (3)$$

which exceeds the upper one percentile threshold range, *i.e.*, 285 nmi, for the most powerful transmitter-receiver pair in Table 5. This result hinges on the CAS signal format selected by Sierra, and, in particular, on the pulse-spacing parameters in Fig. 4 and Table 6. These, in turn, are driven by (1) multipath guard time factors and by (2) altitude decoding accuracy. Improvements in one or both will increase interpulse spacings which will increase interslot interference probabilities.

The ANTC-117 specifies (Ref. 2, pp. 109, 127, and 135) that:

> Altitude shall be decoded with a maximum error in the mean of ±0.1 microseconds and a standard deviation of less than 0.1 microseconds for input signals within the dynamic range of the equipment.

Since the altitude code is specified as 250 ft/μsec (Ref. 2, p. 99), we infer that the standard deviation of the altitude decode accuracy should be

$$(250 \text{ ft}/\mu\text{sec}) \times (0.1\ \mu\text{sec}) = 25 \text{ ft} \tag{4}$$

The DME/CAS altitude decoding accuracy is estimated from the relationships between decode accuracy, pulse time of arrival (TOA) measurement accuracy, signal-to-noise ratio, and the power budget relationships. Thus, the standard deviation, $\sigma_{toa}$, of leading-edge time-of-arrival measurements is estimated from*

$$\sigma_{toa} = \frac{T_r}{\sqrt{2\ \text{SNR}}} \tag{5}$$

and

$$\text{SNR} = \frac{PG^2\lambda^2}{(4\pi)^2R^2LN} \tag{6}$$

where $T_r$ is the pulse rise time after filtering through IF stages; SNR is the peak pulse-to-average noise power ratio after filtering; P, G, λ, and L were defined below Eq. 1 and are given in Table 3; R is the range between transmitting and receiving aircraft; and N is the average noise power which is 9 dB below the receiver sensitivities shown in Table 3. In order to protect against adjacent channel interference, DME receiver

*Equation 5 is derived in Appendix A.

bandwidths have been restricted to 250 kHz so that the pulse rise time, $T_r$, could not be less than 4 μsec. The results of the calculation are shown in Table 8. Thus, to meet the altitude decode accuracy specification (Eq. 4), the decode scale will have to be changed from 250 ft/μsec to

$$\frac{25 \text{ ft}}{64 \text{ ft}} \times 250 \text{ ft/}\mu\text{sec} \approx 100 \text{ ft/}\mu\text{sec}. \tag{6a}$$

Conclusion: In order to meet the altitude decode accuracy, the altitude decode scale should be changed from 250 ft/μsec to 100 ft/μsec.

The consequences of this change, are as follows:

1. Item (d) in Table 6 is changed from 384 μsec to 60 μsec + 81,000 ft x 1 μsec/100 ft = 870 μsec.
2. Item (f) in Table 6 is changed from 599 μsec to 599 + (870 - 384) = 1085 μsec.
3. Equation 3 is changed to $\frac{3000 - 1085}{6.18} = 310$ nmi

which still exceeds the upper one percentile threshold range, *i.e.*, 285 nmi, for the most powerful link in Table 5, *i.e.*, airliner-to-airliner link.

The number of candidates for airliner CAS equipments within the 1982 Los Angeles traffic model, is 81 out of 797. Thus, a remote high-altitude airliner will be exposed, on the average, to one slot (1 percent out of 81) with a spillover interference signal. The probability that an intruding aircraft, within 15 nmi, selects the same slot for CAS transmission is bounded by

$$0.5\% \leq \frac{1}{2000 - N_1} \times 99\% \leq \frac{99\%}{2000 - 797} = 0.8\% \ ,$$

TABLE 8. ALTITUDE DECODE ACCURACIES

| Error Characteristics | Transmit-Receive Links | | | |
|---|---|---|---|---|
| | Airline-to-Airline | Airline-to GA | GA-to Airline | GA-to GA |
| a. One-sigma TOA error[1] in nanoseconds as a functioning range R in nmi | 6.50R | 16.34R | 11.57R | 29.1R |
| b. Required range in nmi[2] | 15.13 | 10.69 | 10.69 | 6.24 |
| c. One-sigma TOA error, in microseconds, at required range | 0.0983 | 0.1747 | 0.1236 | 0.1814 |
| d. Altitude decode accuracy,[3] one sigma in ft, at a scale of 250 ft/μsec | 34.8 | 61.8 | 43.7 | 64.2 |

(1) This is obtained from Eq. 5.

(2) The required range corresponds to a Tau two alarm for the closing rates of 1200 knots, 800 knots, and 400 knots, respectively.

(3) TOA accuracies have to be multiplied by $\sqrt{2}$ because altitude is decoded relative to the marker (*i.e.*, range) pulse pair position.

where 2000 is the total number of slots; $N_i$ is the number of slots that the intruder has detected as occupied slots, $N_i \leq 797$; 99 percent is the probability that the intruder does not "hear" the spillover signal. Consequently, a substantial interference probability may be accumulated in 100 encounters. It should be emphasized at this point that all of the preceding estimates are based on the behavior at the "tails" (*i.e.*, upper one percentile) of the distribution of equipment characteristics (transmitted powers, antenna gains, receiver sensitivities). For this reason, the estimate must be regarded as unreliable. The conservative approach is to equip the airliner (or equivalent) CAS units with non-blocking pulse-pair decoders which are not preempted by the first arriving interference pulse.

Conclusions: Two frequency channels allocated to the CAS function should provide adequate protection against inter-slot spillover interference in DME/CAS. However, the air-line (or equivalent) CAS units should be equipped with a more efficient, non-blocking, pulse decoder which will not be preempted by the first-arriving interference pulse.

Implicit in the conclusion is the assumption that the inter-pulse spacings used in the previous analysis provide adequate time-guard bands against multipath interference. The specified (Ref. 2, p. 107, paragraph 2.5.1) maximum multipath levels is 10 dB below the direct signal. This should cause no decode ambiguities* provided that the first-arriving pulse of the CAS quadruplet (two range pulses and two altitude pulses) is used to set an amplitude acceptance threshold, (say, 3 dB below the first pulse) for the subsequent three pulses.

The need for some form of amplitude discrimination is further emphasized by the problem of undetected co-slot occupants addressed in Appendix D.

*At low altitudes, multipath pulses will overlap the direct pulse and produce measurement errors which are treated at the end of Chapter VII.

## V. ACQUISITION OF THE CAS TIME REFERENCE SIGNAL (CASTRS)

The basic CASTRS, as indicated in Chapter III, contains a 12-ms periodic component which is used by the airborne CAS to update its clock. To acquire the CASTRS, the airborne unit will initiate a search with a 20 μsec search gate which is swept relative to a locally (in the aircraft) generated 12-ms periodic reference. The gate is swept in 20-μsec increments in successive 12-ms intervals until the CASTRS pulse pair is detected within the gate. At this point, a tentative lockup occurs: the gate sweep is arrested and a three-out-of-five test is initiated. If three, or more, of the next five detection opportunities, spaced at 12-ms intervals, confirm the initial lockup detection, then a fine search is initiated within the 20-μsec gate. For this purpose, a narrower 4-μsec gate is swept through the wider gate in an attempt to localize the CASTRS. The sweep employs 0.8-μsec increments in successive 12-ms intervals. The gate is arrested when the CASTRS pulse pair is detected and a two-out-of-two confirmation test is applied in two successive 12-ms periods.

The first lockup opportunity occurs at the time that the wide gate sweeps through the point corresponding to scheduled CASTRS pulse pair transmission (plus the one-way propagation delay). However, the probability of a CASTRS pulse pair transmission at the scheduled time will be 70 percent if it has no priority over DME replies.* Thus, the wide gate lockup

*To prevent DME transponder overloading, only 70 percent of the DME interrogations are guaranteed a reply (Ref. 5, p. 26, paragraph 5.3.8.1). If the CAS time reference signal generator (inside the DME facility) is treated like any DME interrogator, only 70 percent of the generated timing pulse will be transmitted on the air.

probability, defined as the probability of a tentative lockup and subsequent confirmation, is given by

$$\Pr\,[\text{wide gate lockup per sweep}] =$$

$$0.7 \sum_{n=3}^{n=5} C_n^5 (0.7)^n (0.3)^{5-n} = 0.585, \qquad (7)$$

where $C_n^5$ are the binominal coefficients. If no lockup occurs on the first sweep, and the corresponding probability is $1 - 0.585 = 0.415$, then the gate will continue to sweep, in 20-μsec increments per 12-ms interval, until the first sweep is completed and a second sweep is carried through to the second lockup opportunity. Thus, the probability of missing n or more lockup opportunities is

$$\Pr\,[\text{wide gate lockup delay} \geq n \text{ sweeps}] = (0.415)^n. \qquad (8)$$

In the absence of any coarse synchronization information, the wide gate will have to sweep through 12-ms intervals between successive lockup opportunities. Thus, the time required to complete one sweep, if the sweep is not arrested by "fruit" detections (to be analyzed later in this section) is

$$\frac{12 \text{ ms}}{20\ \mu\text{sec}} \times 12 \text{ ms} = 7.2 \text{ sec}. \qquad (9)$$

After lockup of the wide gate, the narrow gate sweep is initiated. The probability of a tentative lockup followed by a confirmation in a two-out-of-two test is

$$\Pr\,[\text{narrow gate lockup per sweep}] = 0.7 \times (0.7)^2 = 0.343 \qquad (10)$$

and

$$\Pr\,[\text{narrow gate lockup delay} \geq n \text{ sweeps}] = (1 - 0.343)^n = (0.657)^n . \qquad (11)$$

If the narrow gate sweep is not arrested by fruit, then the time required to complete a 20-μsec sweep, at the rate of 0.8 μsec per 12 msec, is

$$\frac{20\ \mu\text{sec}}{0.8\ \mu\text{sec}} \times 12\ \text{msec} = 0.3\ \text{sec}. \tag{12}$$

A range rate (between aircraft and ground station) of 600 knots will sweep the CASTRS pulse through the wide gate at the rate of

$$\frac{600\ \text{nmi}}{3600\ \text{sec}} \times 6.18\ \mu\text{sec/nmi} = 1.03\ \mu\text{sec/sec}, \tag{13}$$

so that the maximum dwell time within the 20 μsec gate is (20/1.03) sec and the maximum number of lockup opportunities for the narrow gate is

$$\frac{20\ \mu\text{sec}}{1.03\ \mu\text{sec/sec} \times 0.3\ \text{sec}} = 65\ \text{sweeps}. \tag{14}$$

If the wide gate lockup error (equal to the difference between gate center and pulse center) is uniformly distributed over 20 μsec, then the probability that the narrow gate fails to lock up during the time that the CASTRS remains within the wide gate is obtained by averaging Eq. 11 over 65 sweeps, *i.e.*,

$$\frac{1}{65} \sum_{k=1}^{65} (0.657)^k = 0.0295. \tag{15}$$

Fruit is introduced into the CASTRS acquisition circuitry because the DME replies appear on the same uplink frequency (see discussion in Chapter III) and the same pulse code interval, 12 msec, as the CASTRS transmissions. The probability that a pulse of a fruit pulse pair falls within the wide gate is the product of gate width, 20 μsec, and fruit rate, 2800

pulse pairs per sec, *i.e.*, 0.056. In analogy with Eq. 7, the probability that the wide gate locks up on fruit on any given step during its sweep, is given by

$$(0.056)\sum_{n=3}^{5} C_n^5(0.056)^n(1 - 0.056)^{5-n} = 1.17 \times 10^{-4}. \qquad (16)$$

Since the number of gate steps in one sweep is

$$\frac{12 \text{ ms}}{20 \ \mu\text{sec}} = 600, \qquad (17)$$

the conditional probability that the wide gate locks on to fruit in one sweep, given that it has not locked on to signal, is

$$1 - \left(1 - 1.17 \times 10^{-4}\right)^{600} = 0.0678. \qquad (18)$$

An analogous calculation for the narrow gate yields:

1. The probability that a pulse of a fruit pulse pair falls into the narrow (4-μsec) gate is

$$4 \times 10^{-6} \times 2800 = 0.0112. \qquad (19)$$

2. The probability that fruit will arrest the narrow gate sweep and pass the narrow gate confirmation test (described in connection with Eq. 10) is

$$0.0112 \times (0.0112)^2 = 1.405 \times 10^{-6}. \qquad (20)$$

3. The number of narrow gate steps within one sweep through the wide gate is

$$\frac{20 \ \mu\text{sec}}{0.8 \ \mu\text{sec}} = 25 \text{ steps}, \qquad (21)$$

and the probability that the narrow gate locks up to fruit in one sweep through the wide gate is

$$1 - \left(1 - 1.405 \times 10^{-6}\right)^{25} = 3.5 \times 10^{-5}. \tag{22}$$

Up to 65 sweeps (see Eq. 14) might be allowed in order to insure a high probability of signal acquisition. Thus, the probability that the narrow gate locks up on fruit during this time is

$$1 - \left(1 - 3.5 \times 10^{-5}\right)^{65} = 2.28 \times 10^{-3}, \tag{23}$$

which, when multiplied by Eq. 18, gives $1.5 \times 10^{-4}$ for the probability that both gates lock up on fruit, given no signal lockup by the wide gate. The total time elapsed during this period is one wide gate sweep, *i.e.*, 7.2 sec plus 65 narrow gate sweeps, or 65 x 0.3 sec = 19.5 sec, a total of 26.7 sec. During this interval, the CASTRS could have been acquired through the following events:

1. One wide gate sweep followed by 65 narrow gate sweeps (if aircraft motion were neglected) with the probability (using Eqs. 7 and 10)

$$0.585\left[1 - (1 - 0.343)^{65}\right] = 0.585.$$

2. Two wide gate sweeps followed by 41 narrow gate sweeps with the probability (again neglecting aircraft motion)

$$0.585(1 - 0.585)\left[1 - (1 - 0.343)^{41}\right] = 0.243.$$

3. Three wide gate sweeps followed by 17 narrow gate sweeps

$$0.585(1 - 0.585)^2 \left[1 - (1 - 0.343)^{17}\right] = 0.101.$$

Thus, the overall CASTRS acquisition probability would be less (because aircraft motion was neglected) than the sum of the

above, *i.e.*, 0.93; while the fruit lockon probability will be greater than $1.5 \times 10^{-4}$ (computed below Eq. 23) because this estimate does not include all of the fruit lockon event possibilities within a 26.7-sec interval. Such a performance should be regarded as unsatisfactory from the standpoint of a conservative design approach.

If, on the other hand, CASTRS transmissions were given priority over DME replies, then, for all practical purposes, acquisition would occur in one sweep of the wide gate followed by one sweep of the narrow gate. The probability of a fruit lockup in this time is just the product of Eqs. 18 and 20, *i.e.*, $10^{-7}$.

In order to estimate the CASTRS load on the DME ground transponder, we note that:

1. The CASTRS consists of a component with 83 pulse pairs per second plus two additional pulse pairs every six seconds (see Chapter III), and
2. The DME transponder load limit is rated as 2800 pulse pairs per second, corresponding to 100 interrogating aircraft.

Thus, if CASTRS is given priority, *i.e.*, if all CASTRS pulse pairs are transmitted by the transponder, then the DME capacity is reduced by

$$\frac{83}{2800} \times 100\% = 3\%,$$

or three aircraft out of 100. If only 70 percent of the CASTRS pulse pairs are transmitted (for equal priority with DME replies), then the expected capacity penalty is reduced to 2.1 aircraft instead of 3 aircraft. Thus, the reduced capacity penalty is too small to justify the adverse impact on CASTRS acquisition performance (as calculated in the earlier paragraphs).

Conclusion: The transmission of the CAS time reference pulse pairs should receive priority over DME replies. In this case, the transponder capacity available for DME service will be reduced by about 3 percent.

## VI. UPDATING OF THE AIRBORNE CAS CLOCK

The time of arrival of the CASTRS pulse pair at the airborne receiver depends on the CASTRS transmission time and on the range to the ground station. The difference between the minimum and maximum range (≈120 nmi for class H facilities) corresponds to a time span of 120 nmi x 6.18 μsec/nmi = 741.6 μsec which is too long to be accommodated within the same slot as the reception and transmission of the CAS signal, particularly when the more accurate altitude encoding scale (see Eq. 6a) is to be employed. Consequently, a CAS slot will be preempted for each clock update. Thus, if an update were attempted at each opportunity (≈ 83 times per second), then

$$\frac{3 \text{ sec} \times 83 \text{ sec}^{-1}}{2000} \times 100\% = 12.5\% \qquad (24)$$

of the 2000 CAS slots will be blocked. Furthermore, the same set of slots will be affected at all times. Whether or not an update is needed at every opportunity depends on the clock accuracy requirements and on the implementation of the synchronization maintenance circuitry.

The synchronization update sequence is shown in Fig. 5. At the time $t_1$, the airborne unit transmits the conventional DME interrogation which is received on the ground at time $t_2$. After a fixed and accurately calibrated delay, the ground station transmits the DME reply at time $t_3$. At $t_4$ the reply is received in the air. In addition, at $t_7$, the airborne unit receives the CASTRS pulse pair which was transmitted from the ground at $t_5$. Thus, the airborne unit estimates its clock lag (negative lag being lead) from

$$\text{clock lag} = \frac{1}{2}[(t_4-t_1) - (t_3-t_2)] - (t_7-t_6). \tag{25}$$

An error budget for the clock lag estimation accuracy would include contributions from (1) errors in $t_1$ (see Fig. 5) due to DME transmitter jitter; (2) errors in $t_2$ from time-of-arrival measurement errors on the ground; (3) errors in $(t_3-t_2)$ due to the difference between the presumed beacon delay and the actual delay plus transmitter jitter; (4) errors in $t_4$ due to time-of-arrival measurement errors in the airborne unit; (5) errors in $t_5$ due to ground station transmitter jitter; (6) errors in $t_7$ due to time-of-arrival measurement errors in the airborne unit.

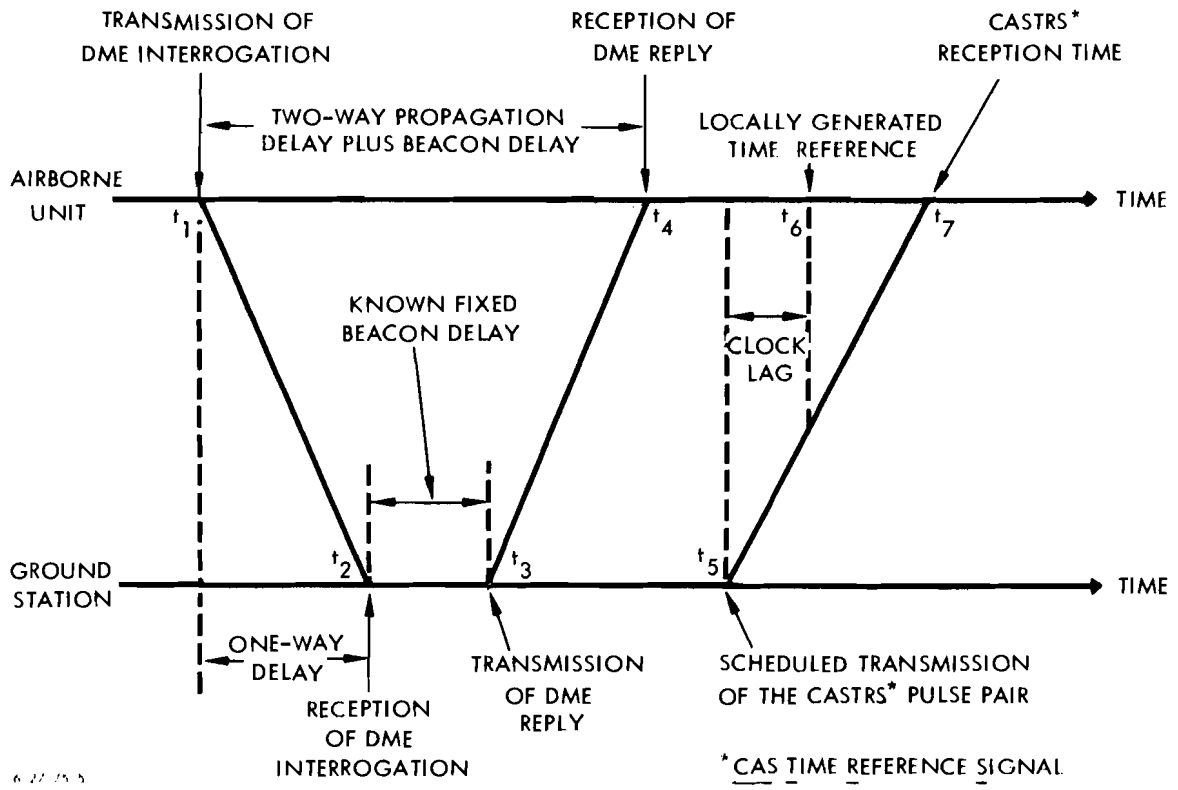


FIGURE 5. Synchronization Sequence

A single lag (or lead) estimate is based on a DME measurement coupled with a time-of-arrival measurement of the CASTRS pulse pair. The CAS/DME concept, envisions that the DME measurements will be made at an average rate of 21 per second (corresponding to a 30 $sec^{-1}$ interrogation rate and a 70 percent reply efficiency) so that the mean time elapsed between a DME measurement and the time-of-arrival of the CASTRS pulse pair is (1/21) = 48 msec; the change in aircraft-to-station range in this time interval is negligible. Pairing of a DME measurement with a CASTRS time-of-arrival measurement has other highly desirable benefits: error components on the uplink (station-to-aircraft) are canceled and errors due to separate filtering of DME replies are eliminated.

The contribution of noise jitter to TOA (time-of-arrival) measurements is estimated from Eq. 5 with

$$SNR = \begin{cases} \dfrac{PG/L_1}{4\pi R^2 \eta} & \text{for the downlink} \\[2ex] \dfrac{SG\lambda^2}{4\pi L_1 N} & \text{for the uplink} \end{cases} , \qquad (26)$$

where P is the airborne transmitter power (see Table 3); G is the airborne antenna gain (2 dB nominal); $L_1$ is the transmitter connector loss (one-half the dB values shown in Table 3); R is the maximum range, *i.e.*, 120 nmi; $\eta$ is the average noise power per unit area as referenced to a plane (perpendicular to the aircraft-to-station line of sight) through the ground-based antenna; the value of $\eta$ is assumed to be 6 dB below the specified sensitivity of -101 dB relative to 1 $W/m^2$ (Ref. 5, p. 23, paragraph V-2.2.1); S is the signal power density ($W/m^2$) received at the aircraft antenna at maximum range; the value of S is specified as -86 dB relative to 1 $W/m^2$ (Ref. 5, p. 24, paragraph

V-3-2); $\lambda$ is the wavelength, assumed to be 0.9374 feet (0.2857 meters) for consistency with Table 3; and where N is the receiver noise power (9 dB below the sensitivities shown in Table 3). The results are shown in Table 9, together with TOA accuracies as computed from Eq. 5.

TABLE 9. UPLINK AND DOWNLINK MEASUREMENT ACCURACIES PER PULSE

| System Parameters | Downlink from | | Uplink to | |
|---|---|---|---|---|
| | Airliner | GA | Airliner | GA |
| SNR at maximum range, dB | 13.6 | 7.6 | 18.6 | 9.6 |
| One-sigma TOA error,* μsec | 0.369 | 0.739 | 0.332 | 0.937 |

*Equation 5 is used here with $T_r$ = 2.5 μsec for downlink measurements and $t_r$ = 4.0 μsec for uplink: the ground station has enough bandwidth to pass the pulse without distortion while the airborne receiver is limited to 250 kHz.

Reference to Fig. 5 and Eq. 25 shows that the lag/lead estimation error is the root sum square of three TOA measurement errors:

1. Downlink DME interrogations
2. Uplink DME replies
3. Uplink CASTRS pulse

Thus we obtain:

$$\text{one-sigma lag/lead estimation errors} = \begin{cases} 0.597 \ \mu\text{sec for airliners} \\ 1.52 \ \mu\text{sec for GA} \end{cases} \tag{27}$$

which applies to the maximum range, 120 nmi, and which scales in proportion to range.*

The clock synchronization accuracy will depend on the processing that is applied to the lag/lead measurements. In one

*The error is inversely proportional to the square root of the SNR (see Eq. 4), while the SNR is inversely proportional to the square of range.

approach, based on the first order control loop, clock oscillator corrections would be proportional and opposite in sign to the lag/lead estimate. The resulting synchronization error is evaluated in Appendix B and plotted in Fig. 6 for a 48 msec update interval. Figure 6 shows five plots as a function of the loop settling time: curves A, B, C, and D give the one-sigma synchronization error due to the lag/lead estimation errors; curve E shows the contribution from clock drift of ±5 parts per $10^9$. The overall rms error is the root sum square of the clock-drift-induced error and the measurement error contribution. It is clear from the figure that an appropriate choice of loop time constant, and this is controlled by selecting loop gain, will minimize the overall rms error. For example, by differentiating the appropriate relations in Appendix B, it can be shown that the RSS error of curves A and E is minimized for a loop settling time of 10 sec. The occurrence of the minimum is characteristic of tracking loop behavior: sluggish loops exhibit good noise performance by sacrificing dynamic tracking performance and vice versa. The specified value shown in Fig. 6 was obtained from the ANTC-117 specifications (Ref. 2, p. 110A, paragraph 2.8)

> Airborne equipment synchronization shall be accomplished with an accuracy of ±0.25 microseconds with respect to the synchronization donor with a probability of 0.995.

For limited equipments, the accuracy requirement is relaxed to ±0.5 μsec (Ref. 2, p. 129, paragraph 4.8). These are interpreted as three-sigma accuracy specifications for airliner (or equivalent) and general aviation equipments. The corresponding one-sigma values are shown by the dotted horizontal lines in Fig. 6. Thus, a loop settling time of 2.5 sec is enough to meet the synchronization accuracy specifications. Unfortunately, the contribution to range-rate error is excessive when a 2.5-sec settling time is used (this will become apparent from the discussion in the subsequent section and from the analysis in

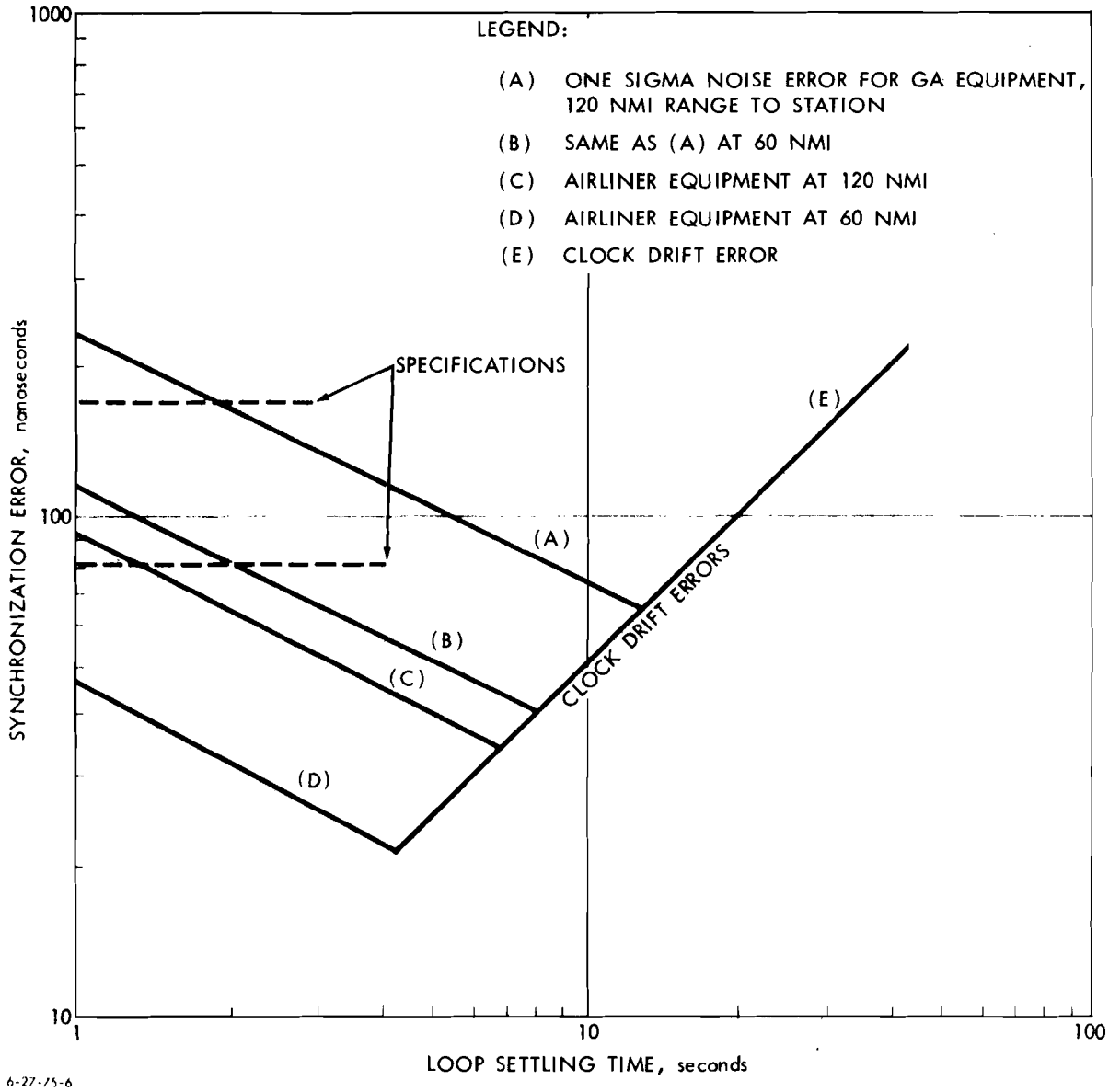


FIGURE 6. Synchronization Error as a Function of Loop Settling Time, for a 48-msec Update Interval

the latter part of Appendix B). For this reason, a 10-sec settling time is selected. The resultant loop gain* is $5 \times 10^{-3}$ which when multiplied by Eq. 27 gives 3 nsec and 8 nsec for the one-sigma value clock corrections. These values are too small for convenient implementation in the timing chain. One solution to the problem is to smooth/average the individual lag/lead measurements prior to clock time corrections. For example, assume that 16 lag/lead measurements are averaged so that:

1. The one-sigma lag/lead error estimate in Eq. 27 is reduced by a factor of 4.
2. The interval between clock corrections is increased by a factor of 16; from 48 msec to 0.768 sec
3. The loop gain is increased by a factor of 16.
4. The loop settling time, which for small loop gains is the ratio of sampling time (equal to time between clock corrections) to loop gain (see Eq. B-4 of Appendix B), remains unchanged.
5. The result of (1) and (2) is that the one-sigma value of clock corrections is increased by a factor of 4; *i.e.*, the 3- and 8-nsec figures obtained earlier are increased, respectively, to 12 and 24.

To simplify implementation, it is desirable to quantize oscillator corrections into 20-nsec steps. This can be implemented by adding or subtracting a pulse in the countdown chain starting at the 50-MHz voltage-controlled oscillator (VCO) proposed for DME/CAS. Such a quantization level is not incompatible with the cited oscillator correction requirements.

The main point to be made here is that lag/lead measurements made** once every 48 msec, together with clock corrections

---

*This is computed from Eq. B-4 in Appendix B for settling time = 10 sec, and update interval = 48 msec.

**Each update preempts one CAS slot and involves a frequency switch from the CAS frequency to the DME uplink frequency where the CASTRS is received.

applied once every 0.768 sec, should provide adequate accuracy for a properly designed synchronization loop. The reduction in update rates from $(12\ \text{msec})^{-1}$ to $(48\ \text{msec})^{-1}$ is reflected as a four-fold reduction in the capacity penalty computed in Eq. 24. It should be emphasized, however, that the reduction applies only to the synchronization maintenance phase; during acquisition, the higher rate is still needed (see Chapter V).

> Conclusion: In the absence of bias errors, a properly designed synchronization loop can meet the synchronization accuracy requirements, with lag/lead measurements every 48 msec. Under such conditions, the synchronization update function will preempt 3 percent of the available CAS slots.

The synchronization maintenance method proposed initially by Sierra (Ref. 1, pp. 3-20, last paragraph, Section III-4-4) could function only in a very high signal-to-noise ratio environment. The original approach should be redesigned to approach the potential performance demonstrated in the preceding analysis.

As far as bias errors are concerned, inspection of Fig. 5 and Eq. 25 reveals that the two uplink biases (*i.e.*, DME replies and CASTRS pulses) cancel. Unfortunately, the downlink bias in TOA measurements, (on the ground) of DME interrogations, will appear as a bias in the airborne clock and may, ultimately, be reflected as a bias in the one-way range measurement of the CAS. Clearly, if two encountering aircraft experience the same bias, no problem exists. However, in an encounter between two aircraft, the ERP (effective radiated power) difference between their downlink interrogations could easily exceed 10 dB. If the encounter takes place near the edge of the coverage volume of the ground station, the difference in the downlink bias errors between the interrogators will amount to one-half the full pulse rise of 2.5 μsec*, i.e., 1.25 μsec.

*This is the difference between the times that the leading edges of a strong and a weak pulse cross the threshold at the DME transponder.

Bias differences between aircraft well within the coverage range of the ground transponder are reduced to 0.6 μsec when both interrogating signals exceed the DME reply threshold by more than 6 dB. In either case, the contribution to the synchronization error exceeds the specifications (±0.25 μsec and ±0.5 μsec, depending on equipment type).

An additional source of potential range bias errors is the reply delay accuracy of the DME transponder. The nominal value of the delay between interrogation reception and reply is 50 μsec, which is compensated by the airborne receiver (see discussion in connection with Fig. 5). The present standard (Ref. 4, p. 35, paragraph 3.5.3.5) allows a maximum delay error of ±1 μsec (two-way) which is also reflected in the requirements (Ref. 5, p. 32, paragraph 5.4.1b) for continuous monitoring of the ground facility. Thus, the combination of the two error sources, one from interrogator amplitude disparity and one from transponder delay errors, may exceed the range error allowance (±0.5 μsec) of ANTC-117.

> Conclusion: DME ground facility standards on range accuracy will have to be upgraded to meet the CAS specifications of ANTC-117.

It is conceivable that many stations provide better accuracies than are called for in the ICAO/FAA specifications. The available measurements (Ref. 6) show a bias error of 0.08 nmi (or 0.5 μsec of one-way delay). However, this result includes aggregated data from short- and long-range measurements, and the transponder delay monitoring and calibration procedures were not identified. Still, the experimental results suggest that sufficient accuracy for CAS operation could be achieved.

## VII. RANGE RATE MEASUREMENT ERRORS

The DME/CAS in its CAS mode extracts range rate from one-way range difference measurements. The required accuracies are specified in ANTC-117 (Ref. 2, p. 110, paragraph 2.7.1.1):

> The overall receiver system shall evaluate the range vs range rate status with the following accuracy. For a specific system and set of test readings at the same range, taken under essentially the same environmental conditions, the alarm outputs shall occur as follows:
>
> The mean of the set of readings shall not exceed the greater of (a) 28 knots or (b) 7% of the difference between the nominal threat line R value and $\dot{R}_o$ (see Figure 7). The standard deviation of the set of alarm points shall not exceed the greater of 11 knots or 1.5% of the nominal range rate.

If B and $\sigma$ denote, respectively, the bias error and the one-sigma error of the range rate estimate, then the specifications can be restated as

$$B = M[28;\ 0.07(\dot{R}-\dot{R}_o)] \tag{28}$$

and

$$\sigma = M[11;\ 0.015\ \dot{R}]\ , \tag{29}$$

where M[a;b] denotes the larger, in magnitude, of the two quantities a and b. The relationship between ranges and range rates along the threat line (see Fig. 7) are:

$$R = R_o + \tau\dot{R} \tag{30}$$

and

$$\dot{R}_o = -R_o/\tau \ , \tag{31}$$

which, when used in Eqs. 28 and 29, lead to

$$B = M[28;\ 0.07R/\tau] \tag{32}$$

and

$$\sigma = M[11;\ 0.015(R-R_o)/\tau] \ . \tag{33}$$

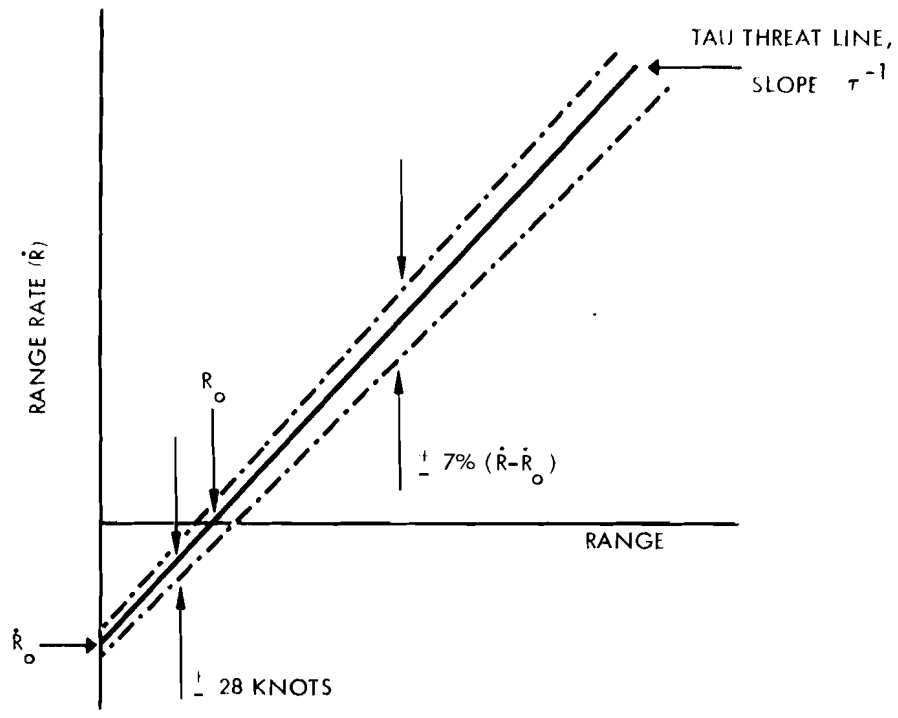


FIGURE 7. Mean Accuracy Requirements (Extracted from Ref. 2, p. 110B)

The appropriate numerical parameters (see Ref. 2, p. 71) are:

$$\tau = \begin{cases} 25 \text{ sec in Tau zone 1} \\ 40 \text{ sec in Tau zone 2} \end{cases} \tag{34}$$

$$R_o = \begin{cases} 0.25 \text{ nmi in Tau zone 1} \\ 1.8 \text{ nmi in Tau zone 2} \end{cases} \tag{35}$$

so that Eqs. 32 and 33 become (after converting Eq. 34 into hours)

$$B = \begin{cases} M[28;\ 10.08R] \text{ in Tau zone 1} \\ M[28;\ 6.3R] \text{ in Tau zone 2} \end{cases} \tag{36}$$

$$\sigma = \begin{cases} M[11;\ 2.16(R - 0.25)] \text{ for Tau zone 1} \\ M[11;\ 1.35(R - 1.8)] \text{ for Tau zone 2} \end{cases} \tag{37}$$

The bias error specification represents an allowance for an error contribution from the FM discriminator characteristic that was originally envisioned for the ATA/CAS doppler (range-rate) measurements. In the absence of range rate bias errors, the one-sigma error allowance might be relaxed to a value given by

$$\sigma_r = \sqrt{\sigma^2 + (B^2/3)} \quad , \tag{38}$$

where $B^2/3$ is the mean square value of a random error uniformly distributed between $-B$ and $+B$.

The RSS contribution, $\sigma_v$, to range rate error from noise jitter in TOA measurements is estimated from*

$$\sigma_v = \frac{\sigma_r \cdot \sqrt{2}}{T_m} \quad , \tag{39}$$

where $\sigma_r$ is the one-sigma range error, obtainable from row a of Table 8 (after multiplication by 0.984 ft/nsec); the factor $\sqrt{2}$ accounts for the contribution from the two range measurements needed to estimate range rate; and $T_m$ is the time between the two range measurements. The results, for $T_m$ = 3 sec, are (with range R in nautical miles):

$$\sigma_v \text{ (knots)} = \begin{cases} 1.79 \text{ R for airliner to airliner} \\ 4.49 \text{ R for airliner to GA} \\ 3.18 \text{ R for GA to airliner} \\ 7.99 \text{ R for GA to GA} \end{cases} \quad , \tag{40}$$

which is plotted in Figs. 8 through 15, together with Eqs. 36, 37, and 38. When the separation is increased to 6 sec, the error is reduced by a factor of two.

Another contributor to range rate estimation error is the clock synchronization error. This component was analyzed in Appendix B and the results are summarized in Table 10.

The resultant range rate error performance is scored in Table 11 in terms of whether or not the error is "within" or "outside" the relaxed specifications (as defined in Eq. 38 and and the associated discussion). Except for the borderline case,

*This expression does not account for the correlation between range and range rate (from range differences) measurement errors. In the worst case, for $\tau$ = 25 sec and $T_m$ = 6 sec, the result is a 12.6 percent increase relative to the error given by Eq. 39 (see Appendix G).

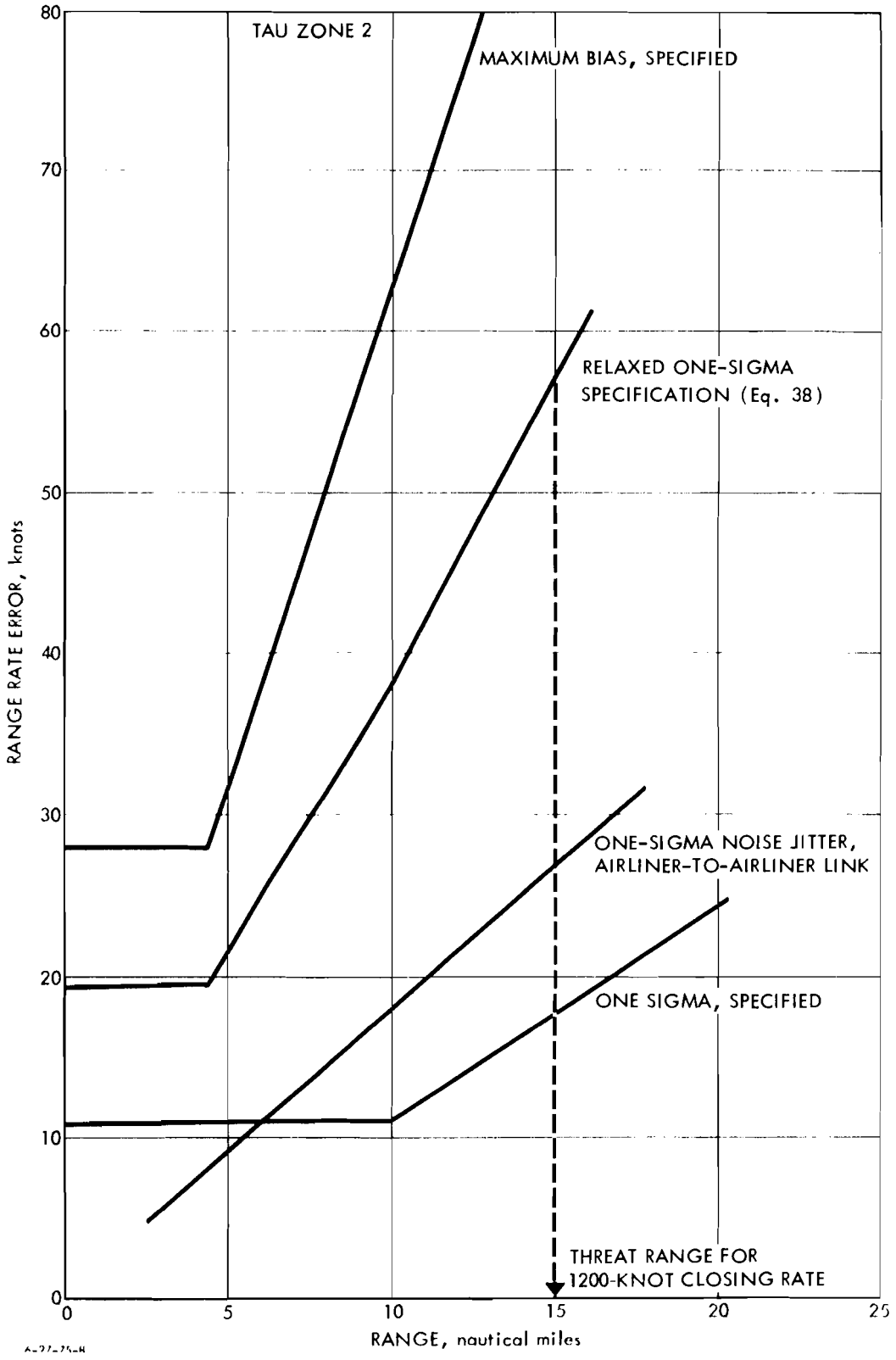


FIGURE 8. Noise Jitter Contribution: Airliner-to-Airliner Link, Tau Zone 2

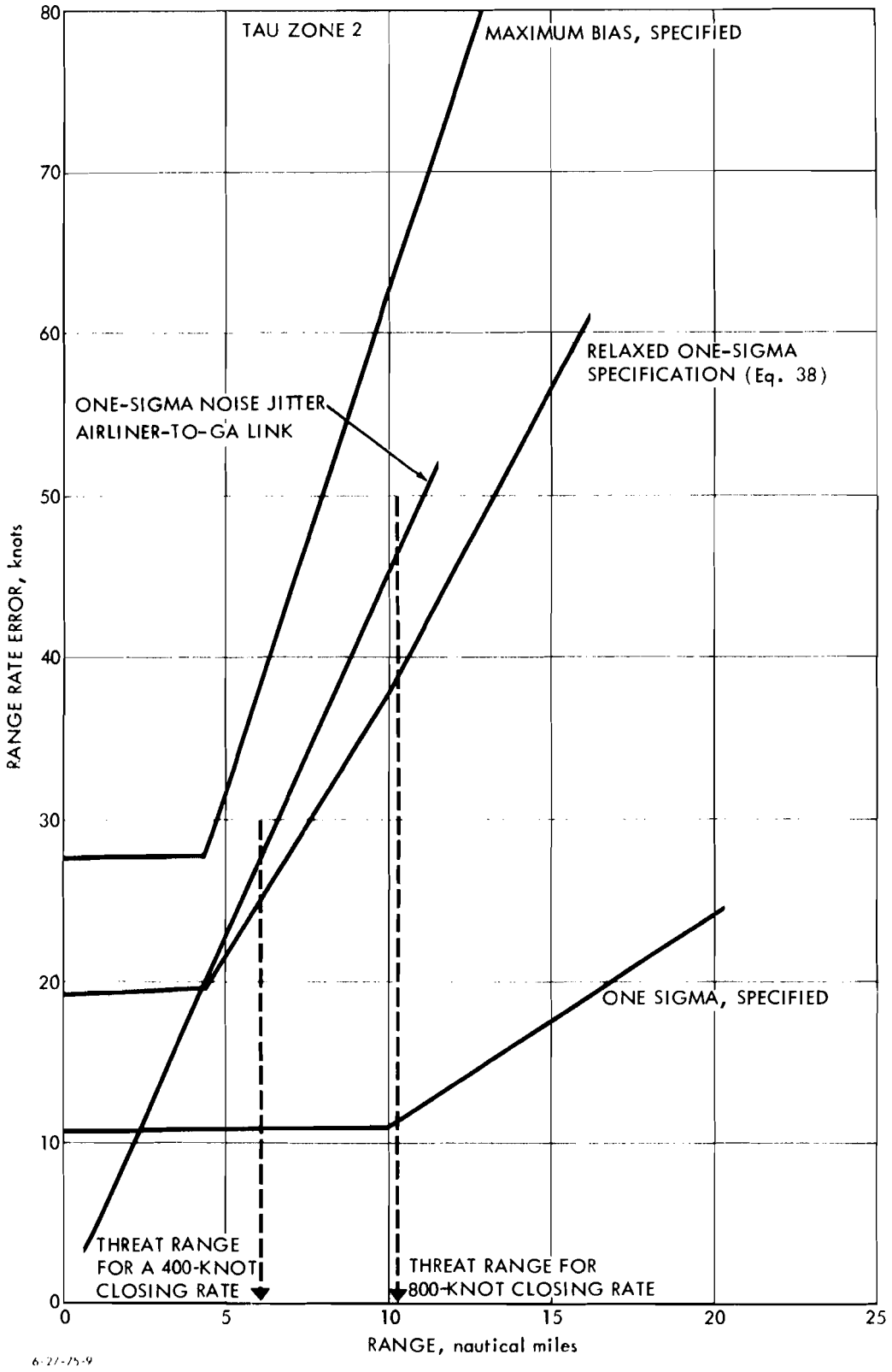


FIGURE 9. Noise Jitter Contribution: Airliner-to-GA Link, Tau Zone 2

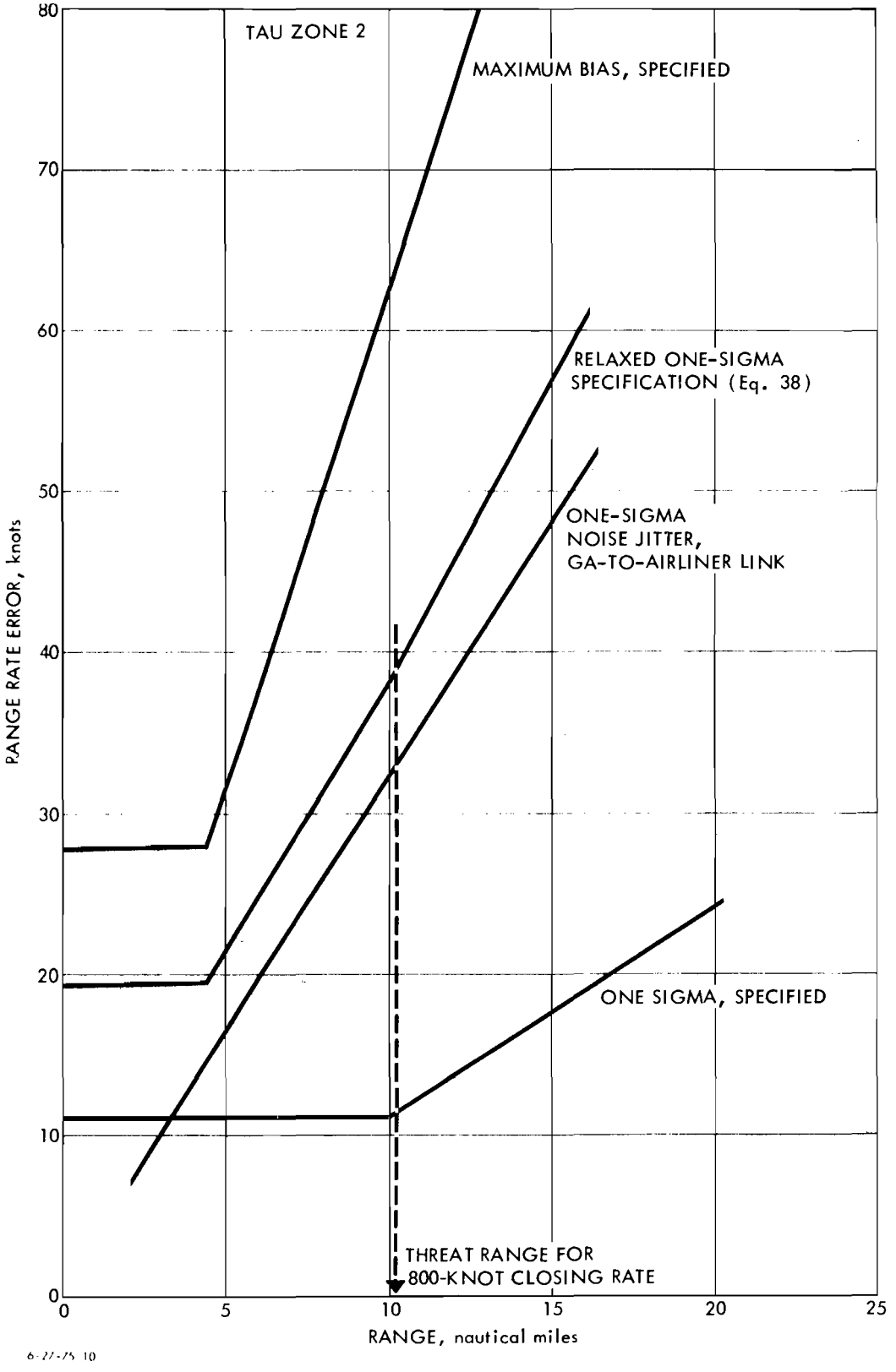


FIGURE 10. Noise Jitter Contribution: GA-to-Airliner Link, Tau Zone 2

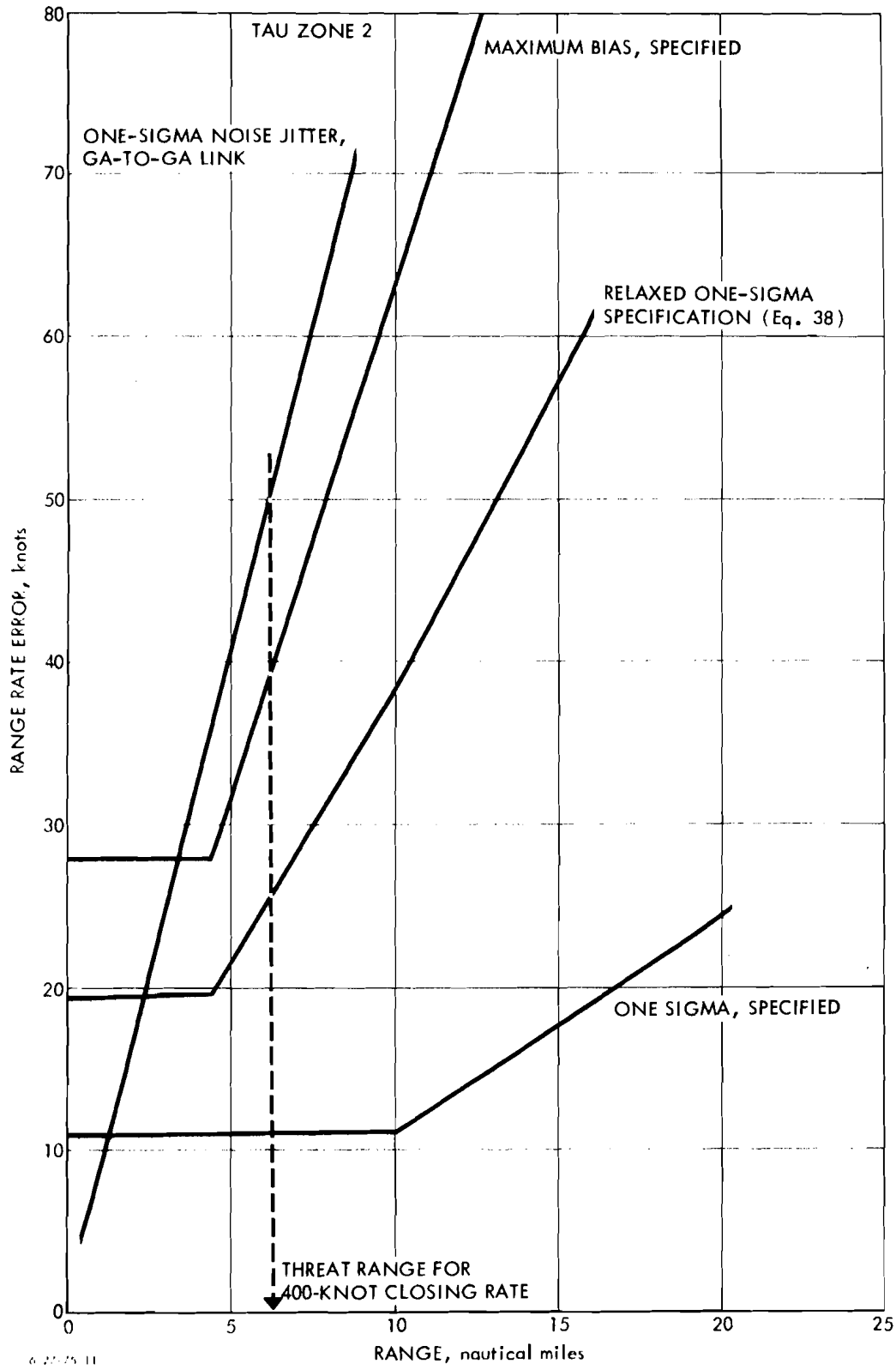


FIGURE 11. Noise Jitter Contribution: GA-to-GA Link, Tau Zone 2

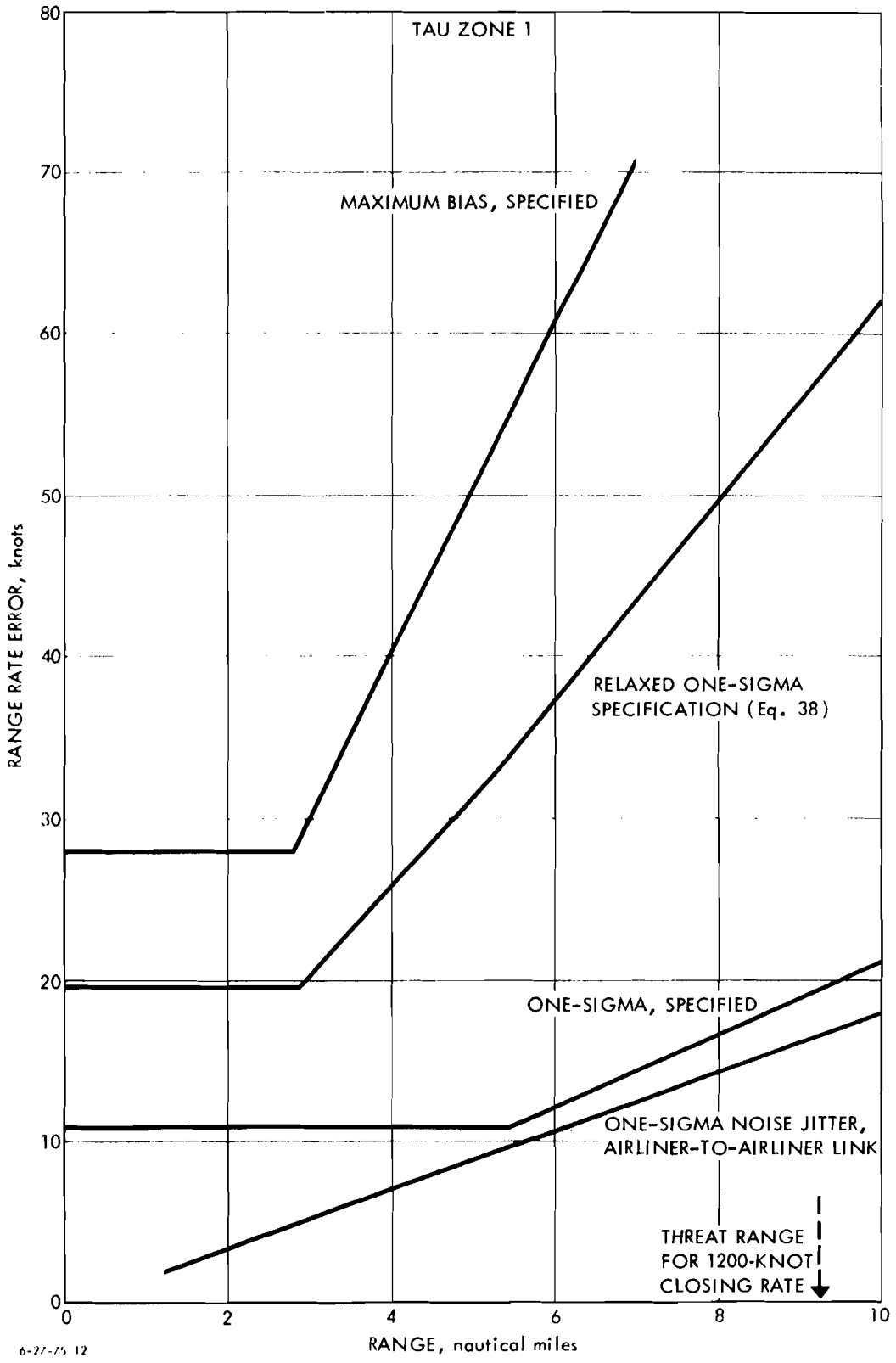


FIGURE 12. Noise Jitter Contribution: Airliner-to-Airliner Link, Tau Zone 1

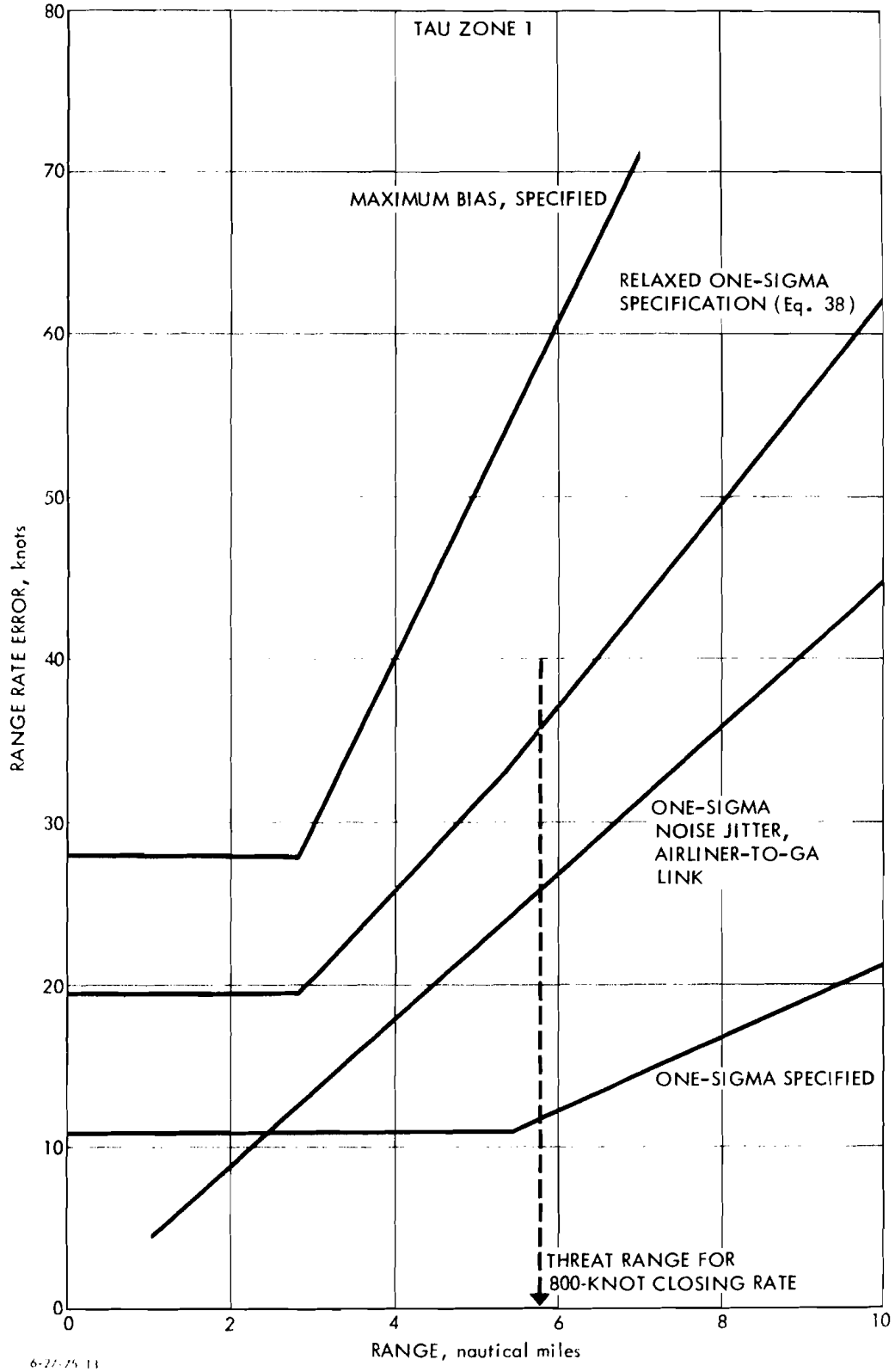


FIGURE 13. Noise Jitter Contribution: Airliner-to-GA Link, Tau Zone 1

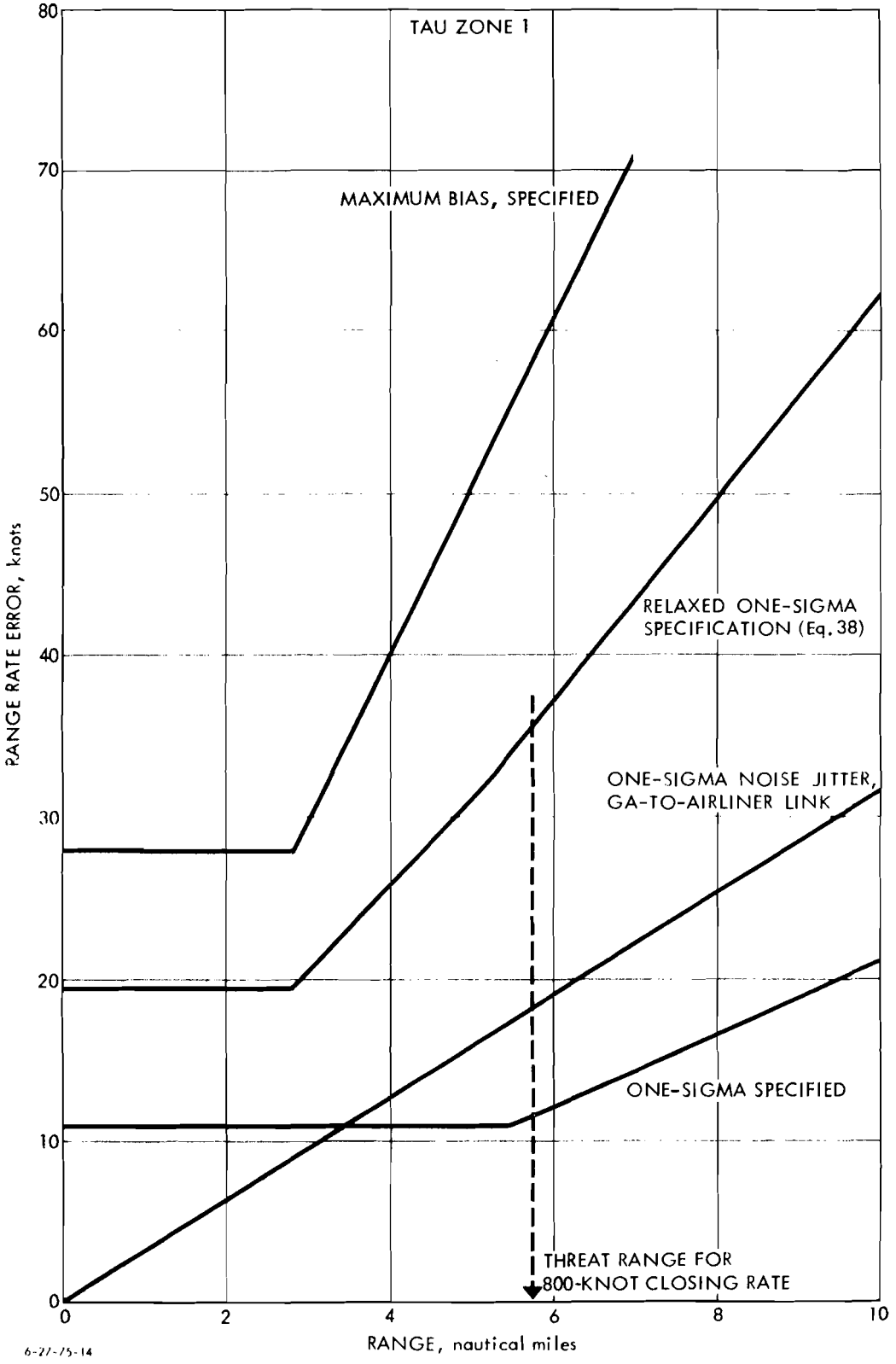


FIGURE 14. Noise Jitter Contribution: GA-to-Airliner Link, Tau Zone 1

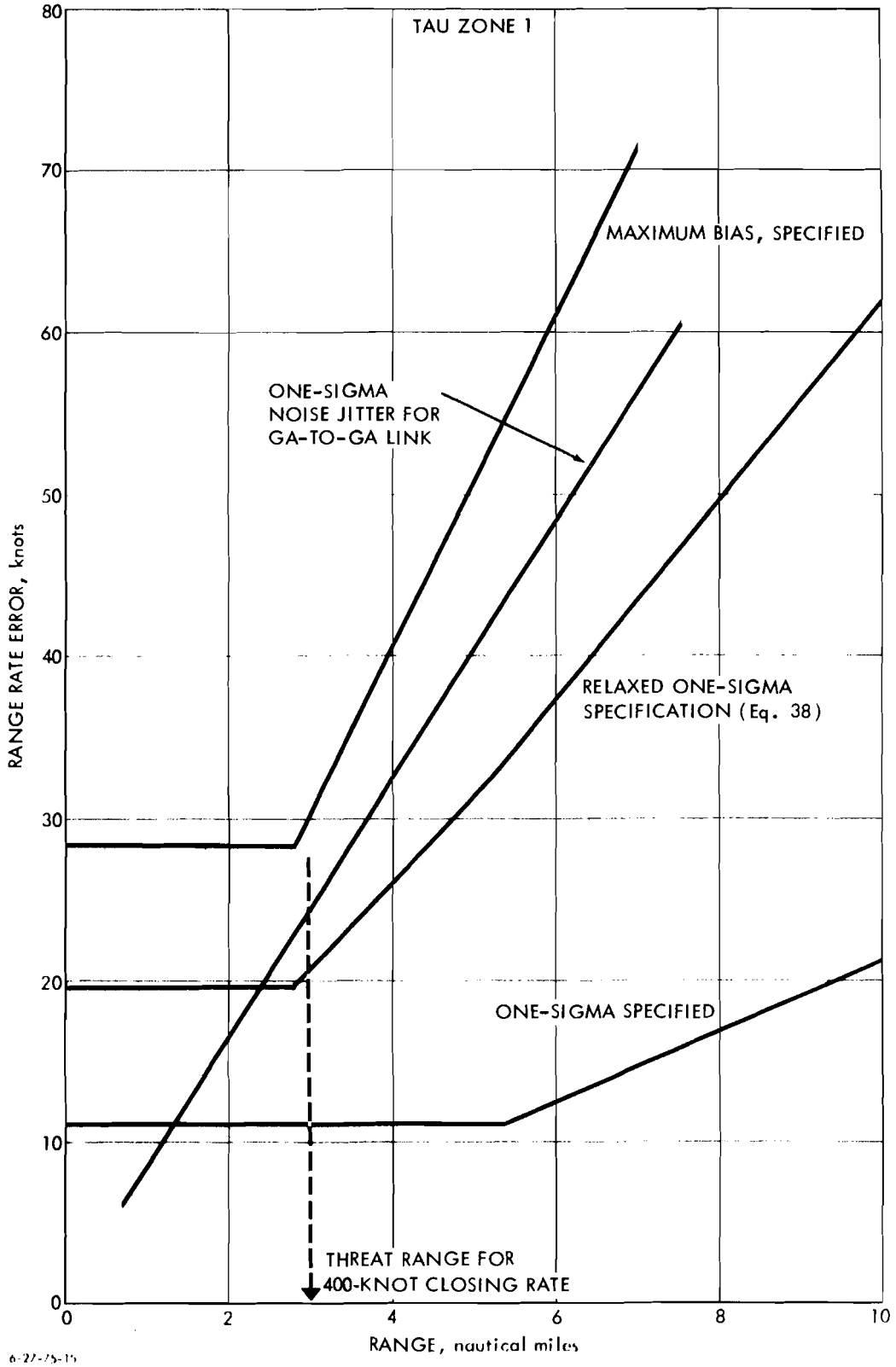


FIGURE 15. Noise Jitter Contribution: GA-to-GA Link, Tau Zone 1

TABLE 10. ONE-SIGMA CONTRIBUTION OF THE SYNCHRONIZATION ERROR TO THE RANGE RATE ESTIMATION ERROR

| Encounters | Range to DME Transponders (nmi) | Time Between Range Measurements (sec) | Error Contribution (knots) |
|---|---|---|---|
| Airliner with Airliner | 120 | 3 | 5.8 |
| | 120 | 6 | 3.8 |
| | 60 | 3 | 2.9 |
| | 60 | 6 | 1.9 |
| Airliner with GA | 120 | 3 | 11.2 |
| | 120 | 6 | 7.4 |
| | 60 | 3 | 5.6 |
| | 60 | 6 | 3.7 |
| GA with GA | 120 | 3 | 14.7 |
| | 120 | 6 | 9.7 |
| | 60 | 3 | 7.4 |
| | 60 | 6 | 4.9 |

TABLE 11. SCORE OF RANGE RATE ERROR PERFORMANCE (NO MULTIPATH)

| Encounters | Time Between Range Measurements (sec) | Relation to Relaxed (1) Overall Error Specification | |
|---|---|---|---|
| | | Tau Zone 1 | Tau Zone 2 |
| Airliner-to-Airliner | 3 | Within | Within |
| | 6 | Within | Within |
| Airliner-to-GA | 3 | Within | Outside |
| | 6 | Within | Within |
| GA-to-Airliner | 3 | Within | Within |
| | 6 | Within | Within |
| GA-to-GA | 3 | Outside | Outside |
| | 6 | Within | Borderline (2) |

(1) See Eq. 38 and associated discussion.

(2) Equal to the specification when the DME transponder facility (Class H) is within 60 nmi; 10 percent above specification when the facility is at 120 nmi.

the score is not affected by the contribution of the synchronization error components (shown in Table 10); in other words, the synchronization error contribution is negligible for the synchronization loop design described in Chapter VI.

> Conclusion (without multipath): When the CAS range data interval is increased from 3 sec to 6 sec, all CAS equipment pair categories can meet the relaxed range rate accuracy specification in both Tau zones. However, the 3-sec epoch specified by ANTC-117 (Ref. 2) implies a data interval requirement of 3 sec. In this case, the bulk of the aircraft population, 90 percent of which is in the GA category, will not meet the relaxed accuracy specification (see Figs. 11 and 15). This applies to GA CAS pairs in both Tau zones as well as to GA CAS units assessing airliner threats in Tau zone 2.

The impact of multipath is examined in Appendix C. The resultant range-rate error is a function of the signal-to-multipath (SMR) ratio, and multipath delay; while the latter is a function of altitude and range. A maximum, one-sigma error is attained when the multipath delay is approximately 2 μsec (equal to one-half the pulse rise time). This maximum is plotted in Fig. 16 as a function of the SMR. Altitudes and ranges producing the maximum error are plotted in Fig. 17.

For shorter delays, the multipath signal tends to merge into the direct signal and errors are reduced. At longer delays, the main multipath return occurs after the signal peak, the impact on the peak detector is reduced, and hence, the error is also reduced.

At an SMR of 10 dB (specified in Ref. 2, p. 107, paragraph 2.5.1) and with a 6-sec time base, the one-sigma error can be as high as 61 knots (see Fig. 16) which exceeds the specifications (see Figs. 11 and 15) cited earlier. However, preliminary

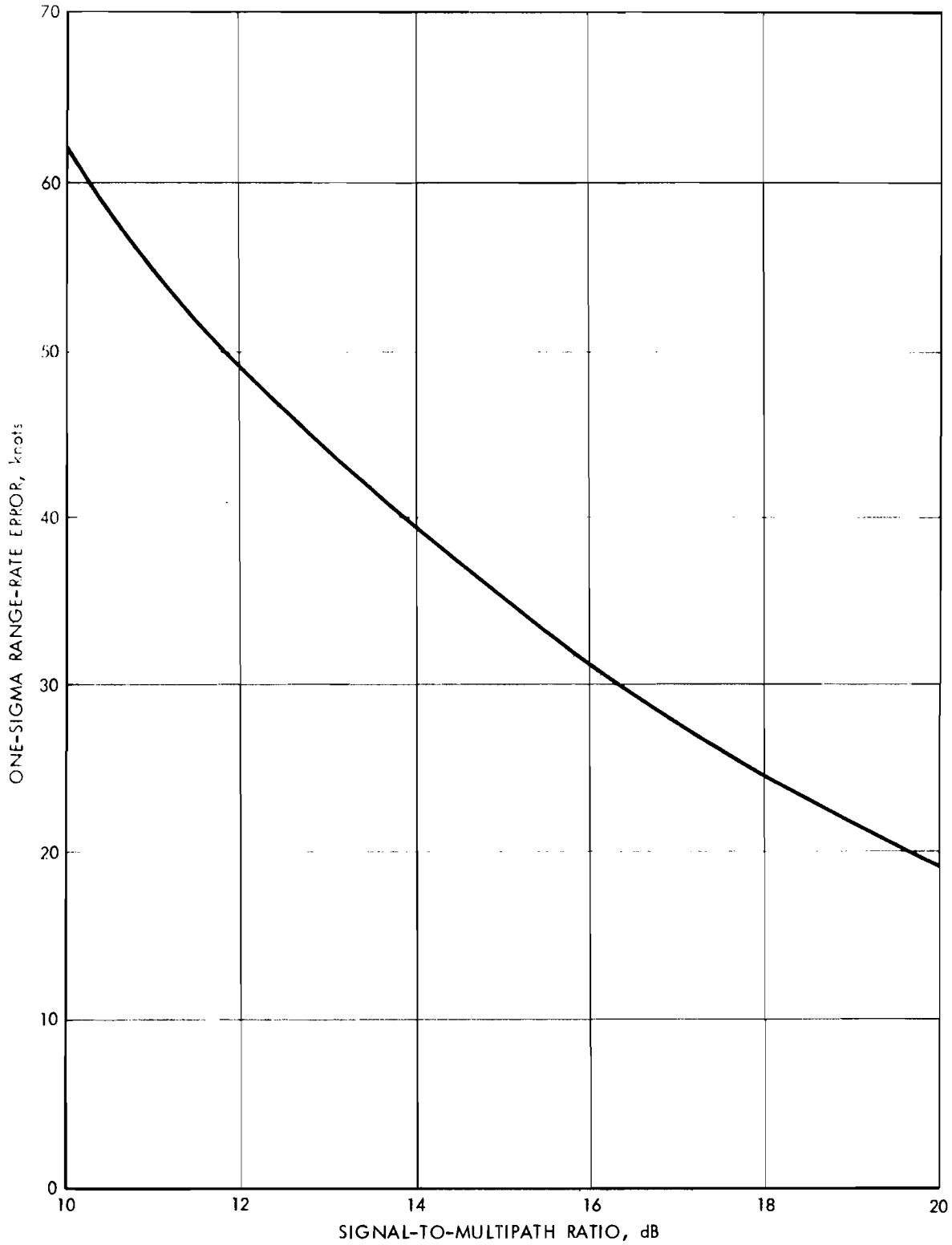


10 29-75-30

FIGURE 16. Maximum Range-Rate Error for 6-sec Data (Ranges and Altitudes Producing Maximum Error are Shown in Fig. 17)

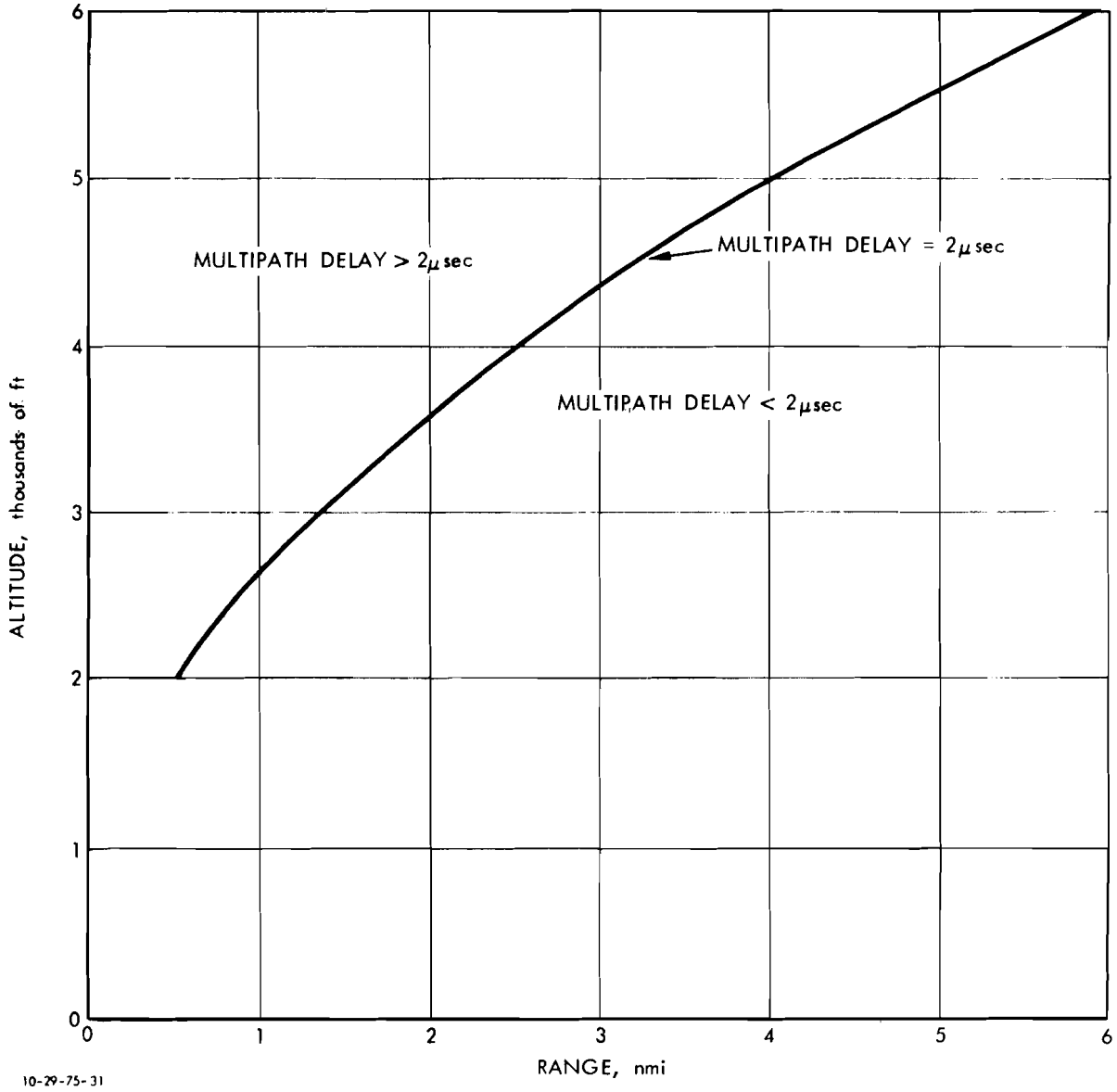


FIGURE 17. Altitude and Range Producing the Maximum Range-Rate Error Shown in Fig. 16

calculations for the doppler system (which is addressed in the ANTC-117 specifications) indicate that this system would also fail to meet the specified accuracies for the specified multipath conditions.

As was indicated throughout the preceding analyses, the random range rate error problem is alleviated when the time base is increased from 3 sec to 6 sec. However, the consequence of such an increase is a range rate bias error due to a consistent overestimate of the actual range rate (see Appendix H). In other words, the range difference divided by the elapsed time is greater than the magnitude of the time derivative of range. The resultant error* is compared with the specified error in Table 12 below.

TABLE 12. RANGE-RATE BIAS ERRORS (FROM APPENDIX H, EQ. H-9) FOR A 600-KNOT RELATIVE SPEED, A 6-SEC TIME BASE, AND TAU ZONE 1 PARAMETERS

| Range (nmi) | Range-Rate Bias Error (knots) | Allowed* Bias Error (knots) |
|---|---|---|
| 1.0 | 290 | 28 |
| 2.0 | 125 | 28 |
| 3.0 | 55 | 28 |
| 3.4 | 32 | 32 |

*Specified by ANTC-117; see quotation at the beginning of this Chapter (VII).

An alternative method for exhibiting the effect of the bias error is shown in Fig. 18. The ordinate and abscissa represent, respectively, crossrange and downrange relative to the

*A more detailed discussion of this source of error is provided in a companion study dealing with the McDonnell Douglas CAS (Ref. 7).

threat-evaluating aircraft. The curve marked "ANTC-117" represents the specified alarm boundary expressed in crossrange and downrange coordinates which are related to range and range-rate variables through obvious kinematic relations (see Eqs. H-16 and H-17 of Appendix H). The same transformation is applied to the actual alarm boundary which includes the effect of the range bias as given in Appendix H (Eq. H-9).

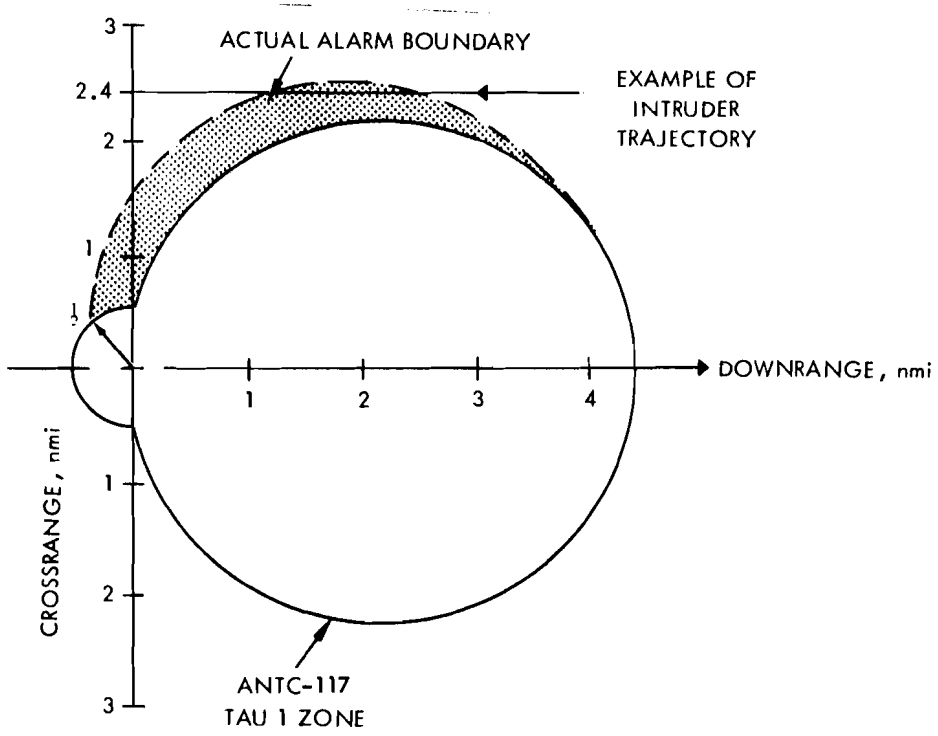


FIGURE 18. Downrange-versus-Crossrange Plot for a Relative Speed of 600 Knots

Two limiting trajectories may be identified; one is tangent to the actual alarm boundary, and the other is tangent to the specified (ANTC-117) boundary. The crossranges for the two tangential trajectories are 2.262 nmi and 2.486 nmi, respectively. False alarms are therefore generated by intruders whose crossranges lie between the two limits (one such intruder is shown in Fig. 18). The percentage difference between these is 10 percent. Thus, for a uniform distribution of crossranges, the overall alarm rate would increase by 10 percent, despite the

fact that the bias error exceeds the ANTC-117 specifications by wide margins (see Table 12).

Repetition of the previous analysis for a relative speed of 180 knots (instead of 600 knots) yields the crossranges for the two tangential trajectories as 0.8068 nmi and 0.8744 nmi. In this case, the alarm rate is increased by 8.4 percent.

> Conclusion: The use of range difference measurements for range-rate estimation introduces bias errors between the actual Tau alarm boundary and the specified boundary. In spite of the fact that the error, at short ranges, exceeds the specified (by ANTC-117) value by wide margins (see Table 12), there is only an 8 percent to 10 percent increase in overall alarm rate.

## REFERENCES


1. SIERRA Research Corporation, Sierra DME Collision Avoidance System, Technical Report TR-1115, December 1973.

2. Air Transport Association of America, Airborne Collision Avoidance System, An Airline Industry Document to provide the Statement of Airline Policy and Requirements and a Technical Description of the System, originally issued June 30, 1967, Revision Nine, July 31, 1970, Revision Ten, May 12, 1971, prepared under the Auspices of the Airline Air Traffic Control Committee CAS Technical Working Group, issued by the Air Navigation/Traffic Control Division, Air Transport Association of America, 1000 Connecticut Avenue, N.W., ANTC Report No. 117, September 20, 1971.

3. J. J. Bagnall, Jr., and I. W. Kay, Review and Analysis of Some Collision Avoidance Algorithms with Particular Reference to ANTC-117, IDA Study S-450, prepared for DOT/FAA, Under Contract No. DOT FA 74WA-3498, June 1975.

4. International Civil Aviation Organization (ICAO), Aeronautical Telecommunications, Annex 10 to the Convention on International Civil Aviation, Second Edition of Vol. 1, April 1968.

5. DOT/FAA, Selection Order: U.S. National Aviation Standard for the VORTAC System, Order No. 1010.55, June 1, 1970.

6. V. J. Luciani, Test and Evaluation of a System for Precise Time-Dissemination Using DME (VORTAC) Synchronization, Final Report, prepared for DOT/FAA, Systems Research and Development Service, August 1973.

7. A. Krinitz, Review and Analysis of the McDonnell Douglas Collision Avoidance System (Phase II), IDA Study S-458, prepared for DOT/FAA, under Contract No. DOT-FA 74WA-3498, October 1975.

# APPENDIX A

## ACCURACY OF LEADING EDGE TIME-OF-ARRIVAL MEASUREMENTS

## APPENDIX A

## ACCURACY OF LEADING EDGE TIME-OF-ARRIVAL MEASUREMENTS

The time, t, at which the signal-plus-noise envelope crosses a threshold H satisfies the equation

$$\sqrt{S^2(t)+2S(t)\ X\cos\phi + X^2} = H \ , \qquad \text{(A-1)}$$

where S(t) is the pulse signal envelope, X is the magnitude of the noise, or interference, envelope and $\phi$ is the phase difference between the signal and noise/interference. Solving for S(t) we get

$$S(t) = \sqrt{H^2 - X^2\sin^2\phi} - X\cos\phi \ , \qquad \text{(A-2)}$$

which is valid only for $X \leq H$ (a complex solution means that the threshold is not crossed). It is assumed that the phase, $\phi$, at the time of threshold crossing, is a random variable uniformly distributed between 0 and $2\pi$. All of the subsequent averages, denoted by a horizontal bar, are averages with respect to $\phi$.

If $\bar{t}$ is the mean value of the threshold crossing time, then, by applying the mean value theorem for derivities, we obtain

$$S(t) - S(\bar{t}) = S'(t_1)(t-\bar{t}) \ , \qquad \text{(A-3)}$$

where $t_1$ is an appropriately chosen point between t and $\bar{t}$ and $S'(t_1)$ is the derivative of S(t) at $t_1$.

Thus,

$$(t-\bar{t})^2 = \left[\frac{S(t)-S(\bar{t})}{S'(t_1)}\right]^2 \tag{A-4}$$

At the point of inflection, $t_i$, on the leading edge of the pulse, we have

$$\left[S'(t_i)\right]^2 \geq \left[S'(t_1)\right]^2 , \tag{A-5}$$

so that Eq. A-4 becomes

$$(t-\bar{t})^2 \geq \left[\frac{S(t)-S(\bar{t})}{S'(t_i)}\right]^2 . \tag{A-6}$$

For any random variable, z, and a parameter, b, we have

$$\overline{(z-b)^2} \geq \overline{(z-\bar{z})^2} . \tag{A-7}$$

This can be proven by squaring, averaging, and differentiating the left-hand side with respect to b, which for $z = S(t)$ and $b = S(\bar{t})$, yields

$$\overline{[S(t)-S(\bar{t})]^2} \geq \overline{[S(t)-\overline{S(t)}]^2} . \tag{A-8}$$

Application to Eq. A-6 leads to

$$\overline{(t-\bar{t})^2} \geq \frac{\overline{[S(t)-S(t)]^2}}{[S'(t_i)]^2} = \frac{\overline{S^2(t)}-\overline{S(t)}^2}{[S'(t_i)]^2} . \tag{A-9}$$

The averages are obtained from Eq. A-2:

$$\overline{S(t)} = \frac{1}{2\pi}\int_0^{2\pi}\sqrt{H^2-X^2\sin^2\phi}\,d\phi - \frac{1}{2\pi}\int_0^{2\pi}X\cos\phi d\phi\ , \qquad \text{(A-10)}$$

where the second integral averages out to zero while the first integral is expressible in terms of the complete elliptic integral* of the second kind:

$$\begin{aligned}\frac{1}{2\pi}\int_0^{2\pi}\sqrt{H^2-X^2\sin^2\phi}\,d\phi &= \frac{H}{2\pi}\cdot 4\int_0^{\pi/2}\sqrt{1-\left(\frac{X}{H}\right)^2\sin^2\phi}\,d\phi \\ &= \frac{H}{2\pi}\cdot 4E\left[\left(\frac{X}{H}\right)^2\right]\end{aligned} \qquad \text{(A-11)}$$

in which E [m] denotes the complete elliptic integral of the second kind, with parameter m, *i.e.*,

$$E(m) = \int_0^{\pi/2}\sqrt{1-m\sin^2\phi}\,d\phi \qquad \text{(A-12)}$$

The other average required in Eq. A-9, $\overline{S^2(t)}$, is obtained from Eq. A-2:

*See, for example "Handbook of Mathematical Functions," U.S. Department of Commerce, National Bureau of Standards, Applied Mathematics Series 55, June 1964, p. 609.

$$\overline{S^2(t)} = \frac{1}{2\pi}\int_0^{2\pi}\left(H^2-X^2\sin^2\phi\right)d\phi$$

$$- \frac{1}{2\pi}\int_0^{2\pi}\sqrt{H^2-X^2\sin^2\phi}\ X\cos\phi d\phi \qquad \text{(A-13)}$$

$$+ \frac{1}{2\pi}\int_0^{2\pi} X^2\cos^2\phi d\phi \ .$$

The integral containing the radical consists of contribution in four regions: (1) 0 to $\pi/2$; (2) $\pi/2$ to $\pi$; (3) $\pi$ to $3\pi/2$, and (4) $3\pi/2$ to $2\pi$. Contributions from region (1) cancel with region (2), while region (3) cancels (4); the net result being zero. Integration of the first and third integrals is obvious so that

$$\overline{S^2(t)} = H^2 \ . \qquad \text{(A-14)}$$

Equations A-11 and A-14 are substituted into Eq. A-9 giving,

$$\overline{(t-t)^2} \geq \frac{1}{\left[S'(t_i)\right]^2}\left[H^2-H^2\left(\frac{2}{\pi}\right)^2 E^2\left(\frac{X^2}{H^2}\right)\right] \qquad \text{(A-15)}$$

or

$$\overline{(t-\bar{t})^2} \geq \frac{X^2}{\left[S'(t_i)\right]^2}\frac{H^2}{X^2}\left[1-\left(\frac{2}{\pi}\right)^2 E^2\left(\frac{X^2}{H^2}\right)\right] \ . \qquad \text{(A-16)}$$

Using tables of elliptic integrals, we obtain

TABLE A-1. CALCULATIONS RELATING TO EQ. A-16

| $(X/H)^2$ | $\left(\frac{H}{X}\right)^2 \left[1 - \left(\frac{2}{\pi}\right)^2 E^2 \left(\frac{X^2}{H^2}\right)\right]$ |
|---|---|
| 0 | 0.5000 |
| 0.05 | 0.5017 |
| 0.25 | 0.5090 |
| 1.00 | 0.5947 |

which shows that the <u>lower bound</u> is not sensitive to the threshold setting, H, although the actual value of $(t-\bar{t})^2$ may be sensitive to the threshold.

The consequence of Table A-1 and Eq. A-16 is

$$\overline{(t-\bar{t})^2} \geq \frac{1}{2} \frac{X^2}{\left[S'(t_i)\right]^2} = \frac{1}{2} \frac{\left[S_o/S'(t_i)\right]^2}{\left(S_o/X\right)^2} \qquad \text{(A-17)}$$

where $S_o$ is the peak signal amplitude; $(S_o/X)^2$ is the peak signal-to-noise/interference power ratio; $t_i$ is the point of inflection on the leading edge of the pulse; $S'(t_i)$ is the maximum slope of the leading edge of the pulse; $S_o/S'(t_i)$ has the dimensions of time and is a measure of the pulse rise time; $S_o/S'(t_i)$ is, in fact, the rise time for a trapezoidal pulse.

It can be shown, by repeating the preceding analysis, that the equality sign holds when the pulse is trapezoidal, and when the signal-to-noise/interference ratio is high.

# APPENDIX B

# SYNCHRONIZATION LOOP ANALYSIS

## APPENDIX B

## SYNCHRONIZATION LOOP ANALYSIS

The relationship between clock oscillator lag (or negative lead), reset corrections, and drift is characterized by

$$S_{n+1} = S_n - g(S_n+x_n) + \delta \ , \qquad \text{(B-1)}$$

where $S_n$ is the clock lag just prior to the nth update, $x_n$ is the lag estimation error at the nth update, $S_n + x_n$ is the estimated clock lag at the nth update, g is the loop gain, $g < 1$, $g(S_n+x_n)$ is the applied correction, $S_n - g(S_n+x_n)$ is the clock lag immediately after the correction, $\delta$ is the drift between the nth update and the n + 1 update, and $S_{n+1}$ is the lag just prior to the n + 1 update.

The solution* to Eq. B-1 is

$$S_n = A(1-g)^n + \frac{\delta}{g} - \frac{g}{1-g} \sum_{m=1}^{\infty} (1-g)^m \, x_{n-m} \ , \qquad \text{(B-2)}$$

where the first term, with A as an arbitrary constant, is the homogeneous solution of Eq. B-1; $\delta/g$ is the component of the particular solution corresponding to oscillator drift; and the remainder, also a component of the particular solution, is the contribution of the lag estimation error. Furthermore, we note that:

1. In the steady state, the first term disappears because $g < 1$; and

*Verifiable by direct substitution into Eq. B-1.

2. The $x_k$ are assumed to be uncorrelated, zero mean random variables (biases are treated separately); with a mean squared value equal to $\sigma^2$.

Thus, in the steady state, the mean square value of Eq. B-2 becomes

$$\langle S^2 \rangle_s = \left(\frac{\delta}{g}\right)^2 + \left(\frac{g}{1-g}\right)^2 \sigma^2 \sum_{m=1}^{\infty} (1-g)^{2m} \quad , \qquad \text{(B-3)}$$

$$= \underbrace{\left(\frac{\delta}{g}\right)^2}_{\substack{\text{drift}\\ \text{component}}} + \underbrace{\sigma^2 \frac{g}{2-g}}_{\substack{\text{noise error}\\ \text{component}}}$$

where the first term represents the clock drift component while the second term is the contribution of the measurement error, and where the subscript, s, denotes the steady state.

Equation B-2 shows that the response of the loop to a single error sample is of the form of $(1-g)^n$. Thus, a loop response time, $\tau$, can be defined as the time that it takes the resultant synchronization error to decay to $e^{-1}$ of its original value, i.e.,

$$(1-g)^{\tau/T} = e^{-1} \qquad \text{(B-4a)}$$

or

$$\tau = -\frac{T}{\ln(1-g)} \quad , \qquad \text{(B-4b)}$$

where T is the time interval between updates. The clock drift, $\delta$, between updates is proportional to T:

$$\delta = \rho T \quad , \qquad \text{(B-5)}$$

in which $\rho$ is the usual oscillator stability specification in dimensionless form.

Substituting Eqs. B-4 and B-5 into Eq. B-3 and using the approximation

$$\ln\,(1-g) \approx -\,g \quad \text{for } g \ll 1, \tag{B-6}$$

we obtain

$$\langle S^2 \rangle_s = \underbrace{\left(\rho\tau\right)^2}_{\substack{\text{clock}\\ \text{drift}\\ \text{component}}} + \underbrace{\frac{1}{2}\,\sigma^2\left(\frac{T}{\tau}\right)}_{\substack{\text{noise error}\\ \text{component}}} \quad \text{for } \left(\frac{T}{\tau}\right) \ll 1 \tag{B-7}$$

The steady state mean square difference between synchronization errors at two points in time, separated by N updates, is obtained from Eq. B-2 (without the transient component):

$$\begin{aligned}\left\langle\left(S_{n+N}-S_n\right)^2\right\rangle_s = {} & \left(\frac{g}{1-g}\right)^2 \sum_{m=1}^{\infty}\sum_{k=1}^{\infty}(1-g)^m(1-g)^k\langle x_{n+N-m}\; x_{n+N-k}\rangle \\ & + \left(\frac{g}{1-g}\right)^2 \sum_{m=1}^{\infty}\sum_{k=1}^{\infty}(1-g)^m(1-g)^k\langle x_{n-m}\; x_{n-k}\rangle \\ & - 2\left(\frac{g}{1-g}\right)^2 \sum_{m=1}^{\infty}\sum_{k=1}^{\infty}(1-g)^m(1-g)^k\langle x_{n+N-m}\; x_{n-k}\rangle\,,\end{aligned} \tag{B-8}$$

where

$$\langle x_i x_j\rangle = \begin{cases}\sigma^2 & \text{for } i = j \\ 0 & \text{for } i \neq j\end{cases}\,. \tag{B-9}$$

Under such conditions, Eq. B-8 becomes

$$\sigma_N^2 = 2\left(\frac{g}{1-g}\right)^2 \sum_{m=1}^{\infty} (1-g)^{2m}\ \sigma^2$$

$$- 2\left(\frac{g}{1-g}\right)^2 \sum_{m=N+1}^{\infty} (1-g)^m (1-g)^{m-N} \sigma^2 \ , \qquad \text{(B-10)}$$

where

$$\sigma_N^2 = \left\langle \left(S_{n+N} - S_n\right)^2 \right\rangle . \qquad \text{(B-11)}$$

The sums are recognized as geometric series so that

$$\sigma_N^2 = 2\left(\frac{g}{1-g}\right)^2 \sigma^2 \ \frac{(1-g)^2}{1-(1-g)^2}$$

$$- 2\left(\frac{g}{1-g}\right)^2 \sigma^2 \ (1-g)^{-N} \frac{(1-g)^{2(N+1)}}{1-(1-g)^2} \qquad \text{(B-12)}$$

$$= \frac{2g\sigma^2}{2-g}\left[1-(1-g)^N\right] .$$

Equation B-4a provides

$$g = 1 - e^{-T/\tau} \ , \qquad \text{(B-13)}$$

so that Eq. B-12 may be rewritten as

$$\sigma_N^2 = \frac{2(1-e^{-T/\tau})}{(1+e^{-T/\tau})}\left[1 - e^{-NT/\tau}\right]\sigma^2 \ . \qquad \text{(B-14)}$$

Equation B-14 gives the contribution of synchronization error to TOA difference measurement errors for two TOA measurements separated by time NT; $\sigma$ being the one-sigma error of the

lag/lead estimate (given by Eq. 27 of the main text). The parameters of interest are

$$\begin{aligned} \text{loop settling time} &= \tau = 10 \text{ seconds} \\ \text{update interval} &= T = 48 \text{ milliseconds} \\ \text{time separation} &= NT = 3,\ 6 \text{ seconds} , \end{aligned}$$

in which case, Eq. B-14 becomes

$$\sigma_N = \begin{cases} 0.03527\sigma & \text{for 3-sec separation} \\ 0.04654\sigma & \text{for 6-sec separation} \end{cases} . \qquad \text{(B-15)}$$

If $\sigma$ is expressed in microseconds, then Eq. B-15 can be converted into range rate error, expressed in knots, by multiplication by

$$\frac{0.1618 \text{ (nmi/}\mu\text{sec)}}{3 \text{ (sec)}} \times 3600 \text{ (sec/hr)} = 194.2 \text{ knots/}\mu\text{sec} \qquad \text{(B-16)}$$

for 3-sec separation; and by half this number for 6-sec separation. Thus, the one-sigma RSS contribution to range rate error, expressed in knots, becomes

$$\begin{aligned} &6.85\sigma \quad \text{for 3-sec separation} \\ &4.52\sigma \quad \text{for 6-sec separation} , \end{aligned}$$

where $\sigma$, in microseconds, is given by Eq. 27 (of the main text) for a 120-nmi range to the DME transponder. Thus, the synchronization error contribution, at the maximum range to the synchronization donor (DME transponder), is as follows:

| Separation | Airliner CAS | GA CAS |
|---|---|---|
| 3 seconds | 4.09 knots | 10.4 knots |
| 6 seconds | 2.70 knots | 6.87 knots |

In any encounter between two aircraft, both the transmission time and reception time measurements will be affected by synchronization errors. Thus, synchronization error contributions from both aircraft in any encounter must be root sum squared. The result is shown in Table 10 of the main text.

# APPENDIX C

# EFFECT OF MULTIPATH ON RANGE RATE ERROR

## APPENDIX C

## EFFECT OF MULTIPATH ON RANGE RATE ERROR

The leading edge of a stylized trapezoidal pulse, together with its multipath return, is shown in Fig. C-1, where

$A$ = direct signal amplitude

$B$ = peak value of signal plus multipath return

$T_r$ = pulse rise time

$X$ = multipath amplitude at the time that the composite signal (direct plus multipath) reaches its peak amplitude B.

$\delta$ = time delay between the leading edge of the multipath return relative to the leading edge of the direct signal

The special case considered here is one where the half-amplitude point, B/2, occurs <u>before</u> the arrival of the leading edge of the multipath signal. The time-of-arrival is defined as the point at which the envelope is equal to one-half of its peak value (the leading edge of the signal must be delayed in order to compensate for the delay through the peak detector). Thus, the error, $\varepsilon$ (see Fig. C-1), is given by

$$\varepsilon = \left(\frac{1}{2}B - \frac{1}{2}A\right)/\text{slope}$$

$$= \frac{B-A}{2A/T_r} \qquad \text{(C-1)}$$

$$= \frac{1}{2}T_r\left(\frac{B}{A} - 1\right) .$$

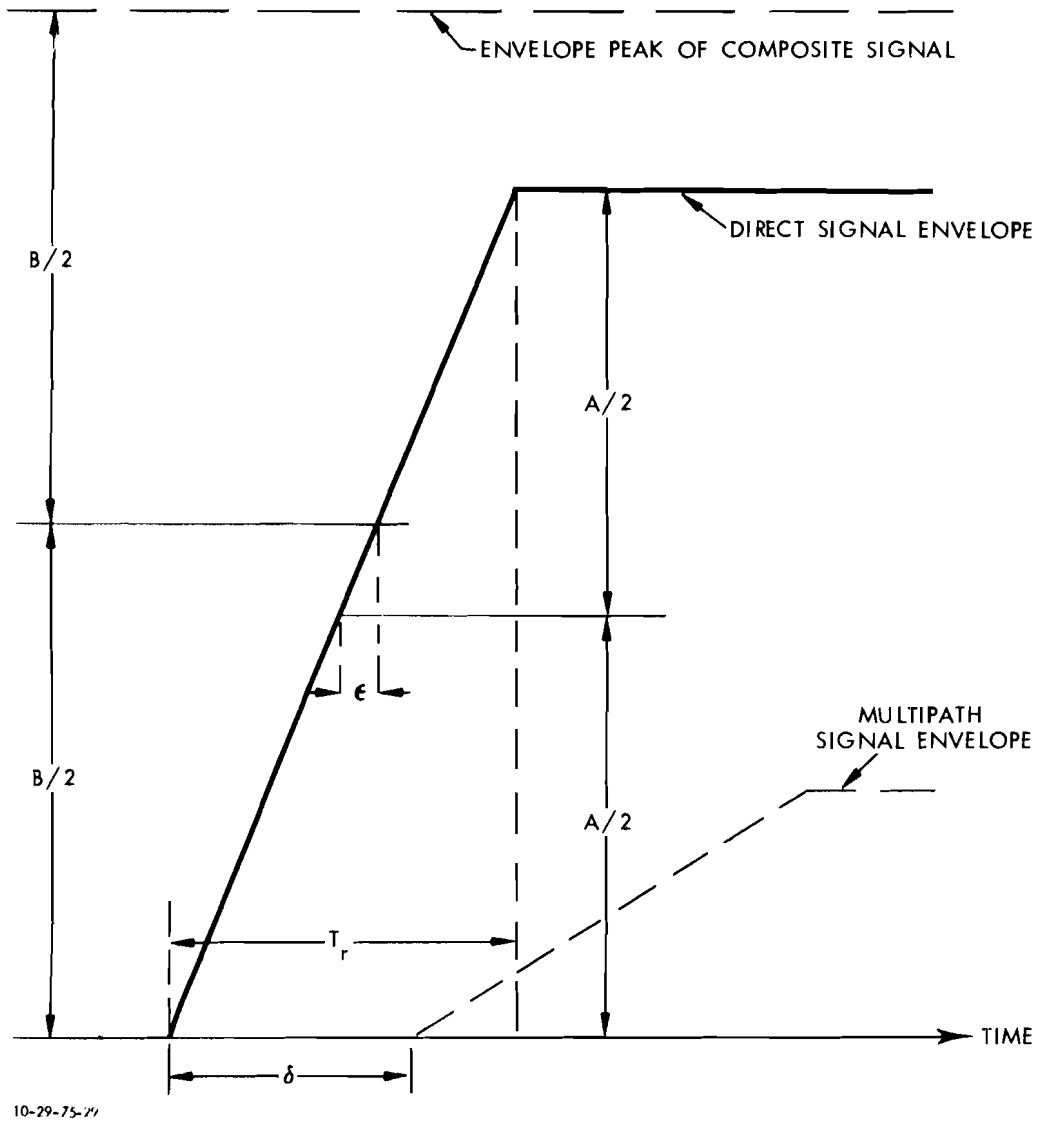


FIGURE C-1. Multipath Parameters

Furthermore, if $\varphi$ is the phase difference between the direct and multipath signals, then

$$B = \sqrt{A^2+X^2+2AX\cos\varphi}$$

$$= \sqrt{(A+X)^2-2AX(1-\cos\varphi)} \qquad \text{(C-2)}$$

$$= (A+X)\sqrt{1 - 4\frac{AX}{(A+X)^2}\sin^2 \varphi/2} \ .$$

For a uniformly distributed phase angle $\varphi$, we have:

$$\overline{B^2} = A^2 + X^2 \qquad \text{(C-3)}$$

and

$$\overline{B} = (A+X)\frac{1}{2\pi}\int_0^{2\pi}\sqrt{1 - 4\frac{AX}{(A+X)^2} \sin^2(\varphi/2)}\,d\varphi$$

$$= (A+X)\ \frac{1}{\pi}\int_0^{\pi}\sqrt{1 - \frac{4AX}{(A+X)^2} \sin^2 u}\ du \qquad \text{(C-4)}$$

$$= (A+X)\ \frac{2}{\pi}\ E\left[\frac{4AX}{(A+X)^2}\right] \ .$$

where $E[\cdot]$ is the complete elliptic integral of the second kind.

The variance of the error $\varepsilon$, given in Eq. C-1, can now be expressed in terms of Eqs. C-3 and C-4:

$$\overline{\varepsilon^2} - \bar{\varepsilon}^2 = \frac{1}{4} T_r^2 \left[ \frac{\overline{B^2}}{A^2} - \frac{\bar{B}^2}{A^2} \right]$$

$$= \frac{1}{4} T_r^2 \left\{ 1 + \frac{X^2}{A^2} - \left[ \frac{2}{\pi} \left( 1 + \frac{X}{A} \right) E\left( \frac{4AX}{(A+X)^2} \right) \right]^2 \right\} , \quad \text{(C-5)}$$

where X/A is the ratio of multipath amplitude to signal amplitude at the time that the composite envelope (direct plus multipath) reaches its peak value B. This ratio is designated by

$$m = X/A , \quad \text{(C-6)}$$

which, after substitution into Eq. C-5, yields the one-sigma error

$$\sigma_{toa} = \sqrt{\overline{\varepsilon^2} - \bar{\varepsilon}^2}$$

$$= \frac{1}{2} T_r \left\{ 1 + m^2 - \left[ \frac{2}{\pi}(1+m) \; E \left( \frac{4m}{(1+m)^2} \right) \right]^2 \right\}^{1/2} . \quad \text{(C-7)}$$

When the signal-to-multipath ratio is 10 dB, $m = 1/\sqrt{10}$, and for 16 dB, $m = 1/2\sqrt{10}$. Thus,

$$\sigma_{toa} = \begin{cases} 0.112 \; T_r & \text{for} \quad \text{SMR} = 10 \text{ dB} \\ 0.056 \; T_r & \text{for} \quad \text{SMR} = 16 \text{ dB} \end{cases} , \quad \text{(C-8)}$$

where SMR denotes the signal-to-multipath ratio.

For a 4-μsec rise time, the one-sigma range error becomes

$$0.112 \times 4\ \mu\text{sec} \times 984\ \text{ft}/\mu\text{sec} = 441\ \text{ft for SMR} = 10\ \text{dB},$$

and 221 ft when SMR = 16 dB. The corresponding range rate error, for 6-sec data, is

$$\frac{\sqrt{2} \times 441\ \text{ft}}{6\ \text{sec}} \times \frac{3600\ \text{sec/hr}}{6080\ \text{ft/nmi}} = 61.5\ \text{knots for SMR} = 10\ \text{dB}, \quad \text{(C-9)}$$

and 31 knots when SMR = 16 dB. The preceding analysis applies to the worst-case error which is attained for multipath delays ($\delta$ in Fig. C-1) of about 2 μsec (the flat part of the pulse is of the order of 2 μsec). As the delay increases, the multipath return moves out beyond the signal peak and the impact on the time-of-arrival measurement is reduced. As the multipath delay decreases, $\delta < 2$ μsec, the waveforms tend to merge and the time-of-arrival measurement error decreases.

The simple analysis, leading up to Eq. C-8, agrees with other results* obtained from an elaborate computer simulation. In this case, it was found that the maximum error occurs when

$$\text{multipath delay} = 0.58\ T_r,$$

and that the corresponding one-sigma errors are 0.11 $T_r$ when SMR = 10 dB, and 0.06 $T_r$ when SMR = 16 dB; results which confirm Eq. C-8.

---

*"A Comparison of Two Approaches for Determining Airborne Aircraft Position in Air Traffic Control," IDA Paper P-912, November 1972, p. 65, Fig. 14. This analysis assumes an exponentially shaped leading edge and the rise time is defined as the time needed to reach 90 percent of the peak amplitude.

The ranges and amplitudes at which the 2-μsec delay (equal to one-half the rise time) obtains are related by

$$\frac{1}{C}\left[\sqrt{\left(\frac{R}{2}\right)^2 + h^2} - R\right] = 2\ \mu\text{sec}, \qquad \text{(C-10)}$$

where C is the velocity of light (984 ft/μsec), R is the range, h is the altitude of both aircraft, and where the multipath is assumed to arrive from the ground midpoint between the two aircraft.

Equations C-7 and C-10 are used in Figs. 16 and 17 in the main text.

# APPENDIX D

# UNDETECTED CO-SLOT OCCUPANTS

## APPENDIX D

## UNDETECTED CO-SLOT OCCUPANTS

Within a 40-sec interval (equal to mean time between checks for co-slot occupancy) a certain number of new transmitters will appear within the communication range of an airliner approaching the Los Angeles Basin. The expected number is calculated from the geometry shown in Fig. D-1, where:

1. Two nmi is the product of 40 sec and a mean magnitude of range rate of 180 knots;
2. The 2-nmi annulus centered at airliner position contains the aircraft (primarily GA) which will enter within communication range (60 nmi) of the airliner within a 40-sec interval (equal to the time between

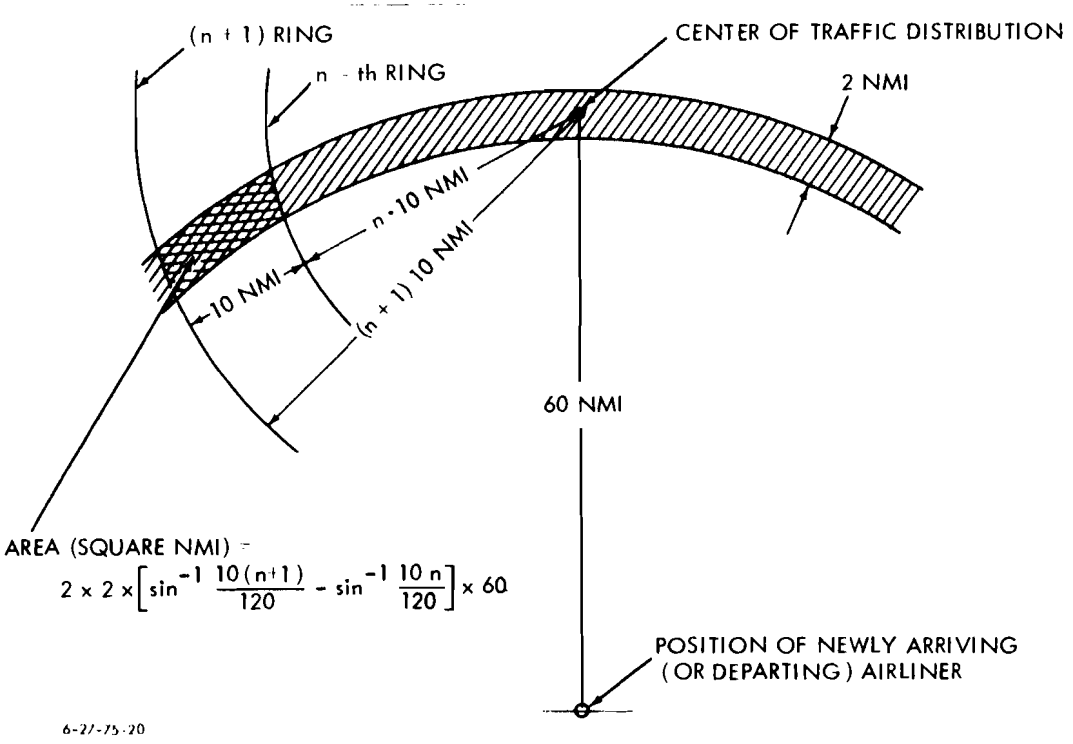


FIGURE D-1. Geometrical Factors (Not to Scale)

slot occupancy checks). However, only half of the aircraft will enter communication range because the other half is receding.

3. The nth ring is a circle of radius n x 10 nmi centered about the traffic distribution center.

The expected number of aircraft is summed in Table D-1. For a symmetric distribution (about the center in Fig. D-1) a similar shaded region needs to be added on the other side of the center. However, since the expected number of receding aircraft equals the number approaching, the factor of two is cancelled and the number of new communicants is just 21.

The approaching aircraft can be expected to "hear" half of the 800 (rounded off value of 797) in the Los Angeles Basin so that the number of slots available to the new arrival is 2000 - (800/2) = 1600 slots. Thus, the probability of undetected co-slot occupancy during the most critical point of the airliner's approach (*i.e.*, 60 nmi from the center of the distribution) is

$$\frac{21}{1600} \times 100\% = 1.3\% \text{ per 40-sec interval} . \qquad \text{(D-1)}$$

For the 2-minute interval during which the front edge of the communication zone might remain within the densest portion of the traffic distribution, the probability of undetected co-slot occupancy is

$$1 - (1 - 0.013)^{120/40} = 3.8\% . \qquad \text{(D-2)}$$

Fortunately, the CAS signals from these co-slot occupants will arrive late within the CAS slot, as observed by any potential threat of interest to the new arrival. With properly designed pulse decoders (such as described at the end of Chapter IV), there should be no ambiguity between the range pulse pair of the remote co-slot occupant and the altitude pulse pair of a potential threat.

TABLE D-1. SUMMATION OF EXPECTED NEW AIRCRAFT WITHIN COMMUNICATION RANGE

| Ring Number | Traffic Density* $(\text{sq nmi})^{-1}$ | Shaded Area in Fig. D-1 (sq nmi) | Expected Aircraft in Shaded Area (Fig. D-1) |
|---|---|---|---|
| 1 | 0.471 | 20.0 | 9.43 |
| 2 | 0.229 | 20.19 | 6.91 |
| 3 | 0.109 | 20.45 | 2.22 |
| 4 | 0.053 | 20.92 | 1.11 |
| 5 | 0.028 | 21.59 | 0.60 |
| 6 | 0.015 | 22.51 | 0.34 |
| 7 | 0.003 | 23.82 | 0.07 |
| | | Total: | 21 expected aircraft |

*Los Angeles Basin model, 1982.

# APPENDIX E

## COPY OF DOT/FAA TASK ORDER

## APPENDIX E

## COPY OF DOT/FAA TASK ORDER

TASK C. INDEPENDENT ASSESSMENT OF THE "DME COLLISION AVOIDANCE SYSTEM" DESCRIBED IN DOCUMENT TR-11115

Conduct an independent assessment of the "DME Collision Avoidance System" developed by Sierra Research Corporation as described in their report TR-1115 dated December 1973. Particular emphasis should be placed on the relationship between traffic density and missed alarms (accepting the hypothesis that the intruder is not a hazard when in fact he is, in accordance with the threat evaluation criteria), and false alarms (accepting the hypothesis that the intruder is a hazard when in fact he is not, again in accordance with the threat evaluation criteria). The analysis performed under this task shall consist in part of a review of work already accomplished in this area in order to validate or invalidate previous conclusions reached, and of original analysis where previous work is non-existant, incomplete or invalid. Consideration in the analysis shall be given, but not limited, to: (1) communication reliability as a result of transmitter power, receiver sensitivity, antenna gain and shadowing, signal processing, such as sensitivity time control, etc.; (2) both synchronous and asynchronous garble (including interweaved and overlapped pulse trains); and (3) multipath. The traffic model to be used for evaluation purposes is that furnished you for the previous analysis. Obvious improvements to the system shall be recommended

(although it is not the purpose of this task to do any substantial redesign effort) and inherent limitations in the system, which will preclude satisfactory operations in the designated environment, will be pointed out (due consideration will be given to conclusions reached as a result of TASKS A and B).

# APPENDIX F

# SUMMARY OF ANTC-117 EVALUATION AND MANEUVER LOGIC

# APPENDIX F

## SUMMARY OF ANTC-117 EVALUATION AND MANEUVER LOGIC

### A. SYSTEM CONCEPT

The specifications given by ANTC-117 for a cooperative airborne collision avoidance system are aimed at insuring the safe separation of aircraft in flight independently of ground control, although ground stations may be required to provide time synchronization for participating aircraft. In order to achieve this goal, several algorithms, involving measured values of the separation distance, separation rate, and altitude difference between two aircraft, as well as the rate of altitude change of the aircraft in which an evaluation of threat is being made, are used to generate warnings and alarms. These, in turn, trigger various cautions and commands to pilots, thereby causing them to perform certain avoidance or escaping maneuvers such as to stop turning (also known as "rollout"), to limit vertical speeds, to change altitude. Because bearing information is not assumed to be available, escape maneuvers take place in the vertical plane only.

The algorithms which provide alarm criteria are of two types: (1) those based on the separation distance (range), R, and separation rate (range rate), $\dot{R}$; and (2) those based upon the altitude difference $\Delta h$ between aircraft and altitude rate $\dot{h}$ of an individual aircraft. In principle, since R represents the slant range between aircraft, the R, $\dot{R}$ criteria alone should be sufficient to provide the alarms needed for protection against collision. However, it has been recognized that the use of altitude data is required to reduce the threat volume, and hence the alarm rate, to manageable proportions and also

to determine the proper direction for vertical avoidance maneuvers.

The measurement of R, $\dot{R}$, and $\Delta h$ is accomplished by means of radio communication between aircraft. The arrival time of a communication signal is used to calculate R, while $\dot{R}$ is obtained from a measurement of the doppler shift, although, recently, the tendency in CAS designs has been to obtain $\dot{R}$ from measurements of R at two different times. Each aircraft measures its own altitude with a barometric altimeter and communicates it in digital steps of 100 ft to other aircraft. Each CAS-equipped aircraft measures its own altitude rate for its own evaluation, but does not communicate this data to others.

ANTC-117 requires, in general, that each aircraft limit its horizontal acceleration to 1/2 G, its vertical acceleration to 1/4 G, and its vertical rate to 5000 ft/min. This implies a maximum relative horizontal acceleration of 1 G and vertical acceleration of 1/2 G, and a maximum vertical separation rate of 10,000 ft/min between two aircraft. [See A-4.b(3),(4) of ANTC-117.]

## B. PRIMARY THREAT CRITERIA

In the early days of CAS development, it was proposed that an R, $\dot{R}$ algorithm be based upon a quantity $\tau$, defined by

$$\tau = R/\dot{R} ,$$

representing the time to collision for two aircraft on a non-accelerating collision course. It has since been realized that, because of measurement errors and the possibility that aircraft may be accelerating, a modification of this idea is necessary. Thus, ANTC-117 has adopted two-alarm algorithms based on R and $\dot{R}$. These algorithms, sometimes known as modified $\tau$ criteria, have the same algebraic form, but different parameters:

$$R + \tau_1 \dot{R} \leq R_{o_1} ,$$

$$R + \tau_2 \dot{R} \leq R_{o_2} ,$$

where $\tau_1$, $R_{o_1}$, $\tau_2$, $R_{o_2}$ are designated constants.*

In the first algorithm, known as the $\tau_1$ alarm criterion, the designated constants have the values

$$\tau_1 = 25 \text{ sec}$$

$$R_{o_1} = 1/4 \text{ nmi } (1520 \text{ ft}) .$$

In the second algorithm, known as the $\tau_2$ warning criterion, the constants have the values

$$\tau_2 = 40 \text{ sec}$$

$$R_{o_2} = 1.8 \text{ nmi } (10{,}940 \text{ ft}) .$$

If two aircraft are co-altitude (within 600 ft for altitudes below 10,000 ft or 800 ft for altitudes above 10,000 ft), and if measured values of R and $\dot{R}$ satisfy the $\tau_2$ criterion, the pilot is commanded to limit turns (rollout) to a bank angle no greater than 10 deg and to neither climb nor dive. This is supposed to reduce the relative trajectory of the encountering aircraft to an approximately linear horizontal course. Then conditions are assumed to be suitable for the safe use of the more restrictive $\tau_1$ criterion.

---

*These algorithms are not actually stated by ANTC-117 in equation form, as is done here, but the equations can be deduced from [B-3.b] and Fig. 2 of that document. Note also that the convention $\dot{R}$ positive corresponding to increasing R is used here rather than the converse used in ANTC-117.

If R and $\dot{R}$ satisfy the $\tau_1$ criterion, vertical maneuver commands are issued so that the aircraft at the higher altitude climbs while the aircraft at the lower altitude dives until both aircraft are separated by a safe distance. If three aircraft are involved, the aircraft at the intermediate altitude maintains its course, neither climbing nor diving.

The $\tau_1$ criterion has been modified further by the addition of a minimum range criterion, the purpose of which is to protect against the hazardous case of $\dot{R}$ equal to or near zero, since it was felt that with the presence of acceleration and measurement errors, the time available for maneuver might be reduced below an acceptable minimum in this circumstance. Thus, an alarm also occurs with the same commands as for $\tau_1$ alarms if

$$R \leq R_M ,$$

where the minimum range $R_M$ has been designated as 1/2 nmi (3040 ft). The latter alarm will be referred to also as a $\tau_1$ alarm.

## C. ALTITUDE CRITERIA

The $\tau$ alarms are implemented only if the encountering aircraft are co-altitude, or it is predicted that they may become co-altitude, where "co-altitude" is defined to mean that their vertical separation is less than 600 ft at altitudes below 10,000 ft and 800 ft at altitudes above 10,000 ft. This definition of co-altitude is based upon (1) an altimeter error allowance of ±150 ft (3σ) below 10,000 ft and ±250 ft (3σ) above 10,000 ft, (2) the assumption that a safe vertical separation between aircraft is 150 ft, and (3) what is intended as an allowance for an undetected vertical drift rate of 500 ft/min.

According to ANTC-117, if an aircraft is climbing or diving at a rate greater than 500 ft/min, it is required to extend its co-altitude protection boundary in the direction of its motion by a predicted co-altitude increment. The predicted co-altitude increment is determined by multiplying the aircraft's own altitude rate $\dot{h}$ by 30 sec [B-3.a(3)].

In addition to the co-altitude zone wherein the $\tau$ alarms become operative, relative altitude buffer zones are established out to $\pm 3400$ ft. In each of these zones, vertical altitude rates are limited from 2000 ft/min in the farthest to successively lower values as the zones get narrower [Figs. 4, 4a, 4b, B-3.e].

## D. LIMITED EQUIPMENTS

ANTC-117 allows the existence of aircraft with limited collision avoidance equipments in order to spare general aviation the expense of a full CAS. Several possible variations are mentioned, but it is implied that unmentioned others may also be permitted.

Of those that are mentioned specifically, there are two types whose properties have an effect on threat evaluation. The first consists of the so-called level one and level two CAS, and the second is the beacon-only equipment.

Since ANTC-117 does not mention that level one and level two CAS-equipped aircraft have the ability to measure altitude rate, it has been assumed here that they do not have this capability. It follows, therefore, that this type of aircraft is unable to use the predicted co-altitude algorithm.

The beacon-only-equipped aircraft has no threat evaluation capability but is required to communicate its altitude. Thus, it can provide the necessary data for threat evaluation to a CAS-equipped aircraft, but is unable to make an avoidance maneuver on command.

# APPENDIX G

# EFFECT OF CORRELATED ERRORS

# APPENDIX G

## EFFECT OF CORRELATED ERRORS

This appendix examines the effect on Tau alarm errors due to correlation between range and range rate errors. Let

$R$ = intruder range at time t

$\varepsilon$ = error in the range measurement

$R + \varepsilon$ = estimated intruder range at time t

$R_1$ = intruder range, T seconds earlier

$R_1 + \varepsilon_1$ = estimated intruder range when its true range is $R_1$

The estimated range rate (closing rates being positive) is

$$\frac{(R_1+\varepsilon_1) - (R+\varepsilon)}{T}$$

so that the system will alarm when

$$R + \varepsilon = \left[\frac{(R_1+\varepsilon_1) - (R+\varepsilon)}{T}\right]\tau + R_0 \qquad \text{(G-1)}$$

in which $\tau$ and $R_0$ are the appropriate alarm parameters (see Eqs. 34 and 35 in Chapter VII of the main text). Rearranging terms in Eq. G-1 we obtain

$$R = \left[\frac{R_1-R}{T} + \frac{\varepsilon_1-\varepsilon\left(1+\frac{T}{\tau}\right)}{T}\right]\tau + R_0 \qquad \text{(G-2)}$$

Thus, the Tau alarm range-rate error due to the range measurement errors $\varepsilon$ and $\varepsilon_1$ is represented by the second term within the parentheses, *i.e.*,

$$\frac{\varepsilon_1 - \varepsilon\left(1+\frac{T}{\tau}\right)}{T} .$$

If $\varepsilon_1$ and $\varepsilon$ are independent, zero mean random variables, with one-sigma values equal to $\sigma_r$, then the mean square velocity error becomes

$$\sigma_v^2 = \frac{\sigma_r^2}{T^2}\left[2+2\frac{T}{\tau}+\left(\frac{T}{\tau}\right)^2\right]$$

or

$$\sigma_v = \sqrt{2}\,\frac{\sigma_r}{T}\sqrt{1+\frac{T}{\tau}+\frac{1}{2}\left(\frac{T}{\tau}\right)^2} .$$

For T = 6 sec and $\tau$ = 25 sec, we get

$$\sigma_v = \sqrt{2}\,\frac{\sigma_r}{T} \times 1.126 ,$$

which is 12.6 percent above $\sqrt{2}\,\sigma_r/T$ used in Eq. 39 in Chapter VII of the main text.

# APPENDIX H

# THE IMPACT OF RANGE DIFFERENCE MEASUREMENTS ON THE TAU ALARM CRITERIA

## APPENDIX H

## THE IMPACT OF RANGE-DIFFERENCE MEASUREMENTS ON THE TAU ALARM CRITERIA

The purpose of this appendix is to derive:

1. The range-rate estimate obtained from range-difference measurements
2. The effect of (1) on Tau alarm boundaries and
3. The difference between (2) and the specified alarm boundary and allowable errors.

The appropriate kinematics are obtained from Fig. H-1 where all the distances and the intruder aircraft trajectory are shown in a coordinate system attached to the reference aircraft and moving with it. In such a coordinate system, the reference aircraft remains fixed at point A while the intruder moves along the trajectory $B_1$-B-C. B is a point along the trajectory when the reference aircraft makes a range-rate estimate; $B_1$ is the intruder position T seconds before the intruder reached B; T is the time elapsed between the two range measurements, $R_1$ and R, employed in the range-rate estimate; C would be the point of closest approach if neither aircraft maneuvered; point A and the trajectory $B_1$-B-C define a plane which is taken as the plane of the diagram in Fig. H-1; the angle A-C-B is a right angle; V is the magnitude of the relative velocity between the reference and intruder aircraft; $\theta$ is the angle C-A-B; range rate (taken to be positive for closing geometries) is given by

$$\dot{R} = V \sin \theta \ , \qquad \text{(H-1)}$$

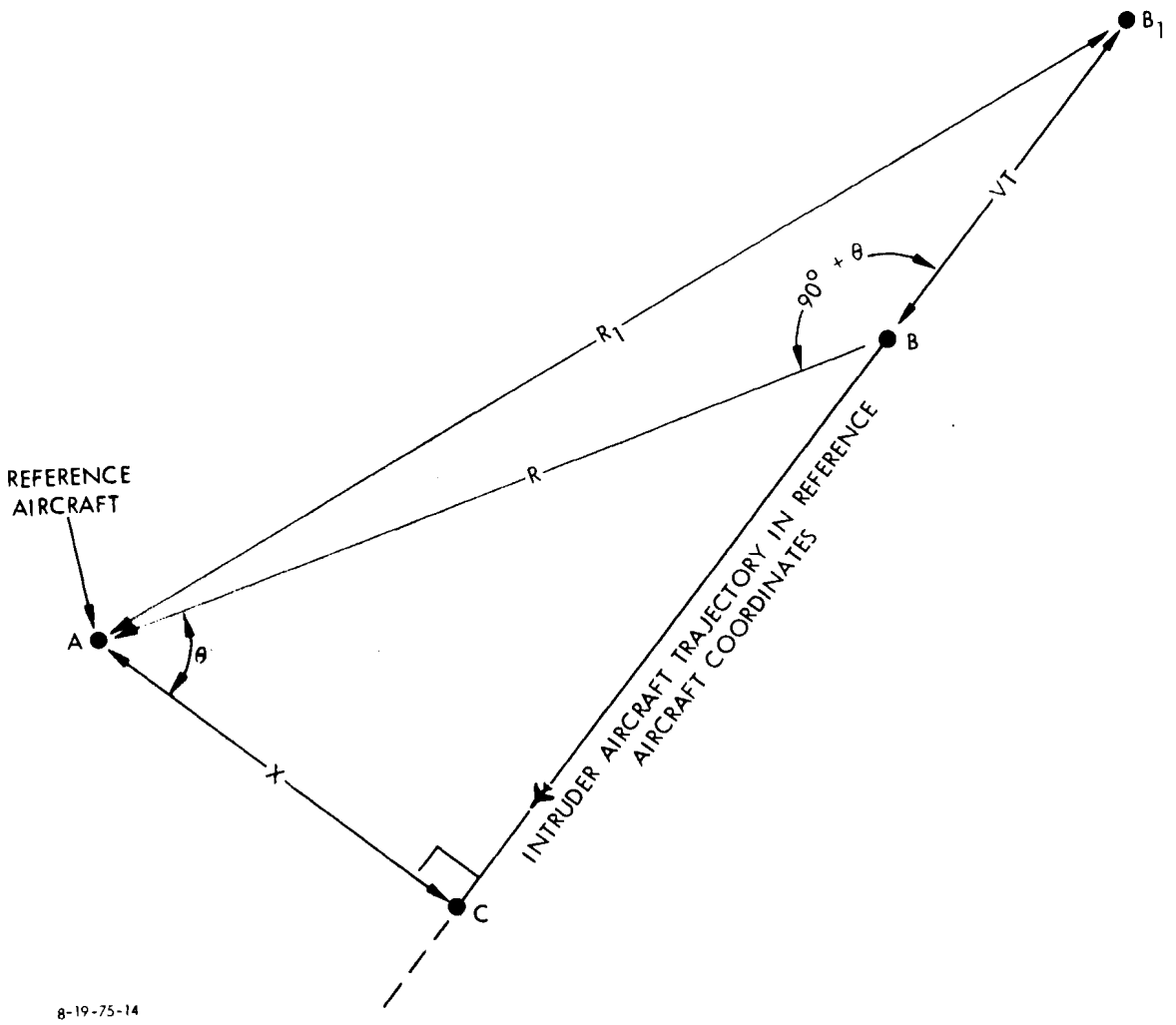


FIGURE H-1. Aircraft Encounter Kinematics in Reference Aircraft Coordinates

while the estimated range rate is

$$\hat{\dot{R}} = \frac{R_1 - R}{T} \ . \tag{H-2}$$

Application of the law of cosines to the triangle A-B-$B_1$ yields

$$R_1^2 = R^2 + 2RVT \sin \theta + (VT)^2 \ , \tag{H-3}$$

which, upon substitution of Eq. C-1, becomes

$$R_1^2 = R^2 + 2R\dot{R}T + (VT)^2 \ . \tag{H-4}$$

The specified (Ref. 2, pp. 71, 73) alarm criteria are shown in Fig. H-2. Thus, for ranges greater than 0.5 nmi, the alarm criteria are

$$\dot{R} \geq (R - R_o)/\tau \ , \tag{H-5}$$

where R is the range, $\dot{R}$ is the range rate (positive for closing geometries and negative for opening geometries) and where $R_o$ and $\tau$ depend on the Tau zone as shown in Fig. H-2. When the estimated value of $\dot{R}$, i.e., $\hat{\dot{R}}$, is used in place of $\dot{R}$, the alarm criterion becomes

$$\frac{R_1 - R}{T} \geq \frac{R - R_o}{\tau} \tag{H-6}$$

or

$$R_1 \geq R + \frac{T}{\tau}(R - R_o) \ , \tag{H-7}$$

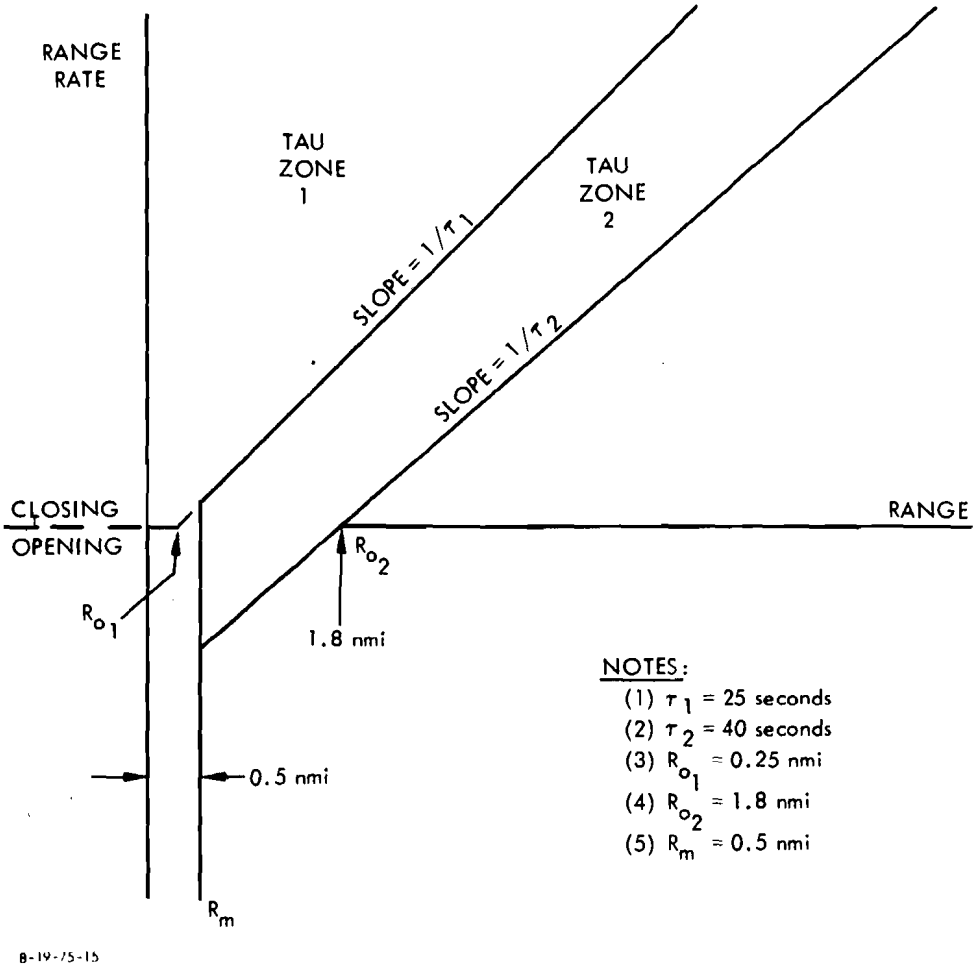


FIGURE H-2. Threat Evaluation Range and Range Rate

which is henceforth understood as applying to $R \geq 0.5$ nmi. As long as the right-hand side remains positive, both sides of the inequality can be squared. Thus, using Eq. H-4 we obtain

$$R^2 + 2R\dot{R}T + (VT)^2 \geq \left[R+\frac{T}{\tau}(R-R_o)\right]^2 \text{ for } \left[R+\frac{T}{\tau}(R-R_o)\right] \geq 0 \qquad \text{(H-8)}$$

or

$$\dot{R} \geq \frac{1}{2RT}\left\{\left[R+\frac{T}{\tau}(R-R_o)\right]^2 - R^2 - (VT)^2\right\} \text{ for } R + \frac{T}{\tau}(R-R_o) \geq 0$$

where $|\dot{R}| < V$ in accordance with Eq. H-1. After some obvious manipulation we get

$$\dot{R} \geq \frac{R-R_o}{\tau} - \underbrace{\frac{T}{2R}\left[V^2 - \left(\frac{R-R_o}{\tau}\right)^2\right]}_{\text{range rate bias error}} \qquad \text{(H-9)}$$

which is used to compute Table 12 in Section VII.

When the right-hand side of Eq. H-7 is negative, then, since $R_1$ is always positive, the alarm region becomes $R_1 \geq 0$ or $R_1^2 \geq 0$. Consequently, with the help of Eq. H-4 we obtain the alarm region as

$$R^2 + 2R\dot{R}T + (VT)^2 \geq 0 \text{ for } R + \frac{T}{\tau}(R-R_o) \leq 0 \qquad \text{(H-10)}$$

or

$$\dot{R} \geq -\frac{R^2+(VT)^2}{2RT} \text{ for } R + \frac{T}{\tau}(R-R_o) \leq 0 \qquad \text{(H-11)}$$

where, in accordance with Eq. H-1, the restriction is that $|\dot{R}| < V$. It should be noted that in Tau zone 1, where $\tau = 25$ sec, $R_o = 0.25$ nmi, and for $T = 6$ sec,

$$R + \frac{T}{\tau}(R-R_o) > 1.24\ R - 0.06 > 0 \text{ for } R > R_m = 0.5 \text{ nmi} \tag{H-12}$$

In other words, Eq. H-11 is never invoked in Tau zone 1. Similarly, in Tau zone 2 ($\tau$ = 40 sec, $R_o$ = 1.8 nmi), and for T = 6 sec, we have

$$R + \frac{T}{\tau}(R-R_o) = 1.15\ R - 0.27 > 0 \text{ for } R \geq 0.5 \text{ nmi} \tag{H-13}$$

so that Eq. H-11 is never invoked.

The additional kinematic relations needed for the analysis in Chapter VII (Fig. 18) are

$$R = \sqrt{X^2 + Y^2} \tag{H-14}$$

$$\dot{R} = \frac{Y\dot{Y}}{\sqrt{X^2 + Y^2}} = \frac{Y}{\sqrt{X^2 + Y^2}}\ V\ , \tag{H-15}$$

where X is the crossrange shown as the interval A-C in Fig. H-1; Y is the downrange, or the distance from C (Fig. H-1) to the intruder along the trajectory C-B-$B_1$; and $\dot{Y}$ is the speed, V, along the trajectory. Solutions for X and Y are

$$X = R\sqrt{1 - \left(\frac{\dot{R}}{V}\right)^2} \tag{H-16}$$

$$Y = \frac{\dot{R}}{V}\ R \tag{H-17}$$